

UNIVERSITY OF MARIBOR
FACULTY OF MECHANICAL ENGINEERING

Doctoral dissertation

**EFFECT OF PEPTIDES' BINDING ON THE
ANTIMICROBIAL ACTIVITY AND BIOCOMPATIBILITY OF
PROTEIN-BASED SUBSTRATES**

Maribor, July 2017

Maja KAISERSBERGER VINCEK



Doctoral dissertation

**EFFECT OF PEPTIDES' BINDING ON THE
ANTIMICROBIAL ACTIVITY AND BIOCOMPATIBILITY OF
PROTEIN-BASED SUBSTRATES**

Doktorska disertacija

**VPLIV VEZAVE PEPTIDOV NA PROTIMIKROBNO
AKTIVNOST IN BIOKOMPATIBILNOST PROTEINSKIH
SUBSTRATOV**

Maribor, July 2017

Author: Maja KAISERSBERGER VINCEK

Supervisor: Prof. Dr. Vanja KOKOL

ACKNOWLEDGEMENTS

I would like to express my deepest gratitude to my family and friends, whose support has sustained me through challenging times. My greatest thank go to my husband Simon and son Oskar, their love, humor and compassion have made all things possible.

I wish my aunt could have lived to see me finish this work, I know it would have meant so much to her. Dearest Tita, this thesis is dedicated to you.

TABLE OF CONTENTS

1	INTRODUCTION	1
1.1	The hypothesis	4
1.2	Original Scientific Contribution.....	4
2	BACKGROUND	6
2.1	Wool	6
2.1.1	Chemical and morphological structure	6
2.1.2	Activation and modification	9
2.2	Gelatine (GEL).....	10
2.2.1	Chemical and morphological structure	10
2.2.2	Activation and modification	12
2.3	Antimicrobial peptides (AMPs)	12
2.3.1	ϵ -poly-L-lysine (ϵ PL)	12
2.3.2	Oligo-acyl-lysyl (OAK).....	14
2.4	Functionalisation of keratinous substrate.....	16
2.4.1	Biochemical modification – carbodiimide conjugation	16
2.4.2	Enzymatic modification	16
3	THEORETICAL PRINCIPLES OF ANALYTICAL METHODS.....	18
3.1	Ultraviolet-visible (UV-Vis) absorption spectroscopy	18
3.2	Fluorescence spectroscopy	19
3.3	Electronic paramagnetic resonance (EPR) spectroscopy.....	20
3.4	Zeta potential (ZP).....	24
3.5	Potentiometric titration	26
3.6	Attenuated total reflectance – Fourier transform infrared (ATR-FTIR) spectroscopy	28

3.7 High pressure liquid chromatography – Size exclusion chromatography (HPLC-SEC)	29
3.8 Capillary zone electrophoresis (CZE)	30
3.9 Antimicrobial susceptibility testing.....	32
3.9.1 Disk-diffusion method	32
3.9.2 Dilution method (broth or agar dilution method)	33
3.9.3 Shake flask test	33
3.10 Cell viability assays	34
3.11 Fluorescence microscopy (FM).....	36
4 EXPERIMENTAL PART	38
4.1 Materials	38
4.2 Methods.....	40
4.2.1 Functionalisation of substrate	40
4.2.2 Evaluation of the efficacy of substrate functionalisation	45
4.2.3 Evaluation of substrate antibacterial activity	52
4.2.4 Determination of substrate cytotoxicity	55
4.2.5 Durability of functionalised wool	56
5 RESULTS AND DISSCUSION.....	57
5.1 The effect of ϵPL/OAK binding on the antimicrobial activity of wool	57
5.1.1 The influence of the coupling strategy of an ϵ PL/OAK graft yield onto wool.....	57
5.1.2 The orientation and localisation of ϵ PL on a wool surface	61
5.1.3 Antibacterial activity of ϵ PL/OAK-functionalised wool	68
5.1.4 Durability of wool’s antibacterial activity to washing	74
5.2 The effect of ϵPL/OAK binding on the antimicrobial activity and biocompatibility of GEL	76
5.2.1 Evaluation of the coupling efficacy of ϵ PL/OAK onto GEL.....	76

5.2.2	Orientation and localization of ϵ PL/OAK on GEL macromolecules.....	85
5.2.3	Antibacterial activity of ϵ PL/OAK-functionalised GEL.....	87
5.2.4	Cytotoxicity of ϵ PL/OAK-functionalised GEL	92
6	SUMMARY AND OUTLOOK.....	96
7	REFERENCES.....	98
8	SUPPLEMENTARY DATA	117
8.1	Curriculum vitae	117
8.2	Bibliography	120

LIST OF ABBREVIATIONS

AATCC	- American Association of Textile Chemists and Colorists
AGC	- Adjustable gap cell
AO7	- Acid Orange 7
Ala	- Alanine
AMP	- Antimicrobial peptide
Arg	- Arginine
Asn	- Asparagine
Asp	- Aspartic acid
ASTM	- American Society for Testing and Materials
ATCC	- American Type Culture Collection
ATR-FTIR	- Attenuated Total Reflectance – Fourier Transform Infrared
BGE	- Background electrolyte
CE	- Capillary Electrophoresis
CFM	- Confocal Fluorescence Microscopy
CFU	- Colony-forming units
CLSI	- Clinical and Laboratory Standards Institute
CMC	- Cell membrane complex
CZE	- Capillary Zone Electrophoresis
Cys	- Cysteine
CySS	- Cystine
DAD	- Diode-array detector
DMEM	- Dulbeco's Modified Eagle's Medium
DNA	- Deoxyribonucleic acid
<i>E. coli</i>	- <i>Escherichia coli</i>
EDC	- 1-ethyl-3-(3-dimethylaminopropyl)-carbodiimide hydrochloride
EPR	- Electron Paramagnetic Resonance
ESR	- Electron Spin Resonance
FBS	- Fetal Bovine Serum
FDA	- Food and Drug Administration

FITC	-	Fluorescein-5-isothiocyanate
FLD	-	Fluorescence detector
FM	-	Fluorescence Microscopy
Fmoc	-	9-fluorenylmethoxycarbonyl
G ⁺	-	Gram-positive
G ⁻	-	Gram-negative
GFC	-	Gel Filtration Chromatography
GHz	-	GigaHertz
Gln	-	Glutamine
Glu	-	Glutamic acid
Gly	-	Glycine
GPC	-	Gel Permeation Chromatography
GRAS	-	Generally recognized as safe
hFOB	-	Human fetal osteoblast cells
His	-	Histidine
HPLC-SEC	-	High Pressure Liquid Chromatography – Size Exclusion Chromatography
Ile	-	Isoleucine
ISO	-	International Standardization Organization
Leu	-	Leucine
LPS	-	Lipopolysaccharides
LSCM	-	Laser Scanning Confocal Microscopy
Lys	-	Lysine
MHA	-	Mueller Hinton agar
Met	-	Methionine
MP	-	Maleimido Proxyl
mTGase	-	microbial Transglutaminase
MTT	-	3-(4,5-dimethylthiazol-2-yl)-2,5-diphenyltetrazolium bromide
MW	-	Molecular weight
MWCO	-	Molecular weight cut off
NHS	-	N-hydroxysuccinimide
NCCLS	-	National Committee for Clinical Laboratory Standards
OAK	-	Oligo-acyl-lysyl

OD	-	Optical density
Phe	-	Phenylalanine
pI	-	Isoelectric point
PI	-	Propidium Iodide
pKa	-	acid dissociation constant
Pro	-	Proline
PVDF	-	Polyvinylidene fluoride
RI	-	Refractive index
RNA	-	Ribonucleic acid
ROS	-	Reactive oxygen species
<i>S. aureus</i>	-	<i>Staphylococcus aureus</i>
Ser	-	Serine
SPPS	-	Solid phase peptide synthesis
t-Boc	-	t-butoxycarbonyl
TFA	-	Trifluoroacetic acid
Thr	-	Threonine
TNBS	-	2,4,6-trinitrobenzenesulfonic acid
TNP	-	2,4,6-trinitro-phenyl
Trp	-	Tryptophan
Tyr	-	Tyrosine
UV-Vis	-	Ultraviolet-visible
Val	-	Valine
VWD	-	Variable wavelength detector
ZP	-	Zeta Potential
ϵ PL	-	ϵ -poly-L-lysine

EFFECT OF PEPTIDES' BINDING ON THE ANTIMICROBIAL ACTIVITY AND BIOCOMPATIBILITY OF PROTEIN-BASED SUBSTRATES

Key words: wool, gelatine, antimicrobial peptides, ϵ -poly-L-lysine, oligo-acyl-lysyl, grafting chemistry, grafting approach, peptide orientation, antibacterial activity, cytotoxicity.

UDK: 677.31.017.86:604.4(043.3)

ABSTRACT

*This work reveals the effect of coupling approach (chemical by using carbodiimide chemistry and grafting-to vs. grafting-from synthesis routes, and enzymatic by using transglutaminase) of a hydrophilic ϵ -poly-L-lysine (ϵ PL) and an amphiphilic oligo-acyl-lysyl (OAK) derivative (K-7 α_{12} -OH) to wool fibers and gelatine (GEL) macromolecules, respectively, and substrates antibacterial activity against Gram-negative *E. coli* and Gram-positive *S. aureus* bacteria after 1–24 h of exposure, as well as their cytotoxicity. Different spectroscopic (ultraviolet-visible, infrared, fluorescence and electron paramagnetic resonance) and separation techniques (size-exclusion chromatography and capillary zone electrophoresis) as well as zeta potential and potentiometric titration analysis, were performed to confirm the covalent coupling of ϵ PL/OAK, and to determine the amount and orientation of its immobilisation.*

*The highest and kinetically the fastest level of bacterial reduction was achieved with wool/GEL functionalised with ϵ PL/OAK by chemical grafting-to approach. This effect correlated with both the highest grafting yield and conformationally the highly-flexible (brush-like) orientation linkage of ϵ PL/OAK, implicating on the highest amount of accessible amino groups interacting with bacterial membrane. However, OAK's amphipathic structure, the cationic charge and the hydrophobic moieties, resulted to relatively high reduction of *S. aureus* for grafting-from and the enzymatic coupling approaches using OAK-functionalised GEL.*

The ϵ PL/OAK-functionalised GEL did not induce toxicity in human osteoblast cells, even at ~25-fold higher concentration than bacterial minimum inhibitory (MIC) concentration of ϵ PL/OAK, supporting their potential usage in biomedical applications.

It was also shown that non-ionic surfactant adsorbs strongly onto the wool surface during the process of washing, thereby blocking the functional sites of immobilized ϵ PL and decreases its antibacterial efficiency.

VPLIV VEZAVE PEPTIDOV NA PROTIMIKROBNO AKTIVNOST IN BIOKOMPATIBILNOST PROTEINSKIH SUBSTRATOV

Ključne besede: volna, želatina, protimikrobni peptidi, α -poli-L-lizin, oligo-acil-lizil, način vezave, konformacija, protibakterijsko delovanje, citotoksičnost.

UDK: 677.31.017.86:604.4(043.3)

POVZETEK

Z naraščanjem zavesti o bakterijskih, glivnih in virusnih obolenjih ter vedno pogostejših vsakdanjih okužbah postajajo protimikrobno aktivni materiali vedno bolj pomembni na številnih področjih uporabe, predvsem pa za biomedicinski, terapevtski in higienski namen.

Glede na proteinsko sestavo z integrirano sekvenčno aminokislinsko strukturo, ki ustreza adheziji različnih človeških celic in biorazgradljivosti, se v zadnjem desetletju preučujejo kot potencialni biomateriali tudi vlakna živalskega izvora, kot je npr. keratinsko volneno vlakno. Tovrstne aplikacije morajo izkazovati določene bioaktivne in protimikrobne aktivnosti, ki jih še zmeraj dosegamo s površinsko ne-permanentno obdelavo s pretežno toksičnimi in okolju neprijaznimi spojinami.

Uporaba polimernih biomaterialov, kot sta kolagen in njegov toplotno denaturiran produkt, želatina, v biomedicinski in farmacevtski namen je ponovno v izrednem porastu zaradi izjemnih biomimetičnih in bioaktivnih lastnosti, izredne resorpcijske sposobnosti in vivo, celične kompatibilnosti, nealergenosti, plastičnosti in visoke adhezije ter sposobnosti predelave v film, vlakno, peno ali 3D nosilec.

Množična uporaba antibiotikov in pogosta odpornost bakterij proti protimikrobnim zdravilom narekuje razvoj novih protimikrobnih biomaterialov. Slednji bi bili uporabni za širok namen in bi zagotovili ne le učinkovito in dolgotrajno protimikrobno zaščito proti širokemu spektru patogenih bakterij, temveč tudi ohranili naravno biološko okolje. Razen tega materiali s protimikrobnimi lastnostmi še vedno ne delujejo kontrolirano in selektivno na patogene mikroorganizme. Za razvoj novih funkcionaliziranih površin je potrebno podrobno poznavanje

osnovnega substrata, kakor tudi uporabljenih reagentov in obdelav. Za razumevanje delovanja protimikrobnih snovi, ki delujejo izključno na mejni površini substrata, pa je potrebno preučiti njihove interakcije, kar je bil eden izmed temeljnih ciljev te doktorske disertacije. Nadalje je nujno razumevanje pojavov na aktivni mejni površini med funkcionaliziranim materialom in biološko okolico.

V prvem delu je prikazan študij načina vezave (kemijski napram encimski način, »vezava-na« napram »vezava-iz« načinu sinteze) različnih protimikrobnih peptidov (PMP) na osnovi lizina (ϵ -poli-L-lizin, ϵ PL in oligo-acil-lizil, OAK) na volnena vlakna in makromolekule želatine (GEL). Cilj doktorske disertacije je bil ohraniti njihovo protimikrobna aktivnost ter doseči stabilno in trajno delovanje tako pripravljenih substratov. Kovalentne vezi namreč igrajo pomembno vlogo pri konformaciji proteinov in njihovi stabilnosti, saj lahko blokirajo aktivna mesta. Zato morajo biti eksperimentalni pogoji dobro nadzorovani. V drugem delu je z uporabo različnih spektroskopskih (ultravioletna-vidna, infra-rdeča, fluorescenčna, elektronsko paramagnetno resonančna spektroskopija) in separacijskih (visokotlačna tekočinska izločitvena kromatografija, kapilarna conska elektroforeza) analiznih metod, ter zeta potenciala in potenciometrične titracije, bila potrjena kovalentna vezava ϵ PL/OAK na proteinska substrata. S kombinacijo različnih raziskovalnih metod in razvojem eksperimentalne metodologije je bila določena kvantiteta in orientacija imobiliziranih PMP.

Najučinkovitejši in najhitrejši učinek redukcije po Gramu negativne bakterije *E. coli* in po Gramu pozitivne bakterije *S. aureus* po 1–24 urni izpostavitvi bakterij je bil dosežen z uporabo volne/GEL funkcionalizirane z ϵ PL/OAK po kemijskem in »vezava-na« načinu. Takšen učinek je povezan tako z največjo količino vezave ϵ PL/OAK kot tudi z njihovo konformacijsko najbolj razvejano orientacijo, ki posledično doprinese največjo količino dostopnih amino skupin za interakcije z bakterijsko membrano. Kljub temu sta oba substrata funkcionalizirana z OAK po kemijskem »vezava-iz« in encimskem načinu vezave izkazala relativno visok inhibitorni učinek na bakterijo *S. aureus* zaradi svoje amfifilne strukture, t.j. pozitivnega naboja in hidrofobnih ostankov. Amfifilne lastnosti OAK omogočajo ciljno in hitro interakcijo z bakterijskimi membranami v primerjavi z bolj hidrofilnim ϵ PL, ki se lažje polimerizira in konjugira.

Tretji del naloge temelji na razumevanju biokompatibilnosti med funkcionaliziranim materialom in okoljskim tkivom ter njegovi specifičnosti in dinamiki, s katero lahko nadalje vplivamo na razvoj medicinsko-negovalnih in zaščitnih materialov s ciljanimi protimikrobnimi lastnostmi. ϵ PL/OAK-funkcionalizirana GEL ni sprožila toksičnega učinka pri človeških

osteoplastnih celicah niti pri ~25-krat višji koncentraciji, kot je bakterijska minimalna inhibitorna koncentracija (MIC) za ϵ PL/OAK, kar kaže na njihovo potencialno uporabo v biomedicini.

Prav tako je bilo pokazano, da se neionsko površinsko-aktivno sredstvo močno adsorbira na volneno površino med procesom pranja in tako blokira funkcionalne skupine imobiliziranega ϵ PL ter posledično zmanjša protibakterijski učinek.

Postopek funkcionalizacije proteinskih substratov s protimikrobnimi peptidi omogoča razvoj novih in bolj varnih tekstilnih in medicinskih biomaterialov z visoko dodano vrednostjo, t.j. specifičnim protimikrobnim in bioaktivnim učinkom. Preučevani materiali lahko predstavljajo alternativo obstoječim biocidom in potencialno antibiotikom, ki se sicer uporabljajo pri bakterijskih okužbah.

1 INTRODUCTION

Antimicrobial activity of fibrous and polymeric materials is increasingly important in many application areas, but above all in biomedical, therapeutic and hygiene applications, to increase the standard of living and reduce the growing awareness of bacterial, fungal and viral diseases.

Lightness, warmth, softness, and smoothness are the properties making **wool fibres** generally used for high-grade textiles. Over the last decade, wool keratins have also been studied as potential biomaterials for human clinical applications as wound dressings and implantable devices, being related to both contents of proteins having cell adhesion sequences [1, 2] and thus being good substrates for fibroblast [3, 4] and osteoblast cells [5], as well as being biodegradable *in vitro* and *in vivo* [6]. However, as a protein fibre, wool suffers degradation easily, causing skin irritation and/or infection due to the generation and propagation of microorganisms under certain temperatures and humidity. In addition, by being used as a biomaterial, it has to meet a wide variety of other demands, above all possessing of relevant bioactive and antimicrobial activities. Still, this is usually obtained by employing quaternary ammonium salts, cationic and amphiphilic polymers, or colloidal nanoparticles such as e.g. SiO₂, Cu and Ag, and using different technologies on nano-functionalised surfaces [7, 8]. A range of cross-linking reagents and coupling strategies for enabling their covalent attachments [9] have been investigated, wherein non-covalently bound (mainly embedded in coatings) metal nanoparticles are still the most important subject studies, although they have shown some weaknesses, such as capped long-term effectiveness and the capacity for developing microbial resistance and low efficiency. On the other hand, increasingly applicable antimicrobial active nanoparticles as e.g metal oxides can penetrate through the skin and/or cell membranes and cause vague threats to our health [10]. In addition, as many heavy metals are applied during the coating of fibres via ultrasound irradiation, such treatments have serious limitations due to technical and environmental problems and, therefore, have not been adopted for commercial production [11, 12].

A biomaterial is a material used to replace part of a living system or to function in intimate contact with living tissue and is generally used to recognize materials for biomedical applications. Applications of polymeric biomaterials are promising for drug delivery, tissue engineering, biomedical sensing, skin grafting, medical adhesives [13] and modern textile-based biomaterials to be used in surgical applications [14]. From a practical perspective, medical applications of polymers fall into three broad categories: i) extracorporeal uses, ii) permanently implanted devices, and iii) temporary implants [15]. In that respect, more and more studies have been recently urged to identify the further impact of collagen and its thermally denatured product, **gelatine (GEL)**, both being categorized as a safe excipient by the US FDA, as biomimetic and bioactive polymers, being extracted from different sources as cattle bones, hides, pig skins, fish and insects [16]. Both, collagen and gelatine, have been evaluated extensively and are currently used in pharmaceuticals, wound dressings and adhesives in clinics due to their good resorption *in vivo*, excellent cytocompatibility, non-immunogenicity, non-antigenity, plasticity and adhesiveness [17, 18, 19], as well as the ability to be processed in films, fibres, foams and scaffolds, thus to engineer various tissues such as bone, as well as cartilage, heart, ligament, and nerves [20, 21]. However, the benefits of lower immunogenicity and aqueous solubility make gelatin more suitable choice as biomaterial compare to collagen [20].

Multi-drug resistance is a world-wide problem, attributed to the extensive use of antibiotics, selection pressure on bacterial strains and lack of new drugs, vaccines and diagnostic aids. These shortcomings urged the development and synthesis of novel antimicrobial biomaterials to be employed in a broad range of applications, ranging from food packaging to medical devices. However, a desired level of protection is to develop materials that would ensure not only effective and long-lasting antimicrobial protection against a wide range of pathogenic bacteria and fungi, but also to maintain a constant and well-defined biological environment. **Antimicrobial active peptides (AMP)** and proteins have been thus recognised as clinically perspective antimicrobial agents, showing high and specific antimicrobial activities at very low (μmol) concentrations [22], as well as low toxicity to mammalian cells, together with the fact that bacterial resistance to them seems inherently difficult to acquire [23, 24].

Amongst them a polipeptide **ϵ -poly-L-lysine (ϵ PL)** is being used within different fields from medicine, food, environment and agriculture as well as the textile industry, due to its low minimum inhibitory concentration (MIC of < 0.05 %) and non-toxic nature [25, 26]. The ϵ PL was initially described to show the analogical antimicrobial kinetics against different bacteria by causing irreversible changes in both the inner and outer cell membranes of pathogens. Good antibacterial activity of covalently bonded ϵ PL can be attributed to its electrostatic interactions with the bacterial membrane, followed by stripping off the membrane and distribution of their cytoplasm [27]. However, amongst different functionalisation procedures that have been studied for the immobilisation of ϵ PL on various types of fibres and polymers, most of them are non-specific and based on electrostatic interactions between positively charged amino groups of ϵ PL and negatively charged polymer surfaces [28]. Stable chemical bonding between lysozyme and wool was also proposed through the cross-linking of lysozymes' amino groups with available Lys residues within wool fibres [29] by using expensive and toxic glutaraldehyde which, however, may reduce the biocompatibility of the final material. Alternatively, using enzymes working site-specifically and regional-selectively, as for example microbial transglutaminase (mTGase) (which catalyses the acyl transfer reaction between the peptide-bound Gln residues as acyl donors and primary amino groups as receptors), have been shown to be a very useful grafting approach [30], resulting in a material with ~96 % reduction of *Escherichia coli* (*E. coli*) [31].

Oligo-acyl-lysines (OAKs) are among the simpler and recently developed AMP molecules, in which the two most important characteristics, the hydrophobicity and the charge, are represented by tandem repeats of amide-linked fatty acids and Lys, thus to mimic the physiological structure and functioning of natural AMPs [32]. These properties were shown to overcome the limitations of conventional AMPs with respect to *in vivo* efficacy and toxicity [33]. In addition, OAKs are generally resistant to bacterial enzymatic degradation and exhibit no or minimal cytotoxicity to mammalian cells. Furthermore, their structures can be fine-tuned to optimise antibacterial activity, which have been shown to be significant *in vivo* against *E. coli* [33, 34] and *Staphylococcus aureus* (*S. aureus*) [35, 36] in infected mouse models.

Although, a wide variety of solid supports has been assessed for production of surfaces with immobilised AMPs [37], including polymeric brushes and resins, metals, glasses, etc. by using

different coupling strategies to render their concentration, stability and orientation and, thus, efficacy, only single studies have been performed on immobilization of OAKs.

The immobilization of an OAK on a polystyrene resin is reported to sequester a broad spectrum of bacterial species, with rapid and efficient bacterial capture to be used for the separation/concentration of a broad spectrum of microbes from large volume samples [38, 39].

1.1 The hypothesis

The primary purpose and objective of this doctoral dissertation was to examine the possibility of AMPs grafting on protein-based substrates (wool/GEL) in a way to interfere with microbes in a different and/or specific (related to Gram-positive or Gram-negative type of bacteria; in a biocidal or biostatic way, and/or by different time scale) mode, thus resulting in the ability for targeted destruction of specific spectrum of pathogens and defiance in the development of long-lasting microbial resistant biomaterials. For this purpose, the ϵ PL as well as recently developed OAK as AMPs were selected.

The hypotheses of the doctoral dissertation are thus:

- AMP can be covalently bonded to a protein-based substrate in a way to entirely maintain its antimicrobial effect,
- by using differently active AMPs it is possible to achieve a targeted anti-microbial activity of the substrate,
- substrate functionalised by AMP is biocompatible.

1.2 Original Scientific Contribution

The aim of this thesis was to define a strategy for the covalent coupling of AMPs to protein-based substrates, whilst maintaining its antibacterial activity. In that respect, different coupling mechanisms and coupling chemistries were used and compared for achieving stable and durable functionalisation. The abundance of Gram-positive and Gram-negative bacteria after incubation with such substrates was evaluated for assessing a biocidal vs. bacteriostatic

effects, depending on the type of bacteria. In addition, differently prepared GEL substrates were screened for cytotoxicity to address their biocompatibility.

2 BACKGROUND

2.1 Wool

2.1.1 Chemical and morphological structure

Wool is a keratin-based polymer consisting of more than 170 different protein residue domains, heterogeneously distributed throughout the fibres that are responsible for its exceptional physical and chemical properties.

At the supramolecular level of organisation, the structure of wool fiber consists of highly organised fibrillary aggregates of proteins (the microfibrils, Fig. 2.2) set in a matrix of globular-type proteins of much less discernible order [40]. Wool fibre consists of two major morphological parts (Fig. 2.1), the sulphur-rich outer layer known as the cuticle and the inner component called cortex [41]. The cuticle acts as a barrier for the diffusion of chemicals, imparts properties such as wettability, tactile properties, and is responsible for the felting of wool. It contains numerous disulphide bonds, which connects the peptide chains and are composed of three layers (the epicuticle, the exocuticle and the endocuticle) among which the exocuticle has the highest sulphur content. The cortex, making up to 90 % of the mass of a fibre, is comprised of cortical cells, which are bounded together with each other and with the cuticle cells by a cell membrane complex (CMC) [42] - composed of protein and lipid [43]. The wool is thus covered with an outer lipid layer, which is covalently bound to the surface to form a hydrophobic barrier.

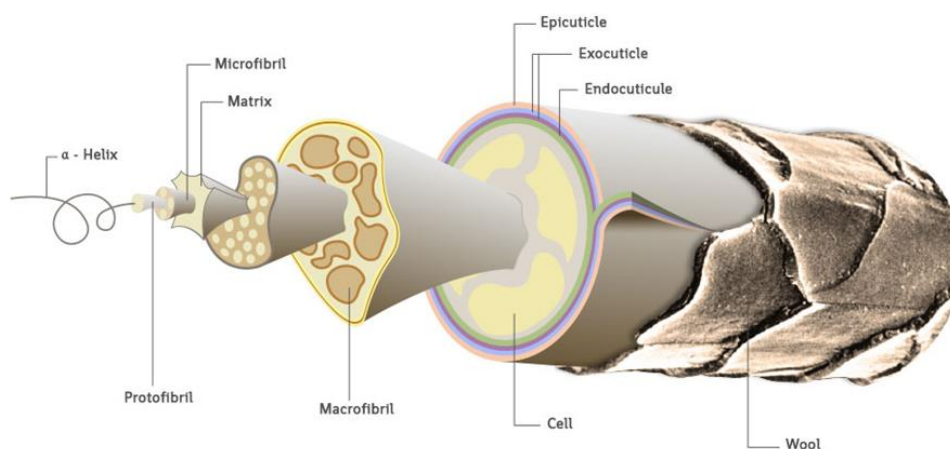


Figure 2.1: A cross-section of the wool fiber [41].

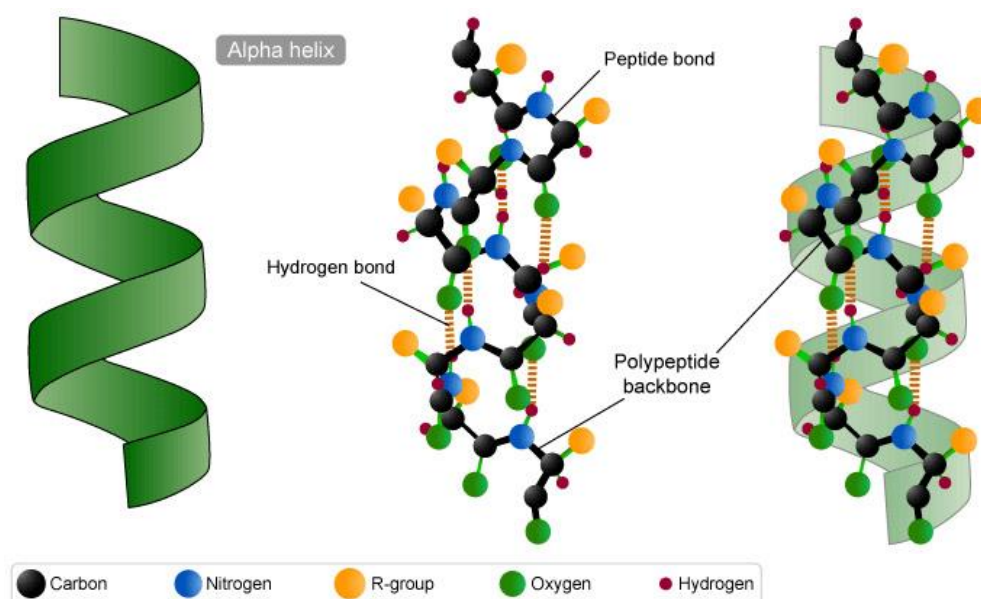


Figure 2.2: Microfibrillar model of an α -helix, showing the intrachain hydrogen bonding between carbonyl oxygen atoms and amide hydrogen atoms. Alpha-helices have 3.6 amino acid residues per turn, *i.e.* a helix of 36 amino acids would form 10 turns [47].

In the microfibrillar region, wool is composed of a complex assembly of proteins with 20 different amino acids sequences, listed in Table 2.1 [44, 45, 46]. They are distinguished by their side chain, which imparts a special character, being either hydrophilic or hydrophobic, acidic or basic based on the containing numerous amino ($-\text{NH}_2$) or acid carboxylic ($-\text{COOH}$) groups. The proportions of acidic and basic groups are approximately the same (800 – 850 $\mu\text{mol/g}$ of each). This high content of oppositely charged side chains facilitates a second kind of crosslinking, *i.e.* ‘salt-bridges’ between an acidic Glu or Asp residues and a protonated Lys or Arg residues, as shown in Fig. 2.3. A third kind of crosslinking element is the isodipeptide bond between Glu or Asp and a Lys residue. Additionally, hydrogen bonds are included as stabilizing elements of wool, notably between amide groups, but also between a variety of other hydrogen donating and accepting groups [47]. Individual protein chains thus exist at α -helices stabilised in part by intra-chain hydrogen bonds. The α -helices in turn are aggregated into 2- and 4-chain units within the microfibril that are held together by a variety of covalent crosslinks and non-covalent physical interactions [48]. At the molecular level the fibre is thus stabilised by inter-chain cross-links formed by the disulphide bridges of Cys residues and by inter-chain secondary bonds, such as hydrogen bonds and salt linkages (especially between $-\text{COO}^-$ and $-\text{NH}_3^+$ groups).

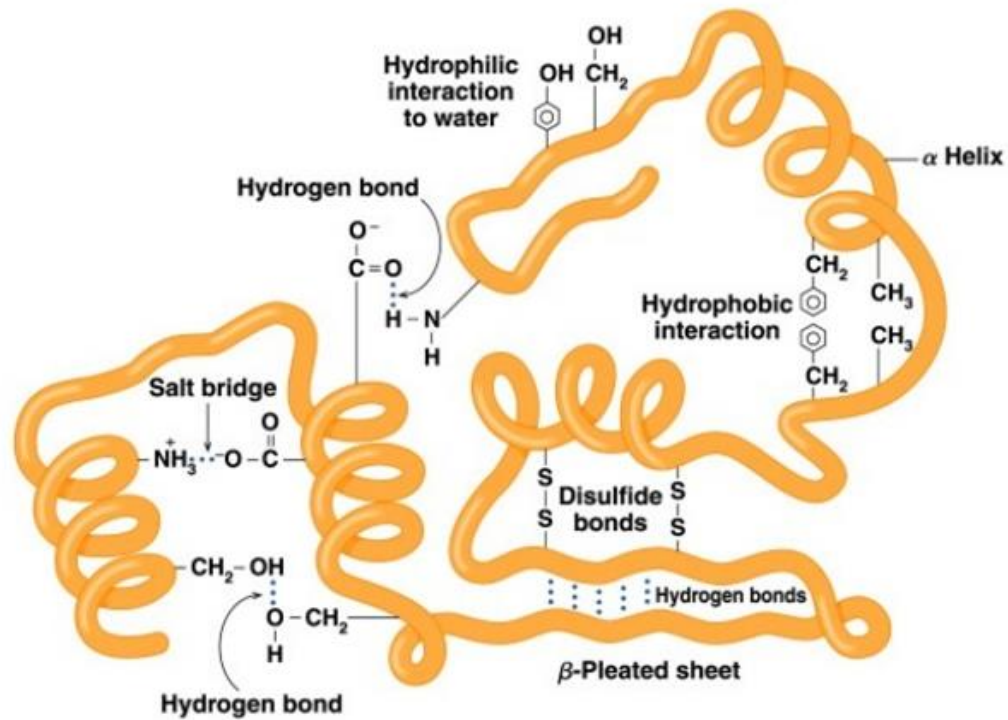


Figure 2.3: An overall three-dimensional tertiary structure of a wool protein.

Table 2.1: The amino acid composition of wool fiber [41]

Chemical character of side group	Name and abbreviation of amino acid	Concentration [μmol/g]
Acidic amino acids and their ω-amides	Aspartic acid (Asp)	200
	Glutamic acid (Glu)	600
	Asparagine (Asn)	360
	Glutamine (Gln)	450
	Arginine (Arg)	600
Basic amino acids and tryptophan	Lysine (Lys)	250
	Histidine (His)	80
	Tryptophan (Trp)	40

Amino acids with hydroxyl groups in the side chain	Serine (Ser)	900
	Threonine (Thr)	570
	Tyrosine (Tyr)	350
Sulphur containing amino acids	Cystine (Cyss)	480
	Methionine (Met)	50
Amino acids without reactive groups in the side chain	Glycine (Gly)	760
	Alanine (Ala)	470
	Valine (Val)	490
	Proline (Pro)	520
	Leucine (Leu)	680
	Isoleucine (Ile)	270
	Phenylalanine (Phe)	260

2.1.2 Activation and modification

Wool protein in general contains three main types of reactive sites: peptide bonds, side chains of amino acid residues and disulphide crosslinks. The presence of many charged groups in the structure of wool provides excellent binding sites for its functionalisation [48]. Amongst different functionalisation procedures that have been studied for the immobilisation of ϵ PL on various types of fibres and polymers, most of them are non-specific and based on electrostatic interactions between positively charged amino groups of ϵ PL and negatively charged polymer surfaces [28, 30, 31, 49, 50, 51]. Stable chemical bonding between lysozyme and wool was also proposed through the cross-linking of lysozymes' amino groups with available Lys residues within the wool fibres [29] by using expensive and toxic glutaraldehyde which, however, may reduce the biocompatibility of the final material.

Alternatively, using enzymes working site-specifically and regional-selectively, for example mTGase (which catalyses the acyl transfer reaction between the peptide-bound Gln residues

as acyl donors and primary amino groups as receptors), have been shown to be a very useful grafting approach [30], resulting in a material with ~96 % reduction of *E. coli* [31]. TGase has been recognised as safe (GRAS) by an independent panel of scientific experts and may be used to incorporate a functional alkyl amine moiety into different proteins that give desired or beneficial effects [52]. TGase mediated grafting of proteins can significant effect on the properties of wool yarn and fabric, resulting for example in increased bursting strength, as well as reduced levels of felting shrinkage and improved fabric softness [53].

2.2 Gelatine (GEL)

GEL is the commercial protein obtained by a controlled hydrolysis from the insoluble protein collagen, the main fibrous protein constituent in bones, cartilages and skins, and as such has all the properties required to meet the technical needs of the pharmaceutical and biomedical application [54, 55]. Conversion of collagen into soluble GEL is due to the cleavage of number of intra- and inter-molecular hydrogen and covalent cross-linking bonds in collagen during heat- and chemical- treatments to destabilize the triple-helix, resulting in helix-to-coil transition and conversion into soluble gelatine [56, 57, 58]. The denaturalization process through which GEL is obtained can be performed by acid hydrolysis leading to GEL type A (pI of 7 – 9), or alkaline hydrolysis resulting in GEL type B (pI of 4.8 – 5.2), and various MWs depending on the source of collagen [20]. GEL contains all amino acids as collagen, except Trp and have low in Met, Cys and Tyr due to the degradation during hydrolysis [59, 60]. GEL type A shows cationic behaviour at pH below its pKa due to protonation of amino groups, while GEL type B is negatively charge at pH values above 4.8.

2.2.1 Chemical and morphological structure

The amino acid composition and sequence in GEL vary, especially the minor constituents, depending on the source of the raw material and processing technique, but always consists of large amounts of Gly, Pro and hydroxy Pro as shown in Table 2.2. Structurally, GEL molecules contain repeating sequences of Gly-X-Y triplets, where X and Y are frequently Pro and hydroxy Pro amino acids. These sequences are responsible for the triple helical structure of GEL and its ability to form gels.

Table 2.2: Typical amino acid profile of 100 g of GEL

Chemical character of side group	Name and abbreviation of amino acid	Concentration [$\mu\text{mol/g}$]
Acidic amino acids and their ω -amides	Aspartic acid (Asp)	5.0
	Glutamic acid (Glu)	8.3
	Arginine (Arg)	4.9
Basic amino acids	Lysine (Lys)	2.9
	Hydroxylysine (hydroxy Lys)	0.6
	Histidine (His)	0.6
Amino acids with hydroxyl groups in the side chain	Serine (Ser)	3.2
	Threonine (Thr)	1.7
	Tyrosine (Tyr)	0.2
Sulphur containing amino acids	Methionine (Met)	0.4
Amino acids without reactive groups in the side chain	Glycine (Gly)	29.3
	Alanine (Ala)	12.1
	Valine (Val)	2.4
	Proline (Pro)	13.2
	Hydroxyproline (hydroxy Pro)	10.0
	Leucine (Leu)	2.5
	Isoleucine (Ile)	1.3
	Phenylalanine (Phe)	1.4

2.2.2 Activation and modification

GEL can be functionalised by many cross-linking approaches, among which chemical methods using highly reactive, but cytotoxic, reagents are frequently employed, such as aldehydes [61]. In effort to improve the biocompatibility of cross-linked protein-based biomaterials, water soluble carbodiimide chemistry using 1-ethyl-3-(3-dimethylaminopropyl)-carbodiimide hydrochloride (EDC) has been developed, that couple carboxyl groups of Glu or Asp with amino groups of Lys or Hyl residues, thus forming stable amide bonds. Reaction efficacy is increased by addition of N-hydroxysuccinimide (NHS) or sulfo-NHS which prevents hydrolysis and rearrangement of the intermediate, thus causing the formation of a coarse structure instead of tougher microstructure, in its absence [62]. Because EDC can only couple groups within distance of 1 nm, this treatment enhances intra- and interhelical linkages within or between tropocollagen molecules, without an inter-microfibrillar cross-links [63] and leads only to the formation of amide linkages without chemical entities remaining in the crosslinked product. By this *in vitro* non-cytotoxic and *in vivo* biocompatible materials can be formed [64, 65, 66].

Improvement of physical and qualitative properties can be made also via enzymatic combination with others proteins [67, 68], protein mixing and enzymatic modification, structure modification and other modifications [69, 70].

2.3 Antimicrobial peptides (AMPs)

Most of the antibacterial agents work under two main principles: inhibition of the growth of the cells (biostatic) and/or killing of the cells (biocidal). Almost all the commercial antimicrobial agents are biocides. They damage the cell wall or inhibit the metabolism of the cell by stopping nutrient penetration inside the cell, be necessary for their survival [71].

2.3.1 ϵ -poly-L-lysine (ϵ PL)

ϵ PL, a generally used and by FDA approved antimicrobial agent, produced by Gram-positive bacteria, have attracted much attention. ϵ PL is hydrophilic cationic linear homo-polypeptide of approximately 25–30 identical Lys residues, which has strong antimicrobial activity against most Gram-positive and Gram-negative bacteria, fungi, as well as some kinds of viruses. Moreover, it is harmless to humans, biodegradable and has antitumor effect [26, 72, 73].

Apart from being used as a safe preservative in food industry, derivatives of ϵ PL offer a wide range of applications such as emulsifying agents, dietary agents, biodegradable fibres, hydrogels, drug carriers, anticancer agent enhancers, biochip coatings, etc.

THE CHEMICAL STRUCTURE

In contrast to normal peptide bond that is linked by the alpha-carbon group, the Lys amino acids in ϵ PL are molecularly linked by the epsilon amino (ϵ -NH₂) group and the carboxyl (-COOH) group, as shown in Fig. 2.4.

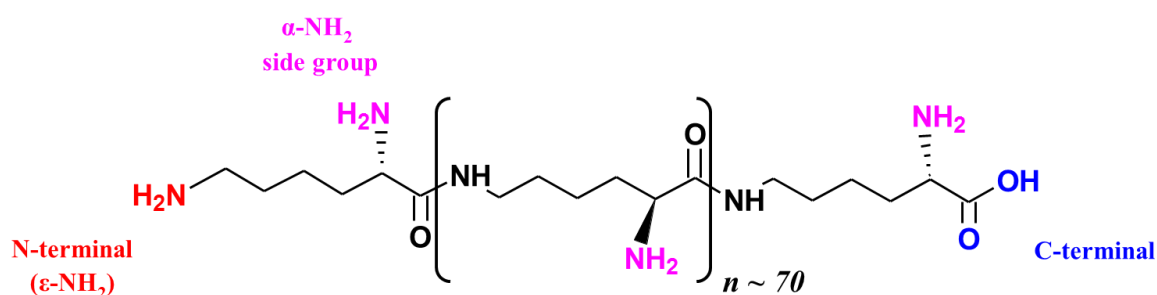


Figure 2.4: Chemical structure of ϵ -poly-L-lysine (ϵ PL).

ANTIMICROBIAL ACTIVITY

ϵ PL's antimicrobial activity is closely related to the number of repetitive Lys residues, and it has been shown that at least ten monomeric Lys residues [27, 74] are required for ϵ PL to exert proper antibacterial activity. Interestingly, the ϵ PL is a more potent antimicrobial compound than α -PL, but the reason for this difference is still unknown [75].

The mechanism of action of ϵ PL has not been fully investigated, but it has been proposed that cationic polypeptide interacts with the negatively charged cell surface by ionic adsorption and that ϵ PL subsequently interferes with cell membranes in a reaction that has been proposed to include stripping of lipopolysaccharide (LPS) layer that leads to a permeabilization of the outer membrane [27, 76]. However, conclusive evidence for the proposed hypotheses together with the molecular mechanism of action of ϵ PL on the cytoplasmic membrane is still lacking. Based on the results of Wei H. et al. [77] and Zhao Y. et al. [78], the potential antimicrobial mechanism of ϵ PL is depicted in Fig. 2.5.

The bacterial cell surfaces are generally negative charged as their cell membranes/walls usually contain LPS, teichoic and lipoteichoic acids, and negatively charged phospholipids

[79]. When positive charges from ϵ PL are exposed to bacteria, it bounds to the membrane surface by electrostatic attraction. The accumulation of such interaction results in the disturbance of the cell membrane, and leads to changes that result in fractures of the membrane structure. Thus, ϵ PL enters the cytoplasm through the membrane fractures, inducing the generation of reactive oxygen species (ROS) and SOS response (it refers to a set of co-regulated genes that are induced in response to DNA damage, causing the lysis of the bacteria and results in the bacterial cell death) [77].

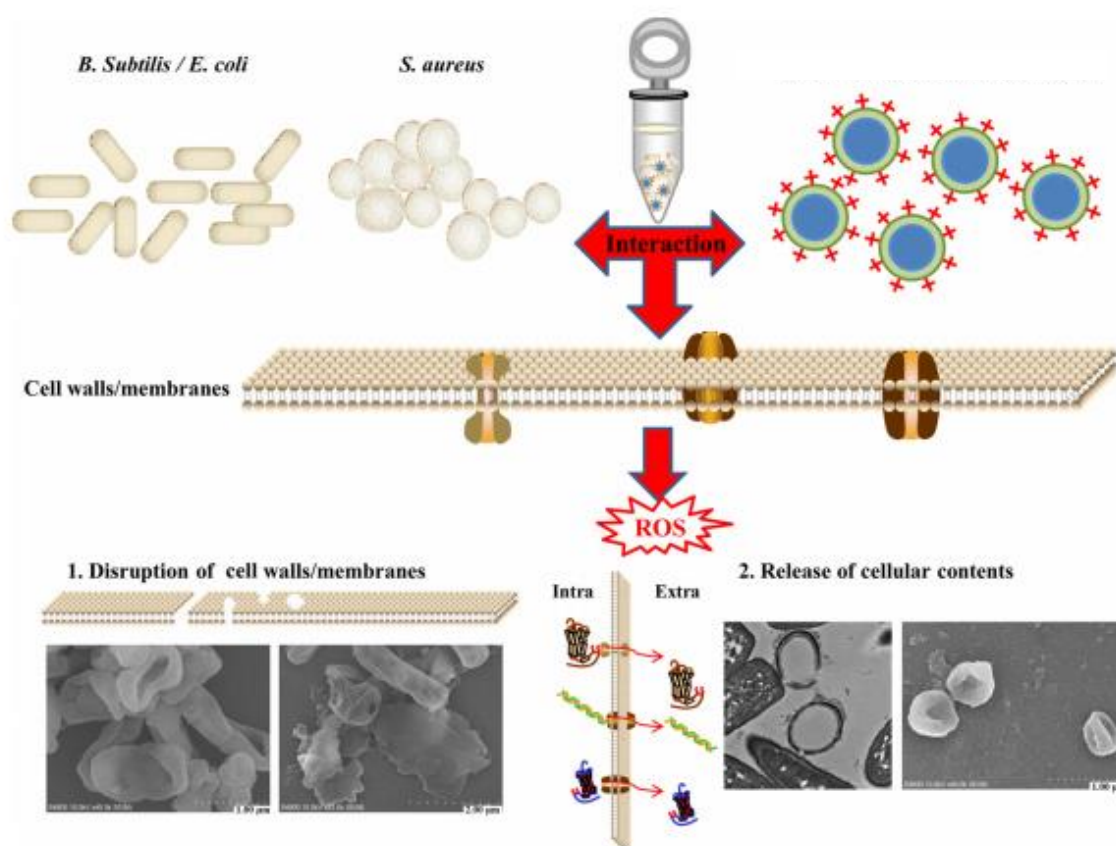


Figure 2.5: Proposed antibacterial mechanisms of the ϵ PL [78].

2.3.2 Oligo-acyl-lysyl (OAK)

OAKs are a novel group of antimicrobial copolymers, designed to mimic the primary structure and function of natural AMPs. Oligomers of acylated lysines are novel synthetic peptidomimetics that consist of alternating amino acyl chains and cationic amino acids that are arranged to create an optimal molecular charge and hydrophobicity [33, 80]. Like most natural AMPs, the OAKs are cationic and form amphipathic structures that associate with

one another to protect the hydrophobic side and expose the cations to interact with the bacterial membrane [81].

However, in contrast to natural AMPs, the OAK design allows for the formation of a simple structure, which allows for the establishment of structure-activity relationships and prevents the formation of secondary structures. These properties are in turn associated with the lack of development of antimicrobial resistance [82]. In addition, the OAK peptides are resistant to bacterial enzymatic degradation [83] and exhibit no or minimal cytotoxicity to mammalian cells [84, 85].

THE CHEMICAL STRUCTURE

In this work, the octameric OAK derivative, lysyl-[aminododecanoyl-lysyl]₇ (K-7 α_{12} -OH, Fig. 2.6) with MW of 2.4 kDa was used, which was produced by the solid-phase peptide synthesis method and further purified to homogeneity by HPLC as described in [86, 87].

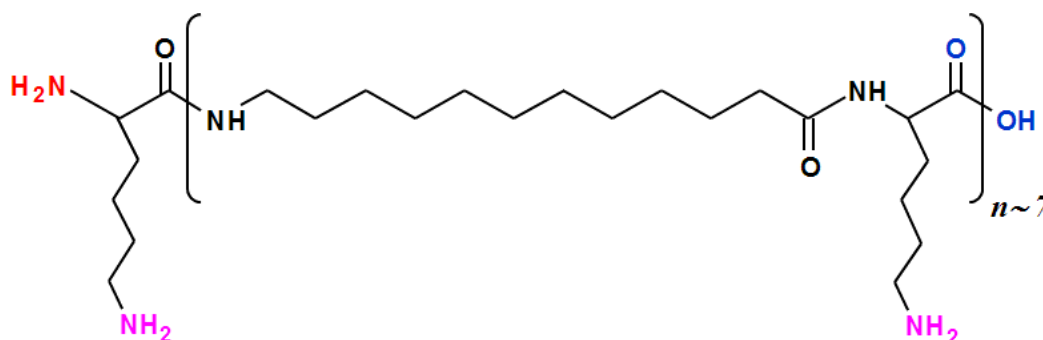


Figure 2.6: Chemical structure of the octameric OAK derivative (K-7 α_{12} -OH), where α_{12} denotes an aminododecanoyl-lysyl subunit.

ANTIMICROBIAL ACTIVITY

Like most natural AMPs, the OAKs are cationic and form amphipathic structures that associate with one another to protect the hydrophobic side and expose the cations to interact with the bacterial membrane. Natural AMPs are usually composed of long acyl chains within a peptide backbone, which can lead to rigid supra-molecular organization, responsible for poor antibacterial activity and enhanced hemolytic activity. In contrast, the OAK design allows for the formation of a structure, enabling the establishment of structure-

activity relationships and preventing the formation of secondary structures. These properties are in turn associated with the lack of development of antimicrobial resistance [33, 80]. In addition, the OAK peptides are resistant to bacterial enzymatic degradation and exhibit no or minimal cytotoxicity to mammalian cells. Furthermore, their structures can be fine-tuned to optimize antibacterial activity and they have been shown to possess significant *in vivo* efficacy against *E. coli* [33, 34] and *S. aureus* [35, 36] in mouse models of infection. Thus, OAKs display characteristic features that are attractive for the development of a potent new class of therapeutic drugs [82].

2.4 Functionalisation of keratinous substrate

2.4.1 Biochemical modification – carbodiimide conjugation

Carbodiimides belong to the zero length cross-linking agents, forming bonds without the introduction of additional atoms or spacers. Their application is favorable in conjugation reactions, where such spacer might be detrimental for the intended use of the corresponding conjugates. Their applicability in both organic and aqueous solvents contributes to the wide spectrum of possible conjugation reactions [88].

Carbodiimides are widely used to activate carboxylate groups by the formation of highly reactive O-acylisourea intermediates. This active species can then react with amine nucleophiles to form stable amide bonds. Water-soluble carbodiimides, such as EDC, allow an aqueous conjugation reaction of water soluble targeting molecules and polymers. To avoid undesirable side reactions, NHS or sulfo-NHS can be added to form more stable NHS ester derivatives as reactive acylating agents. The corresponding NHS or sulfo-NHS esters react readily with nucleophiles to form the acylated product, but only primary or secondary amines form stable amid or imide linkages, respectively [89].

2.4.2 Enzymatic modification

A wide range of enzymatic approaches has been trialled for surface-specific modification of proteins. Enzyme treatments offer the prospect of replacing environmentally unacceptable processes with more “eco-friendly” ones. In that respect, an extensive research and development have been conducted with respect for utilisation of enzymes as antifelting agents for wool, as well as for enhancing its colour [90].

The oxidative enzymes, tyrosinase and laccase, as well as acyltransferase-transglutaminase are capable creating covalent crosslinks in proteinaceous substrates. Tyrosinases and laccases are copper-containing oxidoreductases, which catalyze oxidation of various mono- and polyphenolic compounds. Tyrosinases oxidize p-monophenols and o-diphenols to quinones, whereas laccases are capable to oxidize a larger variety of aromatic compounds by a radical catalyzed reaction mechanism in the presence of oxygen [91].

Transglutaminase (TGase) is able modify the functionality of proteins by inducing intra- and inter-molecular crosslinks. The enzyme catalyzes acyl-transfer transformations between Gln and Lys residues in proteins thereby generating isopeptide bonds [92]. TGase is commercially available crosslinking agent whose use was approved by the US FDA as GRAS.

3 THEORETICAL PRINCIPLES OF ANALYTICAL METHODS

3.1 Ultraviolet-visible (UV-Vis) absorption spectroscopy

UV-Vis spectrophotometry is one of the most powerful and widely used tools for quantitative analysis, being applicable on organic, inorganic, and biochemical systems. Important characteristics of UV-Vis spectrophotometry are good sensitivity, detection limits of 10^{-4} to 10^{-7} M, moderate to high selectivity, reasonable accuracy and precision (relative errors in the 1 to 3 % range and with special techniques, as low as a few tenths of a percent), speed and convenience.

The UV-Vis technique measures the absorption of electromagnetic radiation within wavelength range from 160 nm to 780 nm, by outer (valence) electrons in sample atoms, inducing transition to higher energy level electron orbitals. Energy difference between ground and excited electrons state is quantized, making this technique applicable for identification of functional groups, which absorb at specific wavelength within the region [93].

UV-Vis spectra acquisition may be easily performed in a solution and by using the Beer-Lambert law, compound concentration can be calculated by the following equation:

$$A = -\log T = \log \frac{I_0}{I} = \varepsilon \times b \times c \quad (3.1)$$

A – absorbance

T – transmittance

I_0, I – intensities of incident and transmitted radiation

ε – molar extinction coefficient or molar absorptivity [L/mol cm]

b – beam path length [cm]

c – molar concentration [mol/L]

3.2 Fluorescence spectroscopy

Fluorescence spectroscopy can be applied to a wide range of problems in the chemical and biological sciences. The measurements can provide information on molecular processes, including the interactions of solvent molecules with fluorophores, rotational diffusion of biomolecules, distances between sites on biomolecules, conformational changes, and binding interactions [94].

Fluorescence is the light emitted by an atom or molecule after a finite duration, subsequent to the absorption of electromagnetic energy. The emission spectrum provides information for both qualitative and quantitative analysis. As shown in Fig. 3.1, when light of an appropriate wavelength is absorbed by a molecule (*i.e.* excitation), the electronic state of the molecule changes from the ground state to one of many vibrational levels in one of the excited electronic states, be usually the first one, S_1 . Once the molecule is in this excited state, relaxation can occur via several processes. Fluorescence is one of these processes and results in the emission of light, which is easured [95, 96]. Among instrumental techniques, fluorescence spectroscopy is recognized as one of the most sensitive techniques due to the emission signal that is measured above a low background level. This is inherently 1000 times more sensitive than comparing two relatively large signals in absorption spectroscopy.

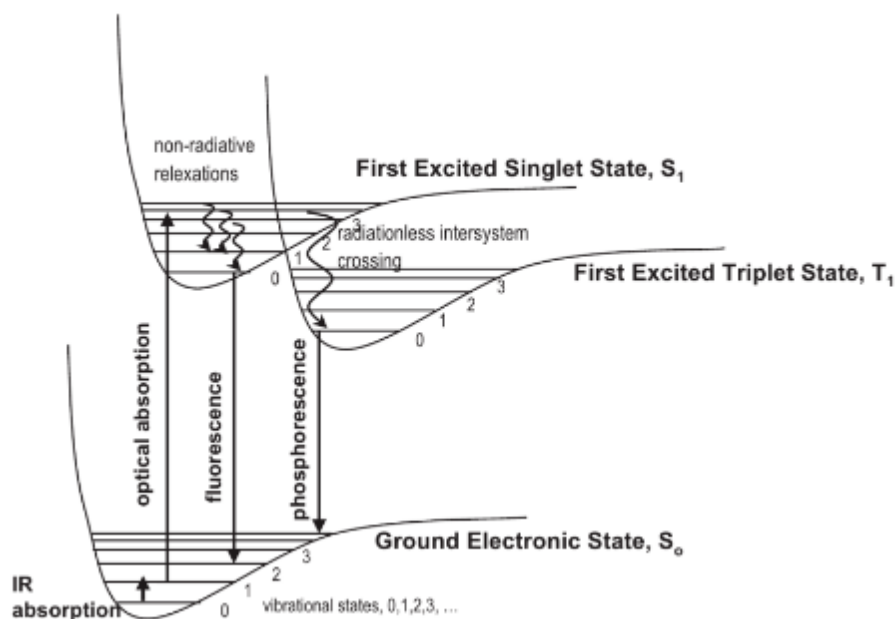


Figure 3.1: Energy level diagram illustrating vibrational and electronic levels of molecules upon light interaction [96].

Excitation and emission are largely decoupled by the relaxations between them. The efficiency of a fluorophore to convert absorbed light into fluorescence, is the quantum efficiency or quantum yield (Φ). Emission spectrum is a mirror image of the absorption spectrum and quantum yield of 1 means that all light absorbed is converted to the fluorescence. The fraction of a parallel beam of light absorbed by a sample is independent of the intensity of the incident beam and is related to the concentration of the absorbing species by the familiar Beer-Lambert Law:

$$\frac{I_0}{I} = e^{-Ecl} \quad (3.2)$$

normally written as:

$$\log_{10} \frac{I_0}{I} = E \times c \times l \quad (3.3)$$

I - intensity of transmitted light

I_0 - intensity of incident light

E - molecular extinction coefficient

c - molar concentration [mol/L]

l - pathlength of sample

and the quantity $\log_{10} \frac{I_0}{I}$ is known as the absorbance or optical density of the sample.

3.3 Electronic paramagnetic resonance (EPR) spectroscopy

EPR spectroscopy, also referred to as electron spin resonance (ESR) spectroscopy, is a remarkably useful form of spectroscopy used to study molecules or atoms with an unpaired electron, in contrast to a spectroscopy that measure the energy difference between atomic or molecular states.

The power of EPR spectroscopy relies on the sensitivity of spectral shapes to the mobility of the label in the nanosecond time window described by the rotational correlation time (τ), a parameter that can be obtained by spectral simulation. Indeed, the magnetic hyperfine interaction between the electron spin and the ^{14}N nucleus is highly anisotropic. This

anisotropy is averaged fully when the radical is highly mobile and the spectrum displays three narrow lines. When the mobility decreases, the averaging becomes partial and the lines broaden progressively until reaching the limit of a fully anisotropic spectrum, corresponding to an immobilised spin label. A spectral modification thus represents a change in the environment of the label affecting its mobility and, thus, indicates a structural transition [97].

The absorption of energy causes a transition of an electron from a lower energy state to a higher energy state under the radiation in the 8 – 12 GHz range. Unlike most traditional spectroscopy techniques, in EPR spectroscopy the frequency of the radiation is held constant while the magnetic field is varied in order to obtain an absorption spectrum. The radiation may be incident on the sample continuously (*i.e.* continuous wave, abbreviated c_w) or pulsed. As shown in Fig. 3.2 the sample is placed in a resonant cavity which admits microwaves through an iris. The cavity is located in the middle of an electromagnet and helps to amplify the weak signals from the sample. Resonance is detected by a decrease in the amount of microwave radiation that is being reflected out of the resonator. Reflected microwaves are channeled specifically into the detector by a special component called a circulator. Resonance will be detected at the field strength that corresponds to the energy splitting of the spin states of the unpaired electron. In practice, most of the external components, such as the source and detector, are contained within a microwave bridge control. Additionally, other components, such as an attenuator, field modulator and amplifier, are also included to enhance the performance of the instrument [97, 98].

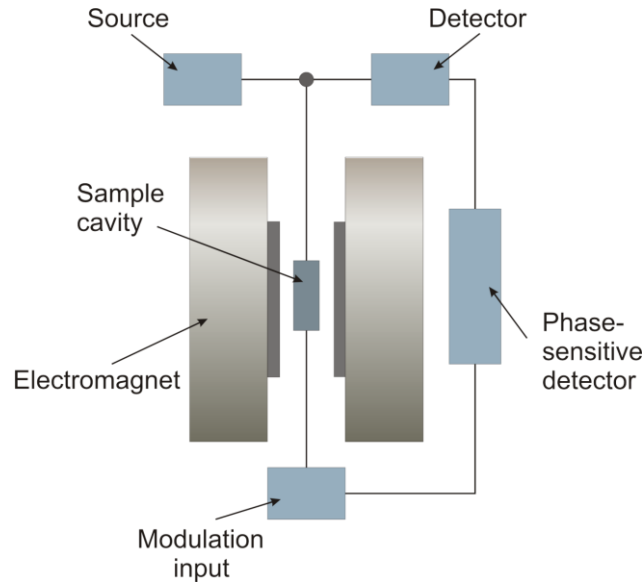


Figure 3.2: Simplified block diagram of a typical EPR spectrometer operating at X-band (8–12 GHz) frequencies [98].

When an external magnetic field is supplied, the spin labels can either orient in a direction parallel ($m_s = -1/2$) or antiparallel ($m_s = +1/2$) to the direction of the magnetic field (Fig. 3.3). This creates two distinct energy levels for the unpaired electrons and allows to measure them as they are driven between the two levels. As the field strength is increased, the energy difference between these two states increases linearly.

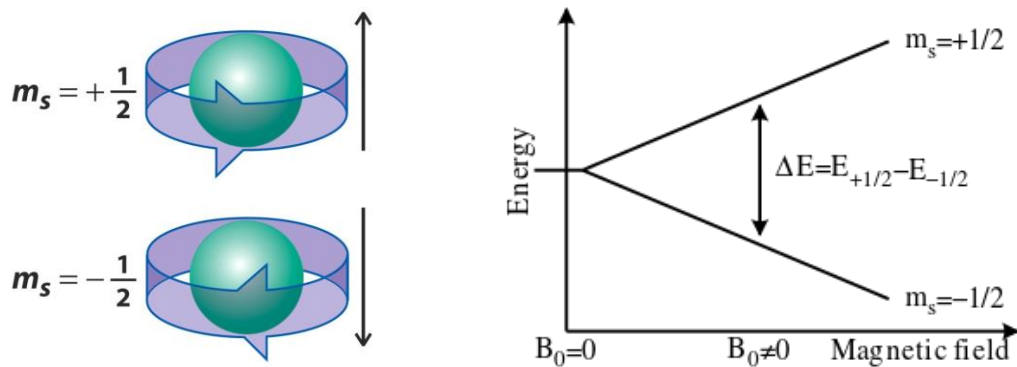


Figure 3.3: Resulting energy levels for an electron spin ($m_s = \pm 1/2$) in an applied magnetic field (B).

Single unpaired electron behaves like a small magnetic bar when placed in a large magnetic field. It will orient itself parallel to the large magnetic field. At a particular magnetic field intensity, the microwave irradiation will induce unpaired electrons to orient against the large magnetic field. This effect will cause Zeeman splitting, when the energy difference (ΔE)

between the two spin states of the electron therefore corresponds to the microwave part of the electromagnetic spectrum and is described by equation:

$$\Delta E = h\nu = g \cdot \beta \cdot B_0 \quad (3.4)$$

ΔE – energy difference [J]

h – Planck constant [6.625×10^{-34} Js]

ν – frequency of electromagnetic radiation [s^{-1}]

g – Zeeman spectroscopy splitting factor

β – Bohr magneton [9.27×10^{-24} J/T]

B_0 – magnetic field strength [T]

These transitions are observed as the absorption of a portion of the microwave intensity. Since these absorptions are fairly broad, an accurate measure of the spacing between the peaks is usually obtained by examining the first-derivative spectrum. Therefore, EPR spectra are conventionally recorded as the rate of change of absorption versus field strength and are conventionally measured as the first derivative (dA) of the absorbance (A) as a function of frequency (ν). The relationship between A and dA is shown diagrammatically in Fig. 3.4.

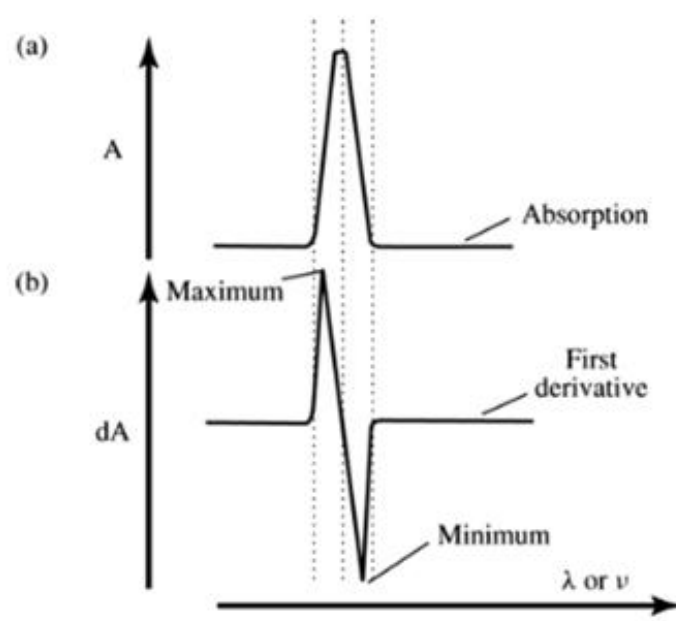


Figure 3.4: EPR spectra recorded as first derivatives of absorption: a) an absorbance spectrum as a plot of absorbance (A) versus frequency (ν), b) a first derivative plot of rate of

change of absorbance (A). The maximum and minimum points of this plot correspond to the half-way points of spectrum [99].

Since the mobility of a spin label covalently attached to a macromolecule is influenced by its microenvironment, analysis of the EPR spectra provides a powerful tool for investigating a variety of applications including: oxidation and reduction processes, bi-radicals and triplet state molecules, reaction kinetics, as well as numerous additional applications in biology, medicine and physics [100].

3.4 Zeta potential (ZP)

ZP represents an electro-kinetic potential, a property that all materials possess, or acquire, when suspended in a fluid and can be used to determine surface isoelectric points (pI) and quantify a change in surface ionisable groups. [101, 102]. In general, electro-positivity at or above +25 mV is used as an arbitrary threshold of low or high- charged surfaces that contributes to suspension stability in colloidal systems [103].

A particle dispersed in a liquid is solvated and the extent of the solvated layer affects the distribution of ions surrounding it, resulting in an increased concentration of counter ions. Consequently, an electric double layer (Fig. 3.5) is formed. This layer consists of two parts: an inner region of strongly bound ions known as the Stern layer and an outer layer of loosely associated ions called the diffuse layer [104, 105]. Within the diffuse layer there is a notional boundary inside which the ions and particles form a stable entity. When a particle moves (e.g. due to gravity), ions within the boundary move with it, but any ions beyond the boundary do not travel with the particle. This boundary is called the surface of hydrodynamic shear or slipping plane. The potential that exists at this boundary is known as the ZP.

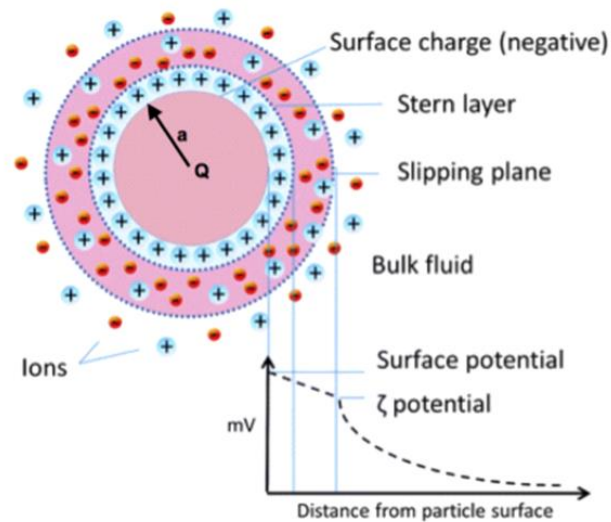


Figure 3.5: Schematic representation of the distribution of ions around a homogeneously charged particle [105].

The ZP is not strictly a phase-boundary potential because it is developed wholly within the fluid region. By measuring the streaming potential and the pressure difference, the zeta potential can be derived using the Smoluchowski equation:

$$ZP = \frac{\Delta U}{\Delta p} \times \frac{L}{Q} \times \frac{\eta}{\varepsilon \times \varepsilon_0} \quad (3.5)$$

$$\frac{L}{Q} = \kappa \times R \quad (3.6)$$

ZP – zeta potential [mV]

ΔU – streaming potential change [mV]

Δp – pressure loss [Pa]

L – length of the flow channel [m]

Q – cross-section of the flow channel [m²]

η – dynamic viscosity of the electrolyte [Pa s]

ε – dielectric constant of the electrolyte solution [C/Vm]

ε_0 – permittivity of vacuum [C/Vm]

κ – conductivity of electrolyte [$\Omega^{-1}m^{-1}$]

R – electrical resistance [Ω]

Changes in the ZP in the presence of polymers may be caused by three different effects, involving: i) the presence of charges arising from the polymer-dissociated functional groups in the by-surface layer of the solid, ii) the shift of the slipping plane by the macromolecules grafted on the polymer surface, or iii) a displacement of the counter-ions in the Stern layer, as result of the polymer grafting [106].

3.5 Potentiometric titration

In a titrimetric methods of analysis, the volume of titrant reacting stoichiometrically with a titrand provides quantitative information about the amount of analyte in a sample. The volume of titrant corresponding to this stoichiometric reaction is called the equivalence point. Experimentally we determine the titration's end point using an indicator that changes color near the equivalence point. Alternatively, we can locate the end point by continuously monitoring a property of the titrand's solution – absorbance, temperature and potential are typical examples – that changes as the titration progresses [107].

One method for determining the equivalence point of an acid–base titration is to use a pH electrode to monitor the change in pH during the titration.

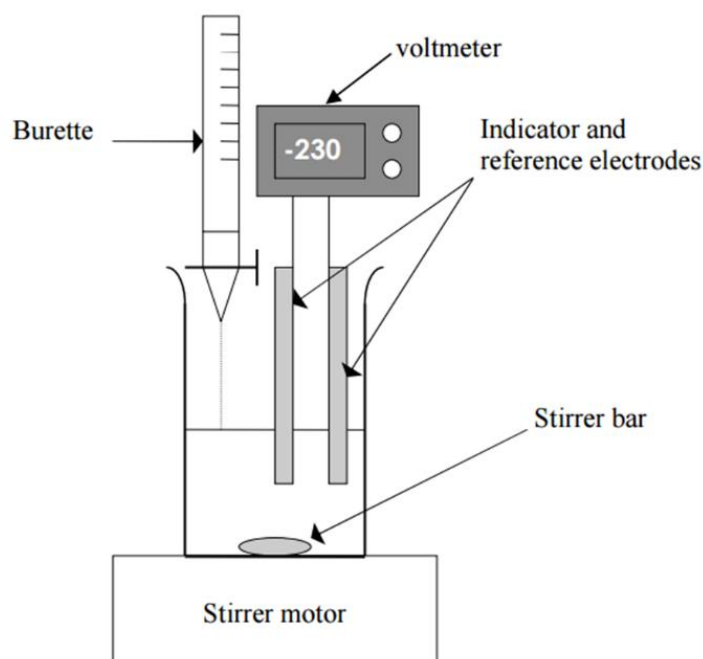


Figure 3.6: Typical apparatus for potentiometric titration [108].

As shown in Fig. 3.6, the voltmeter is used to determine the difference between the potential of two electrodes. The potential of one electrode – the working or indicator electrode, responds to the analyte's activity, and the other electrode – the counter or reference electrode has a known, fixed potential. A relationship between this potential and the incremental volume of the added acid can be established to quantify the present charge group and their respective pKa values in the analysed sample. The addition of titrant in analyte solution (dispersion) causes a pH change, being monitored with calibrated pH sensitive glass electrode [93].

In the titration system, as described above, the ionic species present are H^+ , OH^- , their counter ions K^+ and Cl^- , as well as the species of interest, denoted as A_k^n , where n is the charge number and k is the enumerator.

The total number of charge species Q , due to the presence of A_k^n is calculated using the electro-neutrality condition according to equation:

$$Q = FV_t A = FV_t ([Cl^-] - [K^+] + [OH^-] - [H^+]) \quad (3.7)$$

$$A = \sum_k n [A_k^n] \quad (3.8)$$

Q – total number of charged groups [mol/L]

V_t – total volume of titrating system [L]

F – Faraday's constant [9.649×10^4 C/mol]

A_k – conjugate species of analyte

n – charge number

k – enumerator

The K^+ and Cl^- ions concentration is known from the added volume and concentration of the burette solution, while H^+ and OH^- ions are determined by pH. By including the concentration of K^+ and Cl^- ions from the blank titration (absence of analyte and contaminations), final number of charges can be calculated.

The pKa values for each material can be thus calculated from the plateau region of the charging isotherm by the following equation:

$$pH = pK - \log\left(\frac{Q}{1-Q}\right) \quad (3.9)$$

3.6 Attenuated total reflectance – Fourier transform infrared (ATR-FTIR) spectroscopy

Vibrational spectroscopic techniques, both Raman and Infrared absorption, have significant potential in the field of biomedical analysis, as they can give spatially resolved biochemical information without the use of extrinsic labels and without being invasive or destructive to the system studied. While traditional infrared (IR) spectrometers have been used to analyse samples by means of transmitting the infrared beam directly through the sample, ATR-FTIR spectroscopy uses the reflectance of the sample instead. An ATR-FTIR measures the change that occurs in a totally internally reflected infrared beam when the beam comes in contact with sample [109]. The infrared beam hits an optically dense crystal (*i.e.* diamond, zinc selenide or germanium) which then creates an evanescent wave that subsequently protrudes the sample (0.5 – 5 μm). The regions where sample absorbs energy, the evanescent waves are attenuated. The altered (attenuated) energy from each evanescent wave is passed back to the IR beam, which then exits the opposite end of the crystal and is directed at the detector in the IR spectrometer. The detector records the attenuated IR beam as an interferogram signal, which can then be used to generate an infrared spectrum. With ATR sampling the IR beam is directed into a crystal of relatively higher refractive index. The IR beam reflects from the internal surface of the crystal and creates an evanescent wave which projects orthogonally into the sample in intimate contact with the ATR crystal. Some of the energy of the evanescent wave is absorbed by the sample and the reflected radiation (some new absorbed by the sample) is returned to the detector [110]. This ATR phenomenon is shown graphically for a single reflection ATR in Fig. 3.7.

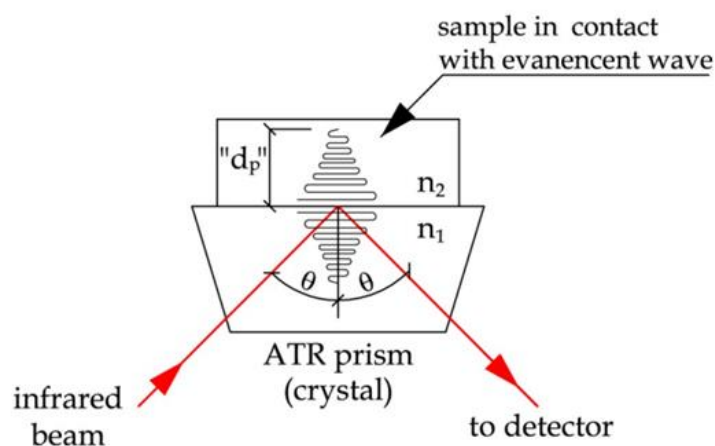


Figure 3.7: Schematic representation of the sampling mode for ATR FTIR spectroscopy.

3.7 High pressure liquid chromatography – Size exclusion chromatography (HPLC-SEC)

SEC is a standard technique for determining molar mass averages and molar mass distributions of polymers. Sometimes the terms gel permeation chromatography (GPC) or gel filtration chromatography (GFC) are also used, but SEC should be preferred, because this term describes the mechanism much better: polymer molecules are separated according to their hydrodynamic volumes (which can be correlated with molar mass), with the larger size molecules exiting first followed by the smaller, as presented in Fig. 3.8. Molar masses are determined either from a calibration or using molar mass sensitive detectors [111]. The major application of SEC is rapid determination of molecular weight (MW) and MW distribution. Beside of this, SEC is commonly applied for separation of low from high MW fractions, homologs and oligomers [112].

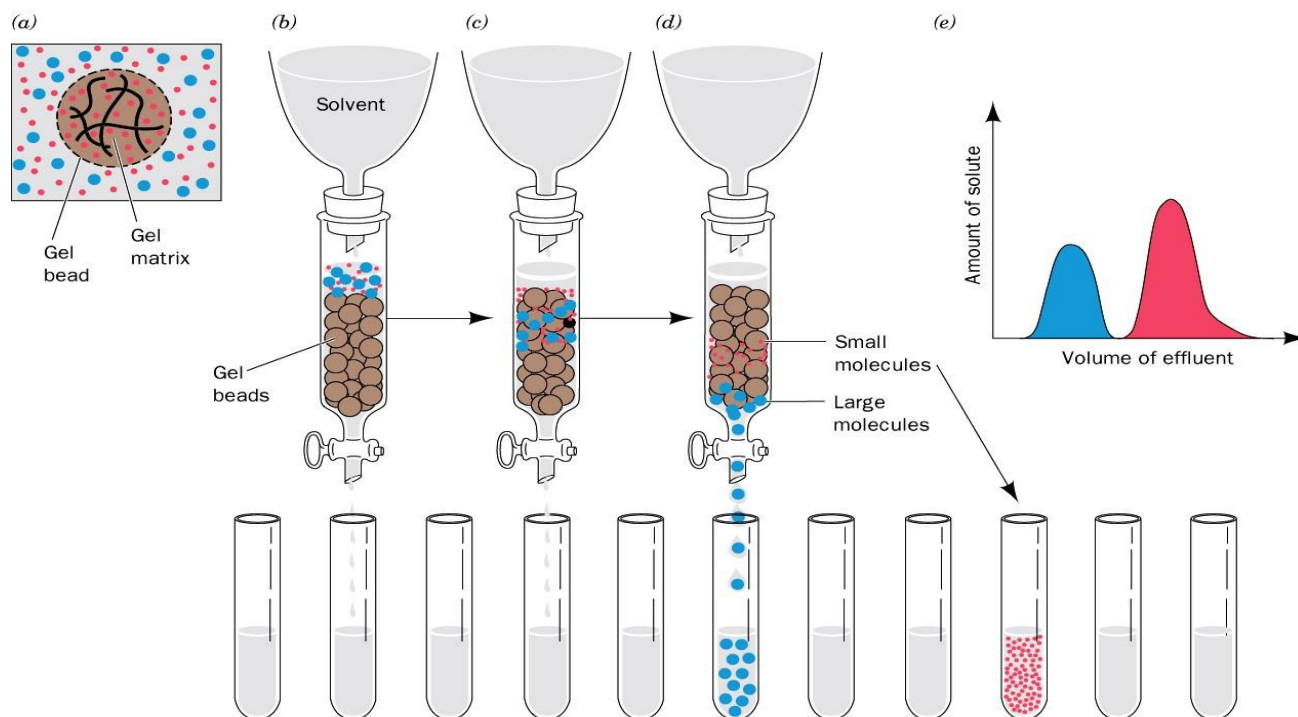


Figure 3.8: Schematic presentation of behaviour of the molecules of different sizes using SEC.

3.8 Capillary zone electrophoresis (CZE)

Capillary electrophoresis (CE) is a special case of using an electrical field to separate the components of a mixture. It is performed in a capillary tube and is the most efficient separation technique available for the analysis of both large and small molecules.

The basic instrumental set-up, which is illustrated in Fig. 3.9, consists of a high voltage power supply (0 to 30 kV), a fused silica (SiO_2) capillary, two buffer reservoirs, two electrodes, and an on-column detector. Sample injection is accomplished by temporarily replacing one of the buffer reservoirs with a sample vial. A specific amount of sample is introduced by controlling either the injection voltage or the injection pressure [113].

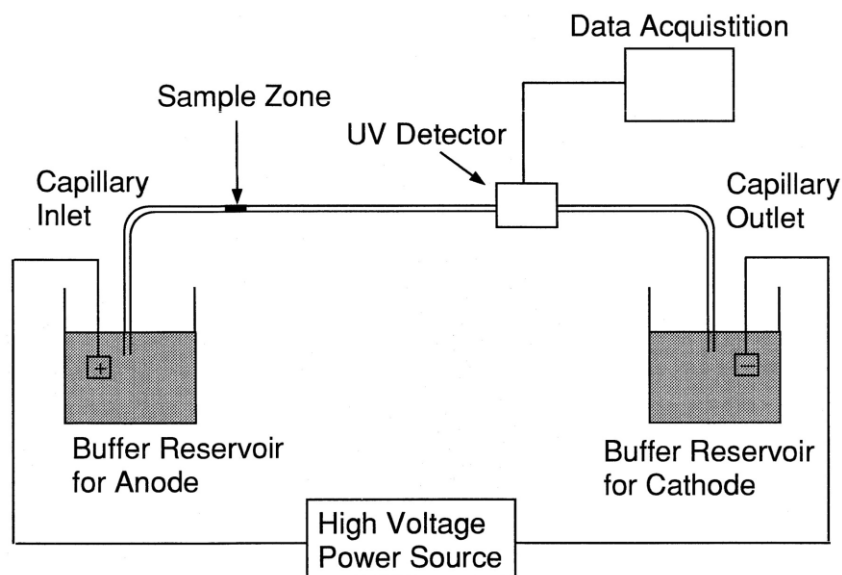


Figure 3.9: A schematic representation of the arrangement of the main components of a typical CE instrument [113].

Capillary zone electrophoresis (CZE) is the simplest form of CE. In this mode sample is applied as a narrow zone (band), which is surrounded by the separation buffer. As an electric field is applied, each component in the sample zone migrates according to its own apparent mobility. Ideally, all sample components will eventually separate from each other to form individual zones of pure material. However, neutral molecules cannot be separated because they migrate at the velocity of electroosmotic flow. The separation of charged molecules is accomplished most efficiently when differences among the apparent velocities of the components are maximized and random dispersion of the individual zones is minimized [114]. The apparent migration time of a sample component, t_{app} , is the time required for the component to move from the beginning of the capillary to the detection window; it can be calculated from the distance between the sample inlet and the detection window, L_d , and the apparent velocity:

$$t_{app} = \frac{L_d}{v_{app}} = \frac{L_d}{\mu_{app}E} \quad (3.10)$$

v_{app} – apparent velocity

μ_{app} – apparent mobility

L_d – distance between the sample inlet and the detection window

E – electric field strength

3.9 Antimicrobial susceptibility testing

To measure the efficacy of antimicrobial-treated substrates, test methods used under controlled conditions for reproducible results are categorized into quantitative and qualitative. Quantitative methods involve actual microbe enumeration, with results reported as a percent or log reduction in the contamination level. Qualitative methods are subjective, using ratings and measured zones of inhibition [115].

The most known and basic methods are the disk-diffusion and broth or agar dilution methods, which have been standardized by the Clinical and laboratory standards institute (CLSI). To further study the antimicrobial effect of an agent in depth, time-kill test and flow cytometric methods are recommended, which provide information on the nature of the inhibitory effect (bactericidal vs. bacteriostatic; time-dependent vs. concentration-dependent) and the cell damage inflicted to the test microorganism [116].

3.9.1 Disk-diffusion method

Disk diffusion is one of the oldest and the most widely used approaches to antimicrobial susceptibility testing – originally described in 1966, when Bauer et al. tested all the variables used in the procedure, such as the media, temperature, and depth of agar [117] and so describe the test that is used today. National committee for clinical laboratory standards (NCCLS) adopted the basic procedural steps in the Bauer paper as the disk diffusion reference method. It is suitable for testing the majority of bacterial pathogens, is versatile in the range of antimicrobial agents that can be tested and requires no special equipment.

A growth medium, usually Mueller-Hinton agar (MHA), is first evenly seeded throughout the plate with the bacterial isolate of interest that has been diluted at a standard concentration (0.5 McFarland, corresponding to approximately 1.5×10^8 CFU/mL). Commercially prepared disks, each of which are pre-impregnated with a standard concentration of a particular antimicrobial, are then evenly dispensed and lightly pressed onto the agar surface. The antimicrobial agent immediately begins to diffuse outward from the disks, creating a

gradient of agent concentration in the agar such that the highest concentration is found close to the disk with decreasing concentrations further away from the disk. After an overnight (or time dependent) incubation, the bacterial growth around each disc is observed.

The zone around disk that has no growth is referred to as the zone of inhibition since this approximates the minimum antimicrobial concentration sufficient to prevent growth of the test isolate. This zone is then measured in mm and compared to a standard interpretation chart used to categorize the agent as susceptible, intermediately susceptible or resistant.

It has been reported that this method is not always reliable for determining the antimicrobial activity of natural antimicrobials, such as plant extract [118], because the polarity of natural compounds can affect the diffusion of compounds onto the culture medium. Compounds with less polarity diffuse slower than more polar ones [119].

3.9.2 Dilution method (broth or agar dilution method)

Compared with disk diffusion method, agar dilution and broth microdilution are quantitative methods, able to determine the minimal inhibitory concentration (MIC). The MIC of an antimicrobial agent is the lowest (*i.e.* minimal) concentration of the antimicrobial agent that inhibits a given bacterial isolate from multiplying and producing visible growth in the test system. The concentration is determined in the laboratory by incubating a known quantity of bacteria with specified dilutions of the antimicrobial agent. Using NCCLS interpretive criteria the results are interpreted as susceptible, intermediate, or resistant. Microdilution testing uses about 0.05 to 0.1 mL total broth volume and can be conveniently performed in a microtiter format. Macrodilution testing uses broth volumes at about 1.0 mL in standard test tubes. MIC tests can be performed using broth or agar media, but broth microdilution is the most widely used method in clinical laboratories.

The test is only valid if the positive control shows growth and the negative control shows no growth. Agar dilution method follows the principle of establishing the lowest concentration of the serially diluted antibiotic concentration at which bacterial growth is still inhibited.

3.9.3 Shake flask test

Standard test method for determining the antimicrobial activity of immobilized antimicrobial agents is designed to evaluate the resistance of non-leaching antimicrobial treated

specimens to the growth of microbes under dynamic contact conditions. This dynamic shake flask test was developed for routine quality control and screening tests in order to overcome difficulties in using classical antimicrobial test methods to evaluate substrate-bound antimicrobials.

Immobilized antimicrobial agents, such as surface bonded materials, are not free to diffuse into their environment under normal conditions of use. Shake flask test ensures good contact between the bacteria and the treated fiber, fabric, or other substrate by shaking samples in a concentrated bacterial suspension for a one hour contact time or other contact times as specified by the investigator. The suspension is serially diluted both, before and after contact, and cultured. The number of viable organisms in the suspension is determined and the percent reduction is calculated based on initial counts or on retrievals from appropriate untreated controls using Eq. 3.11. Results can be presented in either percent reduction when measuring CFU/mL or as a death rate constant when calculating mean \log_{10} density of bacteria [120].

$$\text{Reduction, \% (CFU/mL)} = \frac{B - A}{B} \times 100 \quad (3.11)$$

$$\text{Death Rate Constant (mean } \log_{10} \text{ density)} = B - A \quad (3.12)$$

A - CFU per milliliter (or mean \log_{10} density of bacteria) for the flask containing the treated substrate after the specified contact time

B - "0" contact time CFU per milliliter (or mean \log_{10} density of bacteria) for the flask used to determine "A" before the addition of the treated substrate.

3.10 Cell viability assays

Cell viability assays are effective and very useful tool to assess the cytotoxicity of substrate. Cells exposed to a cytotoxic compound can respond in a number of ways; the cells may undergo necrosis, in which they lose membrane integrity and die rapidly as a result of cell lysis; they can stop growing and dividing; or they can activate a genetic program of controlled cell death, termed apoptosis. It is well accepted that most antimicrobial polymers

such as quaternary ammonium/phosphonium polymers act by a disruptive interaction on the cell wall at the lipid interface [121].

The cell viability assay is using specific fluorescent dyes that can stain certain cell constituents such as DNA, RNA and nucleic acids, thus assess cell physiology. Bacterial viability tests are often performed with premixed, ready for use, dual staining kits, such as the commercially known BacLight™ (**Live/Dead bacterial viability** kit, L-7007, Molecular Probes), having the capability of monitoring the viability of the bacteria as a function of the cell's membrane integrity. The lysis process in a cell can be monitored with these stains by counting the number of intact and permeable cells at different time points [122, 123]. Advantages are a rapid procedure, quantitative analyses, as well as the possibility to measure using various instruments such as flow cytometer, microplate reader and microscope [124]. The Live/Dead BacLight kit utilizes a mixture of SYTO 9, which has a green fluorescent colour, and propidium iodide (PI), which gives a red fluorescent colour. These stains differ both in their spectral characteristics and in their ability to penetrate healthy cells. When used alone, the SYTO 9 stain generally all bacteria in a population – those with intact membranes and those with damaged membranes. In contrast, PI penetrates only bacteria with damaged membranes, causing a reduction in the SYTO 9 stain fluorescence when both dyes are present [124]. Viable bacteria (green) and dead bacteria (red) can be distinguished under a fluorescence microplate reader [125]. The excitation/emission maxima for these dyes are about 480/500 nm for SYTO 9 and 490/635 nm for PI. The background remains virtually nonfluorescent. The fluorescence from both live and dead bacteria may be viewed simultaneously with any standard fluorescein longpass filter set.

Conditions required for measurement of fluorescence in microplate readers are very similar to those required for fluorescence spectroscopy of bacterial cell suspensions.

As in fluorescence spectroscopy experimental protocols, reagent concentrations are the same as those recommended for fluorescence microscopy, and the ratio of green to red fluorescence emission is proportional to the relative numbers of live bacteria.

On the other hand, the assay is used to evaluate the **toxicity to mammalian cells**. Cells are seeded at a density of 10^5 /mL into petri dishes, and grown to a confluency of 70 – 80 %. PI is a membrane-impermeable dye which intercalates with the DNA. Its uptake is therefore an

indication for the loss of membrane integrity, a hallmark of necrotic cell death. In contrast, nuclear condensation (pyknosis) is characterized by condensed chromatin and cell shrinkage, a hall mark of apoptosis [126]. The formation of apoptotic bodies can therefore be assessed by the use of fluorochrome. Both, apoptotic and necrotic cell death provide therefore detailed information regarding cell viability and potential cytotoxic effects.

The **MTT** (3-(4,5-dimethylthiazol-2-yl)-2,5-diphenyltetrazolium bromide) tetrazolium reduction assay is the first homogeneous cell viability assay developed for a 96-well format that is suitable for high throughput screening. Viable cells with active metabolism convert MTT into a purple colored formazan product with an absorbance maximum near 570 nm (Fig. 3.10). When cells die, they lose the ability to convert MTT into formazan, thus color formation serves as a useful and convenient marker of only the viable cells. [127].

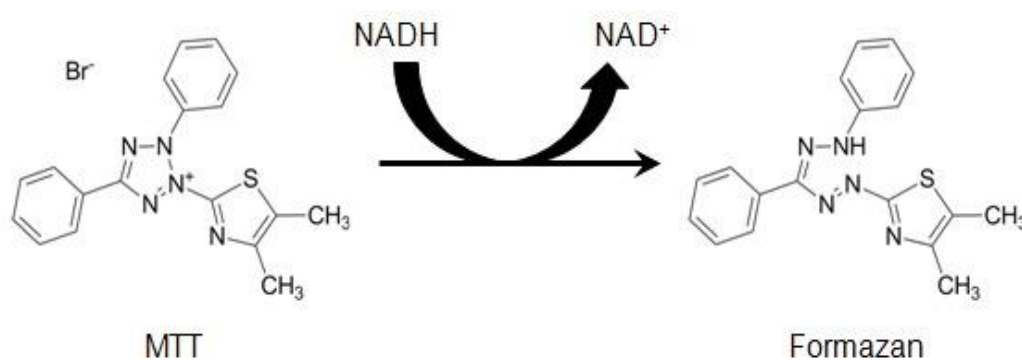


Figure 3.10: Structures of MTT and colored formazan product [127].

3.11 Fluorescence microscopy (FM)

Fluorescence imaging uses high intensity illumination to excite fluorescent molecules in the sample. The sample can either be fluorescing in its natural form like chlorophyll and some minerals, or treated with fluorescing chemicals. FM combines the magnifying properties of the light microscope with fluorescence technology that allows the excitation and detection of emissions from fluorophores - fluorescent chemical compounds [128].

The microscope has a filter that only lets through the radiation with the desired wavelength that matches the fluorescing material. The radiation collides with the atoms in the specimen

and electrons are excited to a higher energy level. When they relax to a lower level, they emit the light. To become visible, the emitted light is separated from the much brighter excitation light in a second filter. Here, the fact that the emitted light is of lower energy and has a longer wavelength is used. The fluorescing areas can be observed in the microscope and shine out against a dark background with high contrast.

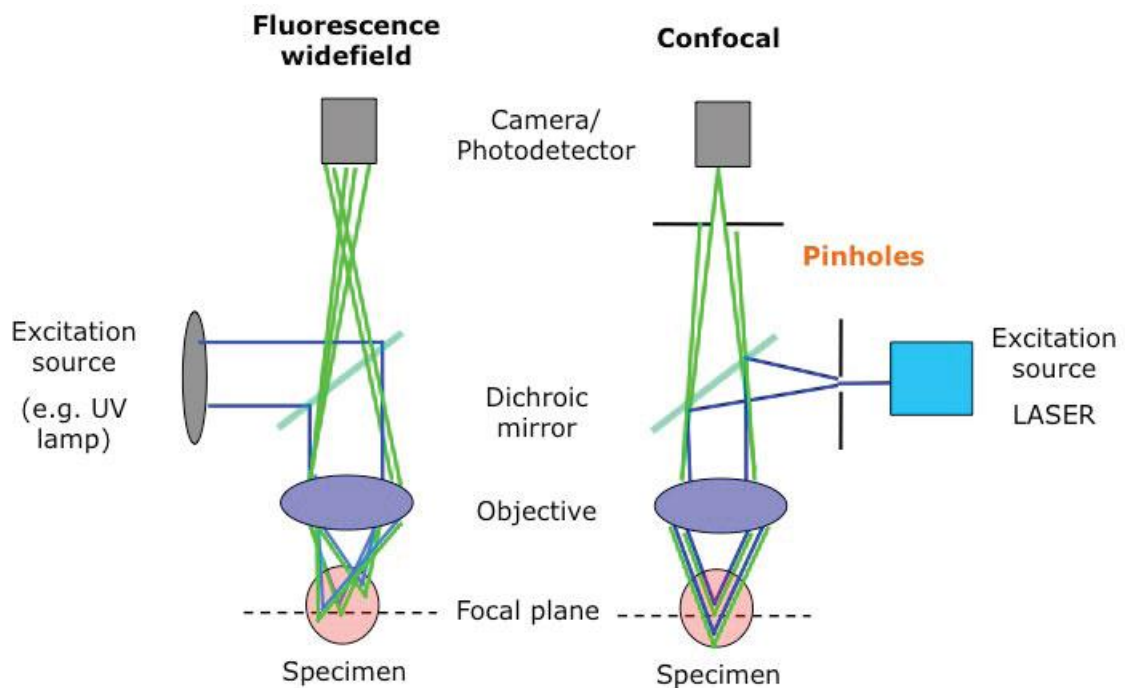


Figure 3.11: Schematic presentation of the typical configuration of fluorescence microscope (wide field) in comparison with confocal fluorescence. Two pin holes used in the confocal geometry restrict the field of view to a single point on the focal plane.

As an improvement of ordinary FM, confocal fluorescence microscopy (CFM) allows imaging of thin optical sections through sample volume, while furthermore fluorescence microspectroscopy can differentiate between labels with substantially overlapping spectra with the ability of microspectroscopic analysis. This added feature is provided by positioning of narrow-band liquid crystal tunable filter (LVTF) in front of a sensitive camera/photodetector (Fig. 3.11). When used in a combination with fluorescence proteins, CFM enables collection of optically sectioned high-resolution images of samples.

4 EXPERIMENTAL PART

The experimental work can be divided in two parts. The first part was focused on the analysis of two different protein-based substrates (wool and GEL) in terms of the presence of functional groups suitable for the activation and grafting of ϵ PL and OAK. In that sense, the mechanisms and quantity as well as durability of grafted ϵ PL/OAK was determined by using different spectroscopic (ATR-FTIR, UV-Vis, fluorescence) and/or separation (HPLC-SEC, CE) techniques. Special emphasis was given to the identification of orientation of immobilized ϵ PL/OAK by using EPR spectroscopy. The surface activity (functional groups) and hydrophobicity of the substrate were evaluated by titration technique and ZP measurements. The second part of the research was focused on the analysis of the substrates related to their antibacterial properties against Gram-negative *Escherichia coli* (*E. Coli*) bacteria and Gram-positive *Staphylococcus aureus* (*S. aureus*) bacteria, as well as cytotoxicity by using human osteoblasts cells (hFOB).

4.1 Materials

Table 4.1: Materials used

Material:	Purchased from	Characteristics
SUBSTRATES and AMPs		
knitted wool fabric	Lokateks d.o.o. (Slovenia)	fine rib 1:1 knit with a mean fibre 23.5 μm diameter and 230 g/m^2 mass/unit area
gelatine (GEL) type B extracted from bovine skin	Sigma Aldrich (Germany)	MW of 47.0 kDa PDI = 2.3 pI at pH 5
ϵ -poly-L-lysine (ϵ PL)	Zhengzhou Bainafo Bioengineering (China)	MW of 9.1 kDa
oligo-acyl-lysyl (OAK, K-7 α_{12} -OH)	produced by the solid-phase peptide synthesis method and purified to homogeneity by HPLC	MW of 2.4 kDa

CROSS-LINKING AGENTS		
EDC (1-ethyl-3-(3-dimethylaminopropyl)-1-carbodiimide hydrochloride)	Sigma Aldrich (Germany)	MW of 191.7 kDa
sulfo-NHS (sulfo-N-hydroxysuccinimide)		MW of 217.1 kDa
tissue transglutaminase (TGase; a protein-glutamine γ -glutamyl-transferase, EC 2.3.2.13) from a guinea-pig's liver		3.1 U/mg
LABELLING AGENTS (reactive dyes)		
2,4,6-trinitrobenzenesulfonic acid (TNBS)	Sigma-Aldrich (Germany)	MW of 293.2 kDa
fluorescein-5-isothiocyanate (FITC)		MW of 389.4 kDa
3-maleimido-2,2,5,5-tetramethyl-1-pyrrolidinyl-oxyl (3-maleimido-PROXYL) spin label		MW of 237.3 kDa
MTT (3-(4,5-dimethylthiazol-2-yl)-2,5-diphenyltetrazolium bromide)		MW of 414.3 kDa
Acid Orange 7 (AO7) dye	Sigma Chemicals (USA)	for colorimetric quantification of the graft yield
Coomassie Brilliant Blue G-250 dye		
Live/Dead BacLight kit consisting of a SYTO 9 dye and Propidium Iodide (PI)	Sigma Aldrich (Germany)	for bacterial viability testing

BACTERIAs and CELLS		
<i>Escherichia coli</i> (ATCC 35218)	the American type culture collection (ATCC)	Gram-negative bacteria
<i>Staphylococcus aureus</i> (ATCC 25923)		Gram-positive bacteria
human osteoblast cells (hFOB; ATCC CRL-11372)	LGC Standards (UK)	/
BUFFERS, SOLVENTS and OTHER CHEMICALS		
dichloromethane, ethanol, methanol, octanol and other solvents	Sigma Aldrich (Germany)	of analytical grades and used without further purification
non-ionic surfactant Dehaclin WP 20	CHT/Bezema (Germany)	/
double distilled water	/	purified using a Milli-Q direct water purification system (Millipore Direct 8) with resistivity of 18.2 M Ω .cm
Spectra/Por dialysis membranes	Thermo Fisher Scientific (USA)	from regenerated cellulose MWCO (molecular weight cut off) of 2 kDa

4.2 Methods

4.2.1 Functionalisation of substrate

PRE-TREATMENT OF WOOL SAMPLES

To improve the availabilities of functional groups for covalent attachment of ϵ PL/OAK, the wool was extracted sequentially with dichloromethane according to the ISO 3074:2014 standard [129], followed by rinsing with Milli-Q water and dried at 40 °C to remove surface lipids and contaminants. Such wool was marked as a reference sample (Ref WO) and was used in all further treatments.

FUNCTIONALISATION OF WOOL WITH ϵ PL/OAK

Wool has an pI at pH of ~ 4.9 (confirmed by potentiometric titration), that offers many reactive sites for its functionalisation with ϵ PL/OAK. The functionalization was performed by chemical approach using EDC/NHS reagents as well as by enzymatic approach using TGase, as schematically presented in Fig. 4.1.

According to the chemical approach, two different coupling routes were thus applied, being generally available in the synthesis of peptide-polymer conjugates using water-soluble EDC and NHS as zero-length and site-specific reaction-mediators [130, 131]. The carboxyl groups (-COOH) in the C-terminal of the wool (*grafting-from*) or ϵ PL/OAK (*grafting-to*) were converted into an unstable amino-reactive intermediate (O-acylisourea) that reacted readily with the available and non-protonated amino (-NH₂) groups of ϵ PL/OAK or wool (R-NH₂ of Lys or Arg residues), respectively, thus forming a stable amide linkage [89]. As the N-terminal ϵ -NH₂ group of peptide (ϵ PL/OAK) has a higher pK_a (~ 10.5) than their numerous sided α -NH₂ groups (pK_a ~ 9.0), this was used to render the Lys α -NH₂ side groups effectively more nucleophilic and thus highly reactive in its reactions.

In the case of the *grafting-from* approach, 1 g of wool was thus activated with EDC/NHS at a molar ratio of 10:10:1 with respect to the available (*i.e.* dissociated) wool carboxyl groups (~ 585 mmol/kg wool as determined by potentiometric titration) in a 100 mM phosphate buffer of pH 4.5 containing 200 mM NaCl and 50 % methanol for 24 h at 23 °C by constant shaking. The fabrics were then added to an equimolar amount of ϵ PL (5 g/L) or OAK (0.05 g/L) with respect to its amino groups. The ϵ PL (pre-dissolved in Milli-Q water) or OAK (pre-dissolved in methanol) were diluted in 100 mM carbonate-bicarbonate buffer before soaking the wool. In the other way around, *i.e.* the *grafting-to* approach, ϵ PL/OAK were incubated with EDC/NHS at a molar ratio of 10:10:1 with respect to the ϵ PL/OAK acidic groups (~ 8.22 mmol/kg for ϵ PL, determined by potentiometric titration) in 100 mM phosphate buffer of pH 4.5 containing 200 mM NaCl for 2 h at 23 °C by constant shaking. The solutions with an activated terminal carboxylic groups of ϵ PL/OAK were then incubated with 1 g of wool (with respect to an equimolar amount of its basic groups determined by potentiometric titration) previously soaked in 100 mM carbonate buffer of pH 10.5. The incubation was carried out for 24 h at 23 °C by constant shaking. In all cases the samples were post-treated by rinsing in a low pH (pH 2) and high salt concentration (2 M NaCl) to

remove residual (non-reacted or ionically-adsorbed) ϵ PL/OAK, as well as ammonia as a by-product being originated during the chemical reaction.

The enzymatic approach of ϵ PL/OAK grafting was performed by TGase, which catalyzed the reactions between the ϵ -amino groups of ϵ PL and the Gln residues of the wool in a two-step reaction, resulting in the formations of new isopeptide bonds [132]. In the initial step the active site of TGase' Cys binds to the γ -carboxamide of the Gln residue by a thioester bond, forming an acyl-enzyme intermediate which interacts forward with the nucleophilic ϵ -amino group of the Lys residue, accelerating the release of ammonia. For that purpose, 1 g of wool was incubated with 5 g/L of ϵ PL or 0.05 g/L OAK and 2 U of TGase in 100 mM phosphate buffer of pH 7.5 containing 5 mM CaCl_2 for 24 h at 50 °C. The reaction was stopped by heating the samples for 5 min at 95 °C and post-treated according to the same procedure as described above to remove residual (non-reacted or ionically-adsorbed) ϵ PL/OAK as well as the ammonia by-product.

In all types of treatments, parallel experiments were conducted being denoted as reference wools, treated in the same way as other samples but with the reagents (Ref-EDC/NHS) or enzyme (Ref-TGase) only and in the absence of ϵ PL. In addition, the wool was treated with ϵ PL/OAK, but without the reagents or enzyme, being denoted as Ref- ϵ PL or Ref-OAK.

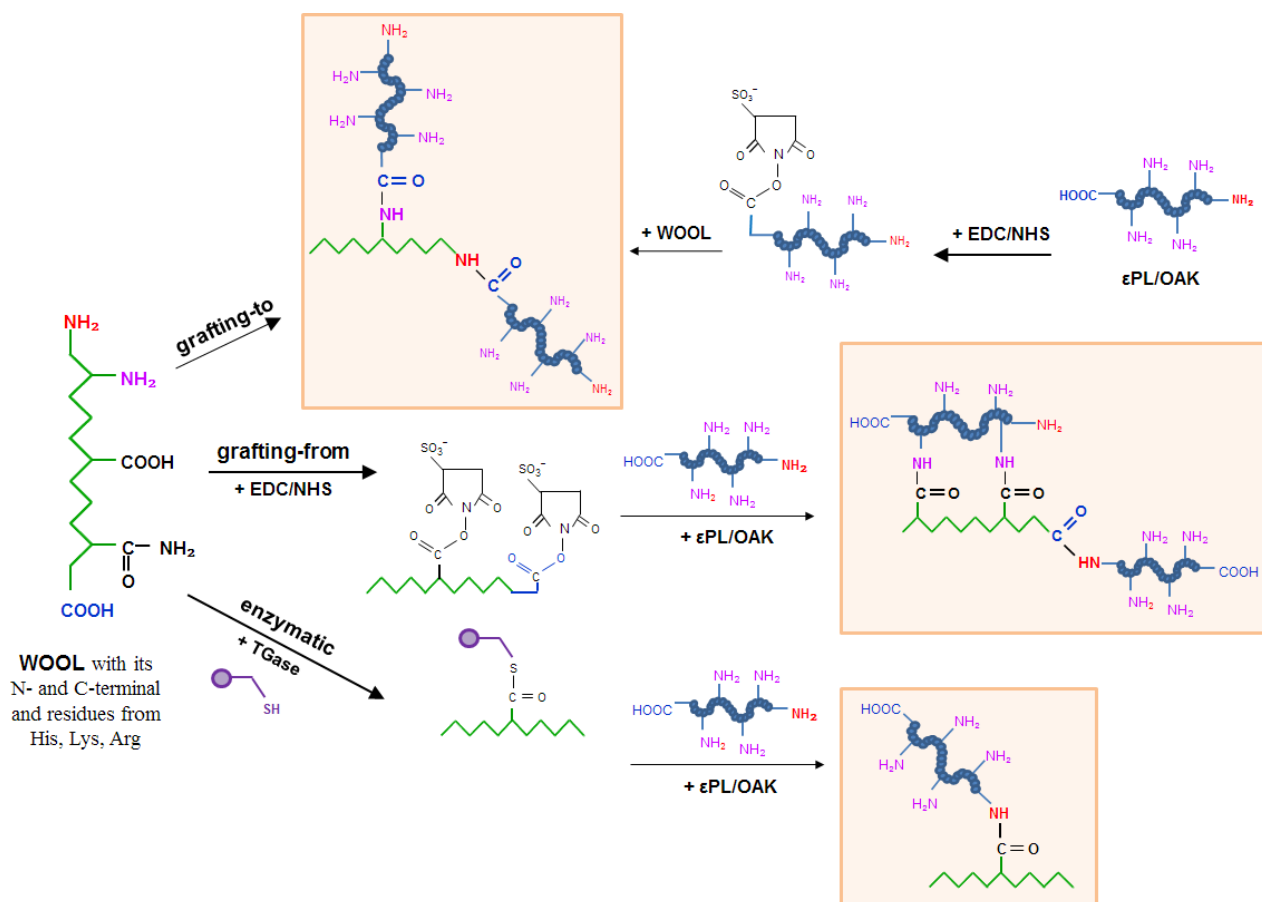


Figure 4.1: Schematic illustration of three routes for εPL/OAK coupling onto the wool using chemical (EDC/NHS, *grafting-to* and *grafting-from*) and enzymatic (TGase) approaches.

FUNCTIONALISATION OF GEL WITH εPL/OAK

GEL was also functionalised with εPL and OAK by using chemical and enzymatic coupling approaches by following the same chemistry as described in 4.2.1, and as presented schematically in Fig. 4.2.

GEL with an pI at pH 5 (determined by potentiometric titration) was - in the case of the *grafting-from* approach - first dissolved at 40 °C in a 100 mM acetate buffer of pH 3 containing 200 mM NaCl (2.5 g/L GEL) and then activated with EDC/NHS at a molar ratio of 10:10:1 with respect to the available (*i.e.* dissociated) GEL carboxylic groups (~0.78 mmol/g, determined by potentiometric titration). The solution was stirred for 1 h before the unreacted and hydrolysed EDC/NHS were removed by dialysis using a Spectra/Por dialysis membrane (Fisher, Germany) with MWCO of 2 kDa against Milli-Q water. The εPL (pre-

dissolved in Milli-Q water) or OAK (pre-dissolved in methanol) were diluted in 100 mM carbonate-bicarbonate buffer of pH 11 to the final concentration of approximately 5 g/L and 0.05 g/L, respectively, before being added to the GEL solution, which caused a pH increase to 6.6. The reaction was left for 24 h under stirring conditions at 40 °C. Conversely, *i.e.* in the *grafting-to* approach, the ϵ PL/OAK was incubated with EDC/NHS at a molar ratio of 10:10:1 with respect to the ϵ PL/OAK carboxyl groups (~ 82 mmol/g for ϵ PL) in 100 mM acetate buffer of pH 3 containing 200 mM of NaCl. Activated ϵ PL/OAK was then added to a 0.25 % solution of GEL, previously dissolved in 150 mM carbonate buffer of pH 11, and incubated under continuous stirring for 24 h at 40 °C. In both cases, the samples were dialysed to remove (non-reacted or ionically-adsorbed) ϵ PL/OAK and reaction by-products such as isourea. The reaction mixtures were dialysed using a Spectra/Por dialysis membrane (Fisher, Germany) with MWCO of 30 kDa for one day against 150 mM NaCl solution with two to three changes, and for an additional three days against Milli-Q water, which was refreshed about six times under stirring until no absorption was observed in the UV-Vis spectrum of the dialysed-out solution. The reaction mixtures were dialysed further against acidic (pH 2) and basic (pH 11) pH medium to remove any electrostatically-bound ϵ PL/OAK.

The enzymatic approach of ϵ PL/OAK grafting using TGase was performed in two-step reaction. In the initial step, the active site of TGase Cys binds to the γ -carboxamide of the Gln residue by a thioester bond, forming an acyl-enzyme intermediate which interacts forward with the nucleophilic ϵ -NH₂ group of the Lys residue of ϵ PL/OAK, accelerating the release of ammonia. For that purpose, GEL (2 g/L) was suspended in a 100 mM acetate buffer of pH 4.5 and mixed with ϵ PL (5 g/L) or OAK (0.05 g/L), previously dissolved in 100 mM carbonate buffer of pH 11 or in methanol, respectively, and re-suspended in 100 mM carbonate buffer of pH 11. The TGase (0.05 U/mg GEL) was added immediately after their mixing. Enzymatic coupling was carried out at pH ~ 7 for 24 h at 40 °C. Control samples were treated without TGase and/or ϵ PL/OAK under the same conditions. The reaction was stopped by heating the samples for 5 min at 95 °C and post-treated according to the same procedure as described above to remove (non-reacted or ionically-adsorbed) ϵ PL/OAK, as well as ammonia as a reaction by-product.

In all types of treatments, parallel experiments were conducted being denoted as reference GEL (Ref GEL), GEL treated in the same way but with the reagents (Ref GEL+EDC/NHS) or

enzyme (Ref GEL+TGase) only and in the absence of ϵ PL/OAK, and GEL treated with (unlabelled or FITC-labelled) ϵ PL/OAK but without the reagents or enzyme (Ref ϵ PL-FITC, Ref OAK). In addition, the ϵ PL/OAK was treated with the reagents only, being denoted as Ref ϵ PL-FITC+EDC/NHS and Ref OAK+EDC/NHS.

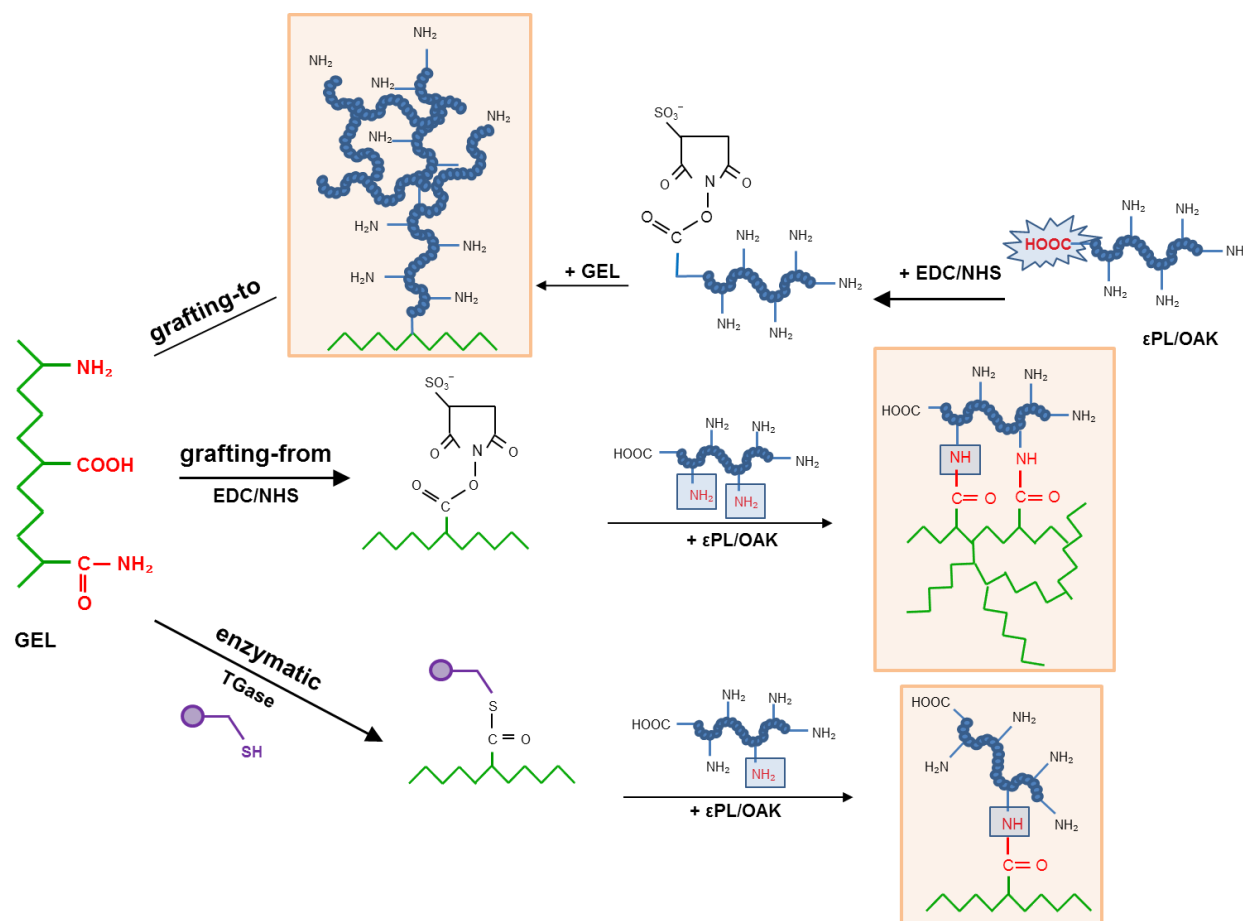


Figure 4.2: Schematic illustration of ϵ PL/OAK coupling onto the GEL using chemical (EDC/NHS, *grafting-to* and *grafting-from*) and enzymatic (TGase) approaches.

4.2.2 Evaluation of the efficacy of substrate functionalisation

COLORIMETRIC EVALUATION OF WOOL/GEL SAMPLES BY ITS STAINING WITH ANIONIC DYES, AND INDIRECT QUANTIFICATION OF AMINO GROUPS

The ϵ PL/OAK deposition on the wool was evaluated directly (colorimetric evaluation of the wool) and indirectly (dye concentration evaluation in the treating solutions) after its staining with two acids dyes (Coomassie Brilliant Blue G–250 and AO7) being related to Van der Waals attractions and ionic interactions between the dye's sulphonate groups ($-\text{SO}_3^-$) and

the available weak base protonated groups ($-\text{NH}_3^+$) of wool protein (arising from side groups of His, Lys, Arg and the $\alpha\text{-NH}_2$ groups at the chain ends) [133], in acidic mediums.

The staining of the wool with an already prepared pre-mixed solution of Coomassie Brilliant Blue G-250 was performed at 50 °C for 30 min using a liquor-to-fabric ratio of 15:1, followed by washing with distilled water for two cycles and then dried at room temperature [134]. The Reflectance (R) of the dyed fabrics was measured using an SF 600+ (Datacolor) Spectrophotometer over a wavelength range of 360 – 700 nm. The relative colour depths of the stained samples expressed as K/S were established according to the Kubelka–Munk equation, $K/S=(1-R)^2/2R$ [135], where K and S are the absorption and scattering coefficients, respectively.

The staining of wool samples with 1 % of AO7 dye solution was performed at pH ~2.2 (being adjusted with 0.05 M sodium acetate and acetic acid, to ensure that the amino groups of $\epsilon\text{PL/OAK}$ and wool were fully protonated) and 50 °C for 30 min using a liquor-to-fabric ratio of 50:1. The remaining solution was analysed spectrometrically at 486 nm to determine the amount of the dye in the solution by calculating the dye concentration based on a standard curve made of dye in the acetic acid. By subtracting the remainder from the initial dye concentration, the amount of dye adsorbed onto the wool was obtained. Data shown are the means of four experiments performed in duplicate, containing the standard deviation. In parallel, the colour depth of stained fabrics, expressed as K/S, were established as described under the previous section.

The $\epsilon\text{PL/OAK}$ immobilization on the GEL was evaluated indirectly (dye concentration evaluation in the treating solutions) after its staining with two acids dyes (TNBS or Coomassie Brilliant Blue G-250) being related to Van der Waals attractions and ionic interactions between the dye's sulfonate groups ($-\text{SO}_3^-$) and the available weak base protonated groups ($-\text{NH}_3^+$) of GEL macromolecules (arising from side groups of His, Lys, hydroxy Lys and the $\epsilon\text{-NH}_2$ groups at the chain ends) [54] in an acidic media.

The staining of GEL samples (1 mL) with 1 mL of 0.5 % TNBS dye was performed at pH 8.5 (adjusted by addition of 1 mL of 4 % NaHCO_3) and 40 °C for 3 h during shaking (50 min^{-1}). 3 mL of 6 M HCl were then added into the mixture, being treated at 60 °C for 1.5 h. The reaction mixtures were diluted using distilled water and the absorbance of TNP-lysyl derivatives generated were measured at 346 nm [136, 137, 138] on a Tecan UV-Vis

spectrophotometer. All samples were read against reagent blank, which represented water prepared with the same procedure. The molar amount of ϵ -NH₂ groups per gram of conjugated products was determined by using the following equation [139]:

$$\frac{\text{Moles of } \epsilon\text{-NH}_2}{\text{mass of protein}} = \frac{2 \cdot \text{Abs} \cdot 0.05L}{(1.46 \cdot 10^4 \text{ L/mol} \cdot \text{cm}) \cdot b[\text{cm}] \cdot x[\text{g}]} \quad (4.1)$$

where 1.46 L/mol·cm is the molar absorptivity of TNP-Lys, b is the cell path length in cm, and x is the sample weight in grams [140].

The amount of ϵ PL/OAK applied to the GEL was evaluated also indirectly by determination of ϵ PL/OAK in the solutions before and after their treatments with GEL using already prepared pre-mixed solution of Coomassie Brilliant Blue G–250 dye (with unknown concentration and pH 3), according to the colorimetric method of Bradford [134] where the dye bound is approximately proportional to the number of positive charges found for the protein [141]. The Coomassie Brilliant Blue G–250 dye reagent from 4 °C storage was placed under ambient temperature. 1 mL of dye reagent was mixed with 1 mL of each sample with slight vortexing. The incubation was maintained at room temperature for ~15 min. After incubation, the absorbance data of the GEL- ϵ PL/OAK samples were measured at 595 nm in Vis-transparent plate pools (Corning 6 Flat) using a Tecan Infinite M200 (Tecan, Mannedorf, Switzerland) UV spectrophotometer, equipped with plate-reader unit. Whereas the absorbance of the dye at 595 nm is proportional to the amount of ϵ PL/OAK bound, the standard curve was created by using the pre-prepared ϵ PL/OAK solutions with known concentrations (being pre-incubated for 15 min at room temperature), which was used to determine the amount of ϵ PL/OAK in the solutions. The efficiency of ϵ PL/OAK coupled was calculated as the ratio of the number of molecules of ϵ PL/OAK to the number of NH₂ groups available before the reaction, so that the quantity of ϵ PL/OAK in GEL was determined by subtracting the supernatant concentrations in the solution after the GEL functionalisation from the starting ϵ PL/OAK concentration. All the reported values are the mean values of triplicate determinations, containing the standard deviation.

QUANTIFICATION OF BASIC GROUPS ON WOOL/GEL SAMPLES BY POTENTIOMETRIC TITRATION

Potentiometric titrations for assessing the pI of wool and GEL samples, before and after chemical modification with ϵ PL, were performed using a dual-burette instrument (Mettler Toledo T-70) equipped with a combined glass electrode (Mettler TDG 117). The burettes were filled with 0.1 M HCl (Merck, Titrisol) and 0.1 M KOH (Baker, Dilut-it). All the GEL solutions were prepared in deionized water with low carbonate content (lower than 10^{-5} M). Different titrant volumes (0.001 mL to 0.25 mL) were dynamically added within 30 s to 180 s periods. Wool samples were rinsed in low pH (0.01 M HCl) to convert polypeptide's basic and acidic residues into a protonated form, soaked in Milli-Q water and, afterwards, dried at 40 °C.

All titration experiments were carried out at room temperature (23 ± 1 °C) in forward and back runs between pH 3 and pH 11. From the potentiometric titration data, the molar concentration relating to the overall charge of the weak ions (arising from side groups of His and Lys, and the α -NH₂ groups at the chain ends) was calculated, a method described in detail by Čakara et al. [142]. All the reported values are the mean values of duplicate determinations, containing the standard deviation.

ATR-FTIR SPECTROSCOPY ANALYSIS OF WOOL SAMPLES

ATR-FTIR spectroscopy was used to identify spectral differences associated with the polymer orientation differences amongst the wool samples. For that purpose, a Perkin–Elmer IR Spectrometer was used with a Golden Gate Attenuated Total Reflection (ATR) attached to a diamond crystal. The spectra were accumulated under ambient conditions from accumulating 16 scans at resolutions of 4 cm^{-1} within a region of $4000\text{--}650\text{ cm}^{-1}$, with air spectrum subtraction performed in parallel as a background. The Perkin Elmer Spectrum 5.0.2 software programme was applied for the data acquisition analysis. A linear baseline was subtracted and the resulting spectra were normalised before determining the differences between the secondary structures of the samples by using Fourier self-deconvolution of the amide I band components ($1700\text{--}1570\text{ cm}^{-1}$), processed by using Peakfit 4.12 software (Galactic Industries Corporation, USA).

The amide I band was resolved by the second-order derivative with respect to the wavelength. Additionally, the spectra were evaluated quantitatively by calculating the intensity ratio between the amide I and amide II bands ($A_{\text{amide I}}/A_{\text{amide II}}$).

ZETA POTENTIAL (ZP) ANALYSIS OF WOOL/GEL SAMPLES

The ZP at the surface of untreated and differently treated wool samples in a supporting electrolyte solution were performed at the Laboratory for water biophysics and membrane processes, Faculty of chemistry and chemical engineering at University of Maribor. ZP values were determined using “SurPASS” electrokinetic analyser, based on the measurements of streaming potential and streaming current, respectively, as a function of pH [143]. The ZP was determined using adjustable gap cell (AGC). Measurements were made at 24 ± 2 °C and for a maximum pressure difference of 500 mbar with flow in the two directions. At least 18 experimental points were collected for each run.

The ZP of untreated and differently treated GEL samples was assessed using a Zetasizer (Nano ZS ZEN360, Malvern instrument LTD., UK) at 20 ± 0.1 °C using the cell ZEN1010, applying the following parameters: a material refractive index (RI) of 1.47, dispersion RI of 1.33 and viscosity of 0.8872 cP. A field of 40 V was applied across the nominal electrode spacing of 16 mm. The samples were diluted in 1:100 ratio with Milli-Q water and measured over a pH range (2–11), being adjusted using 0.1 M NaOH and 0.1 M HCl. The average values, as well as the standard deviation of the mean values, were calculated from 8 individual measurements.

CZE ANALYSIS OF GEL SOLUTIONS

The CZE analyses of native and differently treated GEL dispersions were performed using Agilent 7100 CE instrument with a built-in diode-array detector (DAD), controlled by Agilent Chemstation software. An untreated fused silica capillary tube (Agilent) of 50 µm internal diameter with an effective length of 585 mm (total length of 645 mm) was used. Prior to analysis, the capillary was rinsed for 30 min with 1 mM NaOH, followed by rinsing with Milli-Q water for 10 min and final 20 min with 100 mM sodium borate buffer (pH 9.3), which was

used as a background electrolyte (BGE). Before each run the capillary was preconditioned with 1 M NaOH for 2 min, Milli-Q water for 1 min and BGE for an additional 2 min.

GEL dispersions (~2.5 g/L) were diluted 1:100 (sample:water) in Milli-Q water and filtered by 0.22 µm syringe filters (Roth, Germany) before intensively mixed. Hydrodynamic injection was achieved by injecting samples at 30 mbar for 20 s, followed by a plug of BGE at 30 mbar for 5 s. The 20 kV voltage and constant temperature (45 ± 0.1 °C) were applied as input parameters. The DAD detection was performed at 210 ± 20 nm, according to the absorption maximums of GEL. A total analysis time of 12 min per sample was used. All electrophoresis experiments were carried out three times with similar patterns.

HPLC-SEC ANALYSIS OF GEL SOLUTIONS USING FITC-LABELLED ϵ PL

SEC was employed to evaluate the changes in MW of GEL before and after its treatment with FITC-labelled ϵ PL. The fluorescence labelling of ϵ PL was used to improve the sensitivity and selectivity of detection [144, 145, 146]. For that purpose, the ϵ PL was dissolved in 100 mM carbonate-bicarbonate buffer of pH 10 to the concentration of approximately 5 g/L. FITC was then added at a molar ratio of 1:2 (ϵ PL:FITC), and solution was left under stirring condition for 20 h at room temperature. The reaction mixture was loaded into a Sephadex G-25 column (Sigma-Aldrich, Germany), and the column was washed with 25 mM sodium-acetate pH 5 with 0.8 % NaCl. The unbound label was removed by washing the samples with three column volumes of buffered saline, as shown in Fig. 4.3. Labelled fractions were collected, freeze and lyophilized. The resulting powder of ϵ PL-FITC conjugate was stored in a fridge before further using.

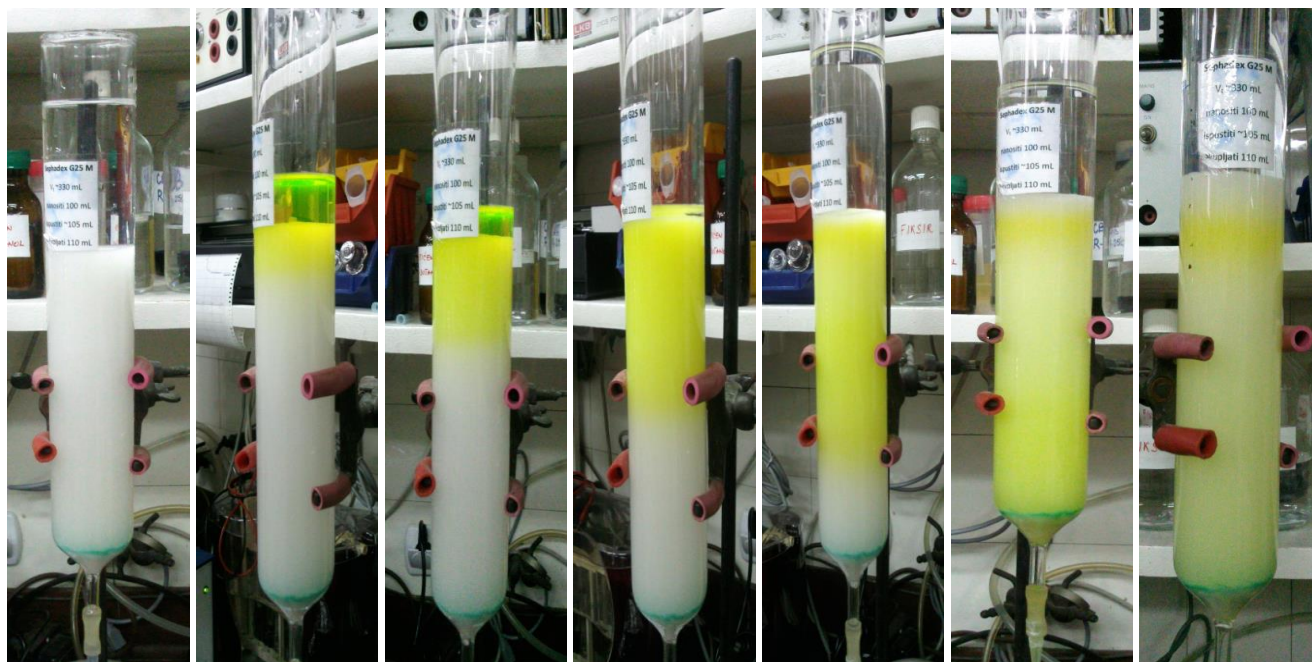


Figure 4.3: Removal of unreacted FITC from ϵ PL-FITC on Sephadex G25 column.

The SEC analysis of differently prepared GEL solutions were performed using a HPLC system (Agilent Technologies 1200 Series) equipped with a variable wavelength detector (VWD) and fluorescence detector (FLD). Separation took place at temperature of 40 ± 1 °C by using an Agilent Bio SEC-3 column with a diameter 4.6 mm, particle size of 3 μ m and pore diameter of 15 nm. Experiments were conducted with 150 mM phosphate buffer and 5 mM sodium azide solution of pH 7.5 as the mobile phase under a flow rate of 0.3 mL/min. Before the injection, samples were filtered through a 0.22 μ m PVDF membrane filter (Rotilabo®-Spritzenfilter, Carl Roth GmbH & Co., Germany). 15 μ L of samples were injected into the system and the measurements were carried out for 15 min, detected by a VWD at a wavelength of 210 ± 5 nm or by FLD by using FITC spectral detection set-up ($\lambda_{ex}=492$ nm and $\lambda_{em}=522$ nm). The software Chem Station (Agilent Technologies) was used for SEC data evaluation. Representative results of analyses performed at least three times are shown.

EPR SPECTROSCOPY ANALYSIS OF WOOL/GEL SAMPLES USING SPIN-LABELED ϵ PL/OAK

The EPR spectroscopy has been applied to elucidate the conformational dynamics and binding of ϵ PL/OAK onto wool and GEL macromolecules [147, 148]. The experiments were assessed at the Laboratory of biophysics, Jozef Stefan Institute, Ljubljana. The ϵ PL and OAK

were site-directed spin-labeled with 3-maleimido proxyl (MP) as a spin probe at room temperature (21 ± 1 °C) for 24 h in 100 mM phosphate buffer containing 200 mM of NaCl (pH 8) at a ratio of spin label to ϵ PL amino groups of 1:10 (mol/mol). The removal of free spin probe and separation of the MP-labelled ϵ PL from unlabeled one was performed by using partitioning between buffer and octanol phase.

The MP- ϵ PL functionalised GEL samples were put into quartz capillary tubes of 1 mm in diameter and transferred into the EPR resonator for analysis without any special preparation steps, while the wool pieces had to be pre-treated by crushing into the powder to be homogenised for EPR analysis. The MP- ϵ PL functionalised wool samples were also put into quartz capillary tubes of 1 mm in diameter and transferred into the EPR resonator for analysis. X-band (9.3 GHz) continuous-wave Electron Paramagnetic Resonance (cw-EPR) spectra were recorded at room temperature using a Bruker EleXsys E500 Spectrometer (Germany) equipped with a high-sensitivity resonator (SHQEW0401) applying a scan range of 100 G, 1.5 G amplitude of modulation, 41.94 s of sweep time, 40.96 ms of time constant, and microwave power of 20 mW. Differently immobilised ϵ PL on wool/GEL were expected to bring local constriction that would restrict the possible motions of the ϵ PL and their associated spin-labels. These changes in motion result in changes in the determined rotational correlation times (τ_c) of the spin-label. The results of the correlation times of differently modified samples thus allowed us to identify the orientation of the grafted ϵ PL.

4.2.3 Evaluation of substrate antibacterial activity

The antibacterial efficacies of differently prepared samples were assessed at the Institute of microbiology and parasitology, Veterinary faculty at University of Ljubljana.

BACTERIAL STRAIN PREPARATION

Stock solutions of selected bacteria (Gram-negative *Escherichia coli* ATCC 35218 and Gram-positive *Staphylococcus aureus* ATCC 25923) were streaked on Petri dishes and cultured for 24 h at 37 °C, before fully grown single colonies were inoculated in sterilised nutrient broth and cultured for 24 h. The incubated culture solutions were diluted using a sterilised physiological saline (0.9 % NaCl), in order to give a final concentration of $1.5\text{--}3.0 \times 10^5$ colony-forming units (CFU)/mL, being used as a working bacterial solution.

ANTIBACTERIAL EFFICACY ASSESSMENT OF WOOL BY SHAKE FLASK TEST

The antibacterial efficacies of wool were examined under dynamic contact conditions by using the dynamic shake flask test method ASTM E2149-10 [120]. Each sample (~0.1 g) was transferred to a sterile 150 mL Erlenmeyer flask containing 10 mL of the working bacterial solution. Control experiments were run during which no wool samples were present within the bacteria culture and treated in the same way. All flasks were capped loosely and incubated for 1 h, 3 h, 6 h and 20 h, respectively, on a rotary shaker (120 min⁻¹) at ~37 °C. At different contact periods, 1 mL of the bacterial suspension was withdrawn, serially diluted using the physiological saline, transferred onto the prepared Petri dish and spread over the nutrient agar using a hockey stick. The inoculated plates were incubated at 37 °C for 24 h and the surviving cells counted. The values were converted to CFU/mL in the flasks by multiplying by the dilution factor, and the mean values of percent reduction were calculated using Eq. 3.11. Experiments were performed in triplicate and the data are shown as the mean values, containing the standard deviation.

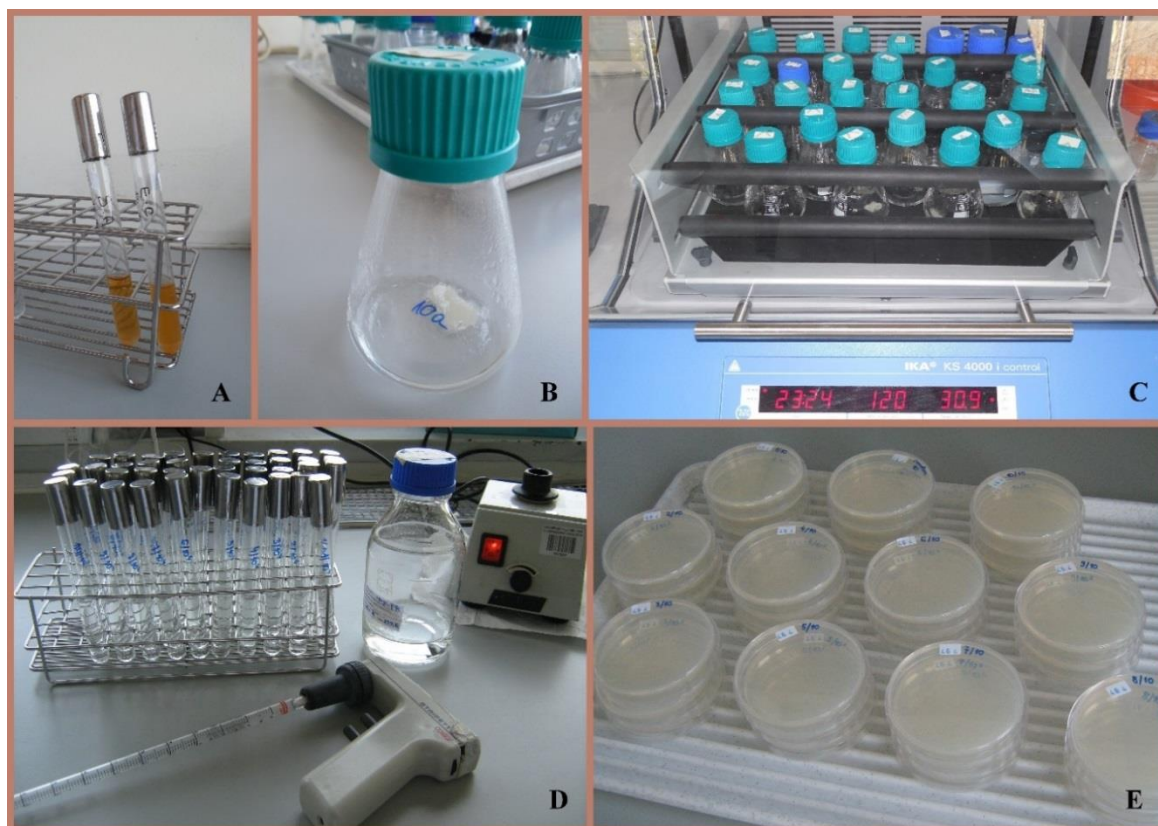


Figure 4.4: Dynamic shake flask test used for determination antibacterial efficacies of wool samples. A – bacterial inoculum, B – Erlenmeyer flask containing WO sample in 10 mL of the

working bacterial solution, C – rotary shaker, D – dilution of withdrawn bacterial suspension, E – inoculated Petri dish plates.

BACTERICIDAL EFFICACY OF WOOL AND BACTERIAL VIABILITY ASSESSMENT USING LIVE-DEAD TEST

The working suspensions of both bacteria, *E. coli* (2×10^8 bacteria/mL) and *S. aureus* (2×10^7 bacteria/mL), were prepared as reported [149]. After 24 h of inoculating wool substrates with bacteria cells using working bacterial suspensions, a stock solution (1.5 mL) of Live/Dead BacLight staining reagent mixture (6 μ M SYTO 9 and 30 μ M PI) was mixed with 1.5 mL of each bacterial suspension which remained after shake flask testing. The solutions were incubated at room temperature in the dark for 15 min and then each pipetted (100 μ L) into separate wells of 96-well flat-bottomed micro-plates and measured using fluorescence emission spectrum using a Tecan Spectrophotometer. By using an excitation wavelength centred at 480 nm, the integrated intensities of the green (G; 530 nm) and red (R; 630 nm) emission were acquired, and the green/red fluorescence ratios (ratio G/R) were calculated for each suspension. The biocidal effect (%) within 24 h against *E. coli* and *S. aureus* were determined by calculating the relationship between live (G, x) bacteria and G/R fluorescence ratio (y) as $[y_1 = 0.0632x + 0.0614]$ for *E. coli* and $[y_2 = 0.0151x + 0.3369]$ for *S. aureus* bacteria.

The biocidal efficiencies of the wool samples were examined further by viability tests performed by using CFM. After 24 h of exposure to the media inoculated with *E. coli* (10^5 CFU/mL) or *S. aureus* (10^5 CFU/mL), the wool samples were stained with a 3.4 μ M of SYTO 9 and 6.0 μ M of PI, respectively, for 30 min in the dark at room temperature, washed with Milli-Q water, air-dried and then visualised by fluorescence microscopy consisting of a Nikon TE2000-E inverted microscope, lambda LS Xe-Hg arc lamp, BD Carv II fluorescence, confocal unit and a Rolera MGi EMCCD camera. The images were excited using 420 nm or 488 nm excitation filters and the emissions collected using a UBG triple-band-pass emission filter cube. Experiments were performed in duplicate and the data are shown as the mean value, containing the standard deviation.

ANTIBACTERIAL EFFICACY ASSESSMENT OF GEL SAMPLES USING AGAR DIFFUSION AND BROTH-DILUTION TEST

The bacterial inoculum (concentration of $1.5\text{--}3.0 \times 10^5$) was uniformly spread using sterile cotton swab on a sterile Petri dish (Deltalab, Spain) MH agar. 50 μL of each GEL dispersion was added to each of the 5 wells (7 mm diameter holes cut in the agar gel, 20 mm apart from one another). The inhibition zone was measured (in mm) after overnight incubation at 37 °C. Experiments were performed in duplicate and the data are shown as the mean values, containing the standard deviation.

Broth-dilution method was based on the [150]. Bacterial pre-cultures were prepared in 10 mL of sterilised nutrient broth with a volume ratio of 1:5 and incubated overnight at 37 °C. Bacterial cell suspensions, diluted to $1.5\text{--}3.0 \times 10^5$ in PBS (pH 7.2), were inoculated in 1 mL of differently prepared GEL solutions for 24 h at 37 °C and 120 rpm. After contact period the samples were submitted to successive serial dilutions using PBS, transferred onto the Mueller Hinton agar (Oxoid) plates and spread over the nutrient agar using a hockey stick. Colony-Forming Units (CFUs) were counted after an overnight incubation at 37 °C, and the mean values of percent reduction (R) were calculated using Eq. 3.11. [120].

4.2.4 Determination of substrate cytotoxicity

DETERMINATION OF GEL CYTOTOXICITY BY USING MTT COLORIMETRIC ASSAY

Cytotoxicity of differently prepared GEL solutions were evaluated at the Institute of biomedical sciences, Faculty of medicine at University of Maribor, by using human osteoblasts cells (hFOB). Cell viability was assessed by MTT (3-(4,5-dimethylthiazol-2-yl)-2,5-diphenyltetrazolium bromide) colorimetric assay. Osteoblast cells were cultured 24 h at 37 °C (5 % CO_2) in Dulbecco's modified Eagle's medium (DMEM) containing 5 % fetal bovine serum (FBS). The cells were seeded onto Eppendorf 96/F-PP microplates at a density of 1×10^4 cells/well; polypropylene plates were chosen to reduce biofilm formation. The dispersions of conjugated products, being diluted in concentrations of 1: 2, 1: 4, 1: 8 and 1:16 in DMEM with 5 % FBS, were added to each well and the cells were cultured for another 24 h at 37 °C. Sample with hFOB cells and no seeded copolymer was used as negative control. After 24 h of incubation, the MTT test was conducted, reviewed and approved by the National Medical Ethics Committee (code 21/09/07). The colour reaction, generated by

the reduction of tetra ring of MTT by mitochondrial dehydrogenases with NADH in the active mitochondria, was measured spectrophotometrically at wavelength 570 nm with a reference at 665 nm using the Tecan Infinite M200 multifunctional spectrophotometer (Tecan, Mannedorf, Switzerland).

DETERMINATION OF CELL DEATH AND CELL MORPHOLOGY BY DIRECT CONTACT WITH GEL SOLUTIONS

Cell death and cell morphology were also assessed using direct contact test. Before the seeding, dispersions were sterilized under UV light for 30 min. Osteoblasts were cultured together with dispersions until cells were formed a single layer. The cells were incubated for 24 h and any morphological changes on the cells in contact with each of the GEL dispersions were visually assessed directly on a microplate by an inverted optical microscope AXIOVERT 40 (Zeiss, Germany) imaging. The boundary between the conjugate sample and the cell monolayer was carefully controlled to check the change of cell's morphology, death or reduction. Cytotoxicity data is expressed as the means of four replicates.

4.2.5 Durability of functionalised wool

To evaluate the durability of the wool's antibacterial effect after washing, the ϵ PL-functionalised wool substrates were washed, according to Standard ISO 105-D01:2010 test method [151].

5 RESULTS AND DISCUSSION

5.1 The effect of ϵ PL/OAK binding on the antimicrobial activity of wool

5.1.1 The influence of the coupling strategy of an ϵ PL/OAK graft yield onto wool

Direct and indirect analytical methods were used in order to evaluate the coupling efficacy of ϵ PL/OAK to wool. Direct methods were related to colorimetric evaluation of the wool stained with different acid dyes, as well as its quantification by potentiometric titration, while the indirect method gave us the information about the remaining AO7 dye content in the treatment bath after the staining.

The potentiometric titration curves (Fig. 5.1) of the reference wool (Ref WO) and differently ϵ PL-treated wool using both chemical and enzymatic approaches were performed to observe the charge reversal in the case of wool functionalisation. The pI of the wool functionalised with ϵ PL using the *grafting-to* approach is the highest and occurs at pH~10, similar to the free ϵ PL (pI~9.5, pre-determined by ZP), while the pI of the Ref WO appeared at pH of ~4.9, which is in accordance with the previous results [2, 152]. The weak basic (arising from side groups of His and Lys residues, as well as the α -NH₂ groups at the chain ends of the wool) group's content (Table 5.1), being determined from the back-titration data, thus increased by ~72 % (to ~1 005 mmol/kg) and by ~42 % (to ~833 mmol/kg) by the *grafting-to* and *grafting-from* approaches, respectively, compared to the Ref WO, where ~585 mmol/kg basic groups were evaluated. Furthermore, the quantity of these groups on the wool treated by the enzymatic approach increased by ~55 % (to ~909 mmol/kg). The control sample treated without EDC/NHS (Ref- ϵ PL) didn't bring any increase of the basic group's content (~563 mmol/kg), which means that the ionic adsorption of ϵ PL to the wool is negligible and that all the non-covalently bound ϵ PL was removed successfully by its rinsing at very low pH (pH 2) at which the strong electrostatic interaction is disrupted [153]. On the other hand, a significant reduction of basic groups (~172 mmol/kg) was detected for Ref-EDC/NHS, indicating the cross-linking between the available carboxylic and amino groups of wool protein residues [89]; a similar but much less pronounced effect can be observed for the Ref-TGase sample, also being well in agreement with other studies, which have shown that

keratin can be self-cross-linked by microbial TGase, resulting in less Lys NH₂ groups availability [154, 155].

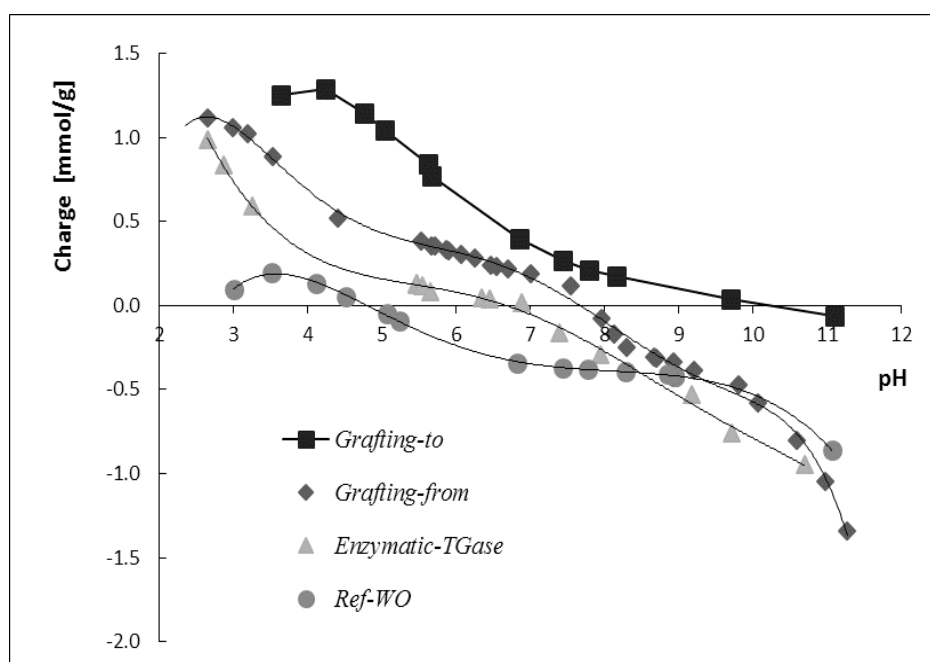


Figure 5.1: Titration curves of the reference and differently ϵ PL-functionalised wool samples.

Indirectly quantified basic groups (arising from side groups of His, Lys, and Arg residues, as well as α -NH₂ groups at the chain ends) of the wool (by determining the AO7 dye concentrations in the solutions of wool samples after their staining at very low pH where the wool is fully protonated and thus available for ionic interactions with acid dye) showed a similar trend. As shown in Table 5.1, the quantity of basic groups present on the wool was the largest (~58 or ~47 % higher) when using the EDC/NHS coupling mechanism and *grafting-to* approach (~928 mmol/kg for ϵ PL or ~863 mmol/kg for OAK), compared to the reference (~587 mmol/kg) as well as *grafting-from* (~711 mmol/kg for ϵ PL or ~814 mmol/kg for OAK) and TGase catalyzed coupling mechanism (~744 mmol/kg for ϵ PL or ~819 mmol/kg for OAK). The basic group reduction was observed for all the reference samples, except for the Ref- ϵ PL or Ref-OAK showing the group's content of ~400 mmol/kg or ~493 mmol/kg, being comparable to that of the Ref WO. The values are well correlated to that from the potentiometric titration analysis.

Table 5.1: The colouration yield (K/S) and quantity of basic groups [mmol/kg wool] of the references and differently ϵ PL/OAK-functionalised wool samples, being evaluated through their staining with different acid dyes as well as by potentiometric titration

Sample	Method	Qualitative by color strength measurement using Kubelka-Munk		Quantitative	
		Coomassie Brilliant Blue G-250	AO7	AO7 by dye concentration evaluation from the exhausted bath	Potentiometric titration
		K/S at λ_{\max} 610 nm	K/S at λ_{\max} 490 nm	(all) basic groups (mmol/kg wool)	(some) basic groups (mmol/kg wool)
Ref - WO		3.2 ± 0.2	19.0 ± 0.7	587 ± 33.8	585 ± 17.0
Ref - EDC/NHS		4.1 ± 0.1	18.9 ± 0.6	169 ± 21.5	172 ± 15.5
Ref - TGase		4.4 ± 0.5	20.4 ± 1.1	441 ± 12.9	448 ± 10.3
Ref - ϵ PL		4.7 ± 0.15	19.2 ± 0.4	400 ± 10.5	563 ± 10.5
Ref - OAK		4.8 ± 0.1	19.1 ± 0.5	493 ± 12.0	n.d.
Enzymatic TGase - ϵ PL		6.7 ± 0.3	31.9 ± 0.8	744 ± 90.5	909 ± 29.6
Grafting from - ϵ PL		6.3 ± 0.3	32.8 ± 1.5	711 ± 10.3	833 ± 13.5
Grafting to - ϵ PL		10.1 ± 1.3	35.9 ± 2.1	928 ± 12.1	1 005 ± 20.3
Enzymatic TGase - OAK		8.2 ± 0.8	30.9 ± 2.0	819 ± 11.6	n.d.
Grafting from - OAK		7.9 ± 0.6	33.3 ± 1.6	814 ± 33.8	n.d.
Grafting to - OAK		8.9 ± 0.4	36.3 ± 3.4	863 ± 63.2	n.d.

On the other hand, direct evaluation of the ϵ PL/OAK grafting yield by **the staining of available amino groups** on wool with both acid dyes (Coomassie Brilliant Blue G–250 and AO7, respectively) showed increased colour strength (K/S) values for all ϵ PL/OAK-treated wools (Table 5.1), as a result of an increased amount of dyes applied [141]. The EDC/NHS treatment resulted in more intensive colouration in the case of *grafting-to* (K/S of 10.1 and 35.9 for ϵ PL or 8.9 and 36.3 for OAK, respectively) compared to the *grafting-from* (K/S of 6.3 and 32.8 for ϵ PL or 7.9 and 33.3 for OAK, respectively) mechanism and the TGase approach (K/S of 6.7 and 31.9 for ϵ PL or 8.2 and 30.9 for OAK, respectively), being again significantly higher compared to all the references showing K/S values between 3.2 – 4.4 for dyeing with Coomassie Brilliant Blue G–250 and between 19 – 20.4 for AO7. The dyeability (K/S) of all AO7 dyed samples is related to much higher initial dye concentration compared to the Coomassie Brilliant Blue G–250, which is available only as a pre-mixed solution with unknown concentration.

It may be concluded that ϵ PL/OAK immobilisation on wool is achieved by all three coupling strategies, being however the highest by using EDC/NHS coupling chemistry and the *grafting-to* approach promoting the basic group's content of the wool- ϵ PL/OAK conjugate. In addition, the resistance of ϵ PL/OAK desorption upon the exposure of functionalised wools to a strong acidic solution under which all the ionic interactions which can cause non-specific attachment should be broken, indicating the specific attachment of the ϵ PL/OAK to the wool's surface via amide bond formation.

Surface charge of wool after different treatment for ϵ PL/OAK-functionalisation was also evaluated as a function of pH medium (range from 2 to 11) by determination of electrokinetic ZP in the contact surface between the wool sample and the fluid (Fig. 5.2). The untreated wool and wool treated with reagents, but without ϵ PL, showed the pI around pH 3.5 and net negative ZP, which indicated that the surface is hydrophilic. The addition of ϵ PL/OAK resulted to an increase in the ZP at almost the entire pH area and the pI was shifted to around pH 4.5. The analyze also shown on the difference in the negative ZP at higher pHs (\sim pH 6) between Ref WO (-60.8 ± 2.5) and sample, functionalised by *grafting-from* approach (-49.3 ± 3.4 for ϵ PL and -35.4 ± 2.1 for OAK), which increases by the pH decreasing, indicating on a tighter structure of wool, functionalised by *grafting-from* coupling mechanism. The highest difference in ZP between samples was identified at pH around 4.0, where the ZP of

Ref WO was -28.1 ± 0.7 , while the potential for sample, functionalised by ϵ PL using *grafting-to* approach, was 14.2 ± 0.6 and for sample, functionalised by OAK using *grafting-from* approach 19.4 ± 1.0 .

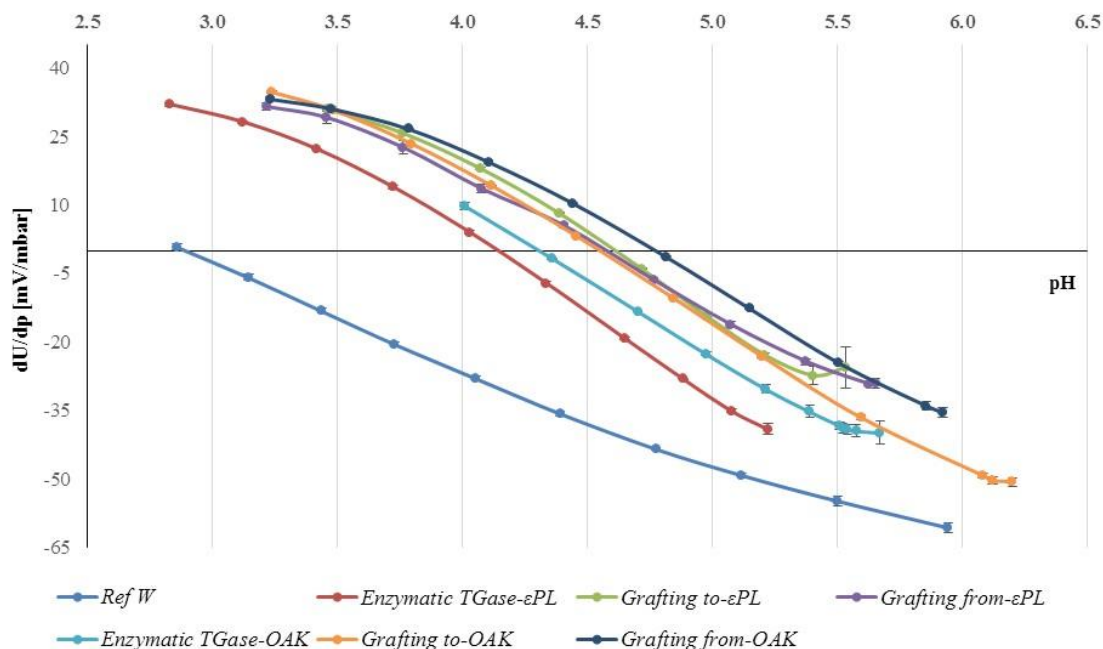


Figure 5.2: Zeta-potential curves of the reference and differently ϵ PL/OAK-functionalised wool samples as a function of pH.

5.1.2 The orientation and localisation of ϵ PL on a wool surface

The ATR-FTIR spectra of the referenced and differently treated wool samples were used to evaluate the interactions of ϵ PL/OAK within the wool protein. The spectra of all the samples presented on Fig. 5.3 exhibited similar absorption bands with a slight difference in two primary amide bands, namely the amide I (at $\sim 1630 \text{ cm}^{-1}$) and amide II (at $\sim 1513 \text{ cm}^{-1}$) regions, being used frequently to assess polymer orientation and their conformations [156]; hence an increase or a decrease in the ratios of their intensities ($I_{\text{AI}}/I_{\text{AII}}$) could be attributed to the changes in the orientation of secondary structures. Furthermore, the change in the amide I band shape is expected to have the same functional dependence as the amide I/amide II intensity ratio [157]. In that respect, the peaks were characterised using the ratio of the peak areas between amide I and amide II, as seen in Table 5.2. The assignments of intensities were determined between the local minima at 1470 cm^{-1} and 1577 cm^{-1} for the amide II and at 1577 cm^{-1} and 1717 cm^{-1} for the amide I ranges.

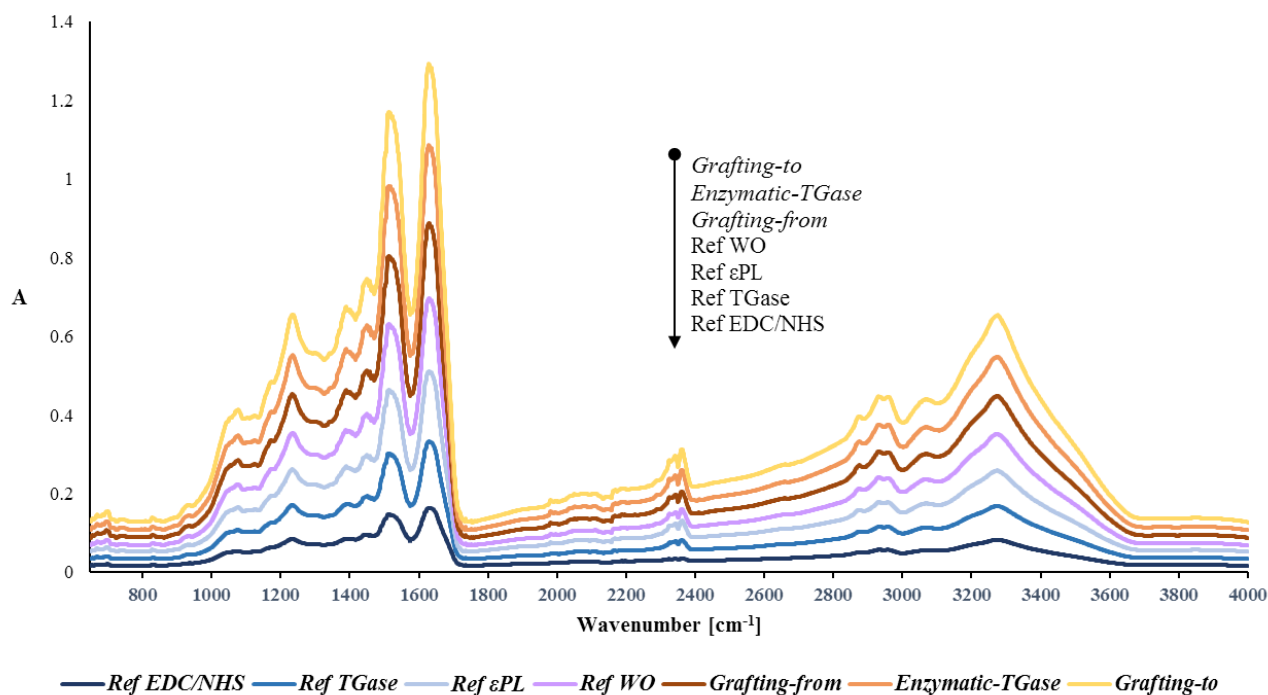


Figure 5.3: ATR-FTIR spectra of the references and differently ϵ PL-functionalised wool.

Table 5.2: Relative peak areas of amide I and amide II regions of FTIR spectra for the references and differently ϵ PL/OAK-functionalised wool samples

Sample	Relative peak area of amide I ($\sim 1630 \text{ cm}^{-1}$)	Relative peak area of amide II ($\sim 1513 \text{ cm}^{-1}$)	Area ratio (amide I/amide II)
Ref - WO	8.313	4.013	2.07
Ref - EDC/NHS	8.937	4.120	2.17
Ref - TGase	7.677	3.576	2.15
Ref - ϵ PL	8.055	3.669	2.18
Ref - OAK	8.168	3.781	2.16
<i>Enzymatic TGase - ϵPL</i>	7.482	3.328	2.24
<i>Grafting from - ϵPL</i>	9.303	4.078	2.28
<i>Grafting to - ϵPL</i>	9.890	4.274	2.32
<i>Enzymatic TGase - OAK</i>	8.364	3.688	2.27
<i>Grafting from - OAK</i>	8.936	4.019	2.22
<i>Grafting to - OAK</i>	8.740	3.772	2.32

All functionalised samples had higher peak area ratios than the references, indicating that the grafting yield affected the protein amide I and II peak areas. The wool being functionalised chemically by the *grafting-to* approach exhibited the highest peak area ratio ($A=2.32$ for ϵ PL and OAK), which had increased by $\sim 12\%$ in comparison with the reference wool ($A=2.07$) and by $\sim 7\%$ compared to all the other references. In the case of *grafting-from* ($\sim 10\%$ increase) or the enzymatic ($\sim 9\%$ increase) coupling approach, the peak area ratios were lower in comparison with the *grafting-to* chemistry, which was also consistent with the quantification of amino groups, evaluated by the spectroscopic method and potentiometric titration.

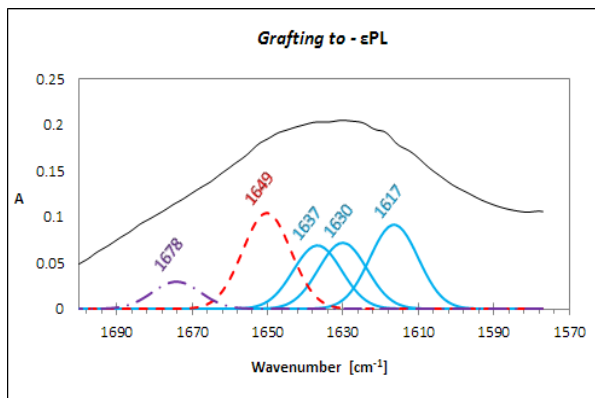
The amide I vibration, absorbing near 1650 cm^{-1} , originates mainly from the C=O stretching of the peptide linkages (approximately 80%) with minor contributions from the out-of-phase CN stretching vibration, the CCN deformation and the NH in-plane bend. The latter is responsible for the sensitivity of the amide I band to N-deuteration of the backbone. The extent to which the several internal coordinates contribute to the amide I normal mode depends on the backbone structure [158]. The amide II mode ($\sim 1550\text{ cm}^{-1}$) is the out-of-phase combination of the NH in-plane bend and the CN stretching vibration with smaller contributions from the CO in-plane bend and the CC and NC stretching vibrations. As for the amide I vibration, the amide II vibration is hardly affected by side-chain vibrations but the correlation between secondary structure and frequency is less straightforward than for the amide I vibration. The amide I is hardly affected by the secondary structures of the proteins and could be used to determine changes in protein after functionalisation, as each type of secondary structure gave rise to somewhat different C=O stretching frequencies due to their unique molecular geometries and hydrogen bonding patterns [159, 160]. Accordingly, the curve fitting procedure was used to quantify the area of α -helix, β -sheet, random and turn structures, representing the secondary structures of the wool protein.

As seen from Fig. 5.4, 25 different peaks were identified in the second derivative spectra within the $1570 - 1700\text{ cm}^{-1}$ amide I region, being assigned to various types of polymer orientation. The band centred at $\sim 1633\text{ cm}^{-1}$ was attributed to the intramolecular β -sheet; the peak at $\sim 1689\text{ cm}^{-1}$ and the bands within the $1618-1627\text{ cm}^{-1}$ regions were due to the intermolecular β -sheets. The contribution of the random coil conformation was identified by a peak centred at $\sim 1647\text{ cm}^{-1}$, the α -helix centred at $\sim 1651\text{ cm}^{-1}$ [161], and disordered

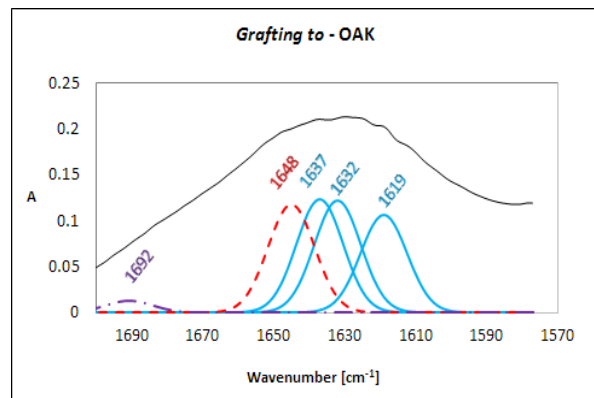
conformations being assigned to the bands between 1675 – 1700 cm^{-1} [162]. The 3_{10} -helix with 15–20 % of all helices is the fourth most common type of secondary structure in proteins after α -helices, β -sheets, and reverse turns, and is commonly found as N- or C-terminal extensions to α -helix [163].

The results of the relative areas of the de-convoluted absorbance bands, shown in the inserted Table in Fig. 5.4, revealed that a change in the secondary structures occurred in all ϵ PL/OAK-functionalised wool samples. Whilst the β -sheet content increased for all the grafting mechanisms, the 3_{10} -helix structure from the Ref WO diminished to about one fifth or even disappeared during the grafting process. New specific bands also occurred after its functionalisation with ϵ PL/OAK: the band at $\sim 1651 \text{ cm}^{-1}$ corresponding to the α -helix structure [159], appeared only in the case of the enzymatic grafting approach, while the peak for β -turn conformation occurred in the case of the *grafting-to* ($\sim 1678 \text{ cm}^{-1}$ for ϵ PL and $\sim 1692 \text{ cm}^{-1}$ for OAK) and enzymatic ($\sim 1688 \text{ cm}^{-1}$ for ϵ PL and $\sim 1689 \text{ cm}^{-1}$ for OAK) coupling approaches. Besides, the band at $\sim 1647 \text{ cm}^{-1}$ which is characteristic for random coil formation, was the highest in the wool functionalised by the *grafting-to* mechanism, which can be assigned to the fact that the *grafting-to* synthesis approach uses available NH_2 groups of wool reacting with the terminal carboxylic group from the ϵ PL/OAK, thus the remaining of free amino groups from the ϵ PL/OAK, which are charged, can affect the forming of random coil structures. In contrast, the *grafting-from* approach uses an initiated terminal carboxylic site on the ϵ PL/OAK to form a peptide bond with the wool NH_2 groups, resulting in the formation of both helical ($\sim 1641 \text{ cm}^{-1}$ for ϵ PL and $\sim 1692 \text{ cm}^{-1}$ for OAK) and random coil ($1645 - 1649 \text{ cm}^{-1}$) structures.

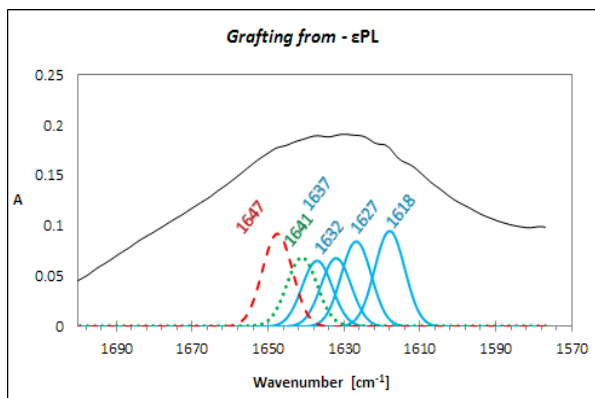
Finally, the contribution of relative areas of the de-convoluted absorbance bands within the amide I region, can thus be attributed to the molecular orientation of the grafted ϵ PL/OAK. In the case of the enzymatic coupling approach, the mobility of ϵ PL/OAK is restricted due to its highly formed branched structure, resulting in the creation of new intra-molecular β -sheet structures, which correspond to ~ 72 % of the relative area. On the other hand, in the case of the *grafting-to* mechanism, molecular flexibility is increased by refolding the ϵ PL/OAK to the random coil structure, representing ~ 29 % of the relative area. In the case of the *grafting-from* coupling mechanism molecular motion and unfolding decreased, and increased the α -helices content to ~ 17 % of the relative area.



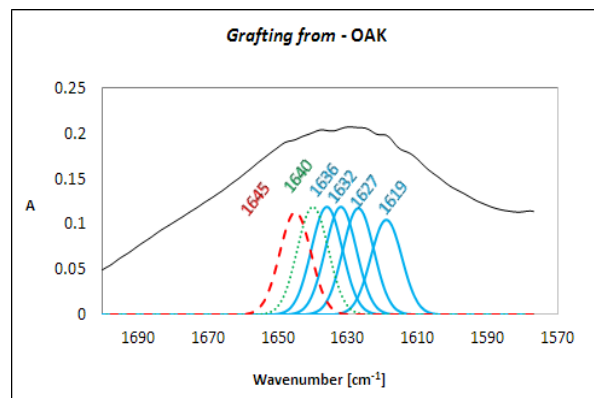
a)



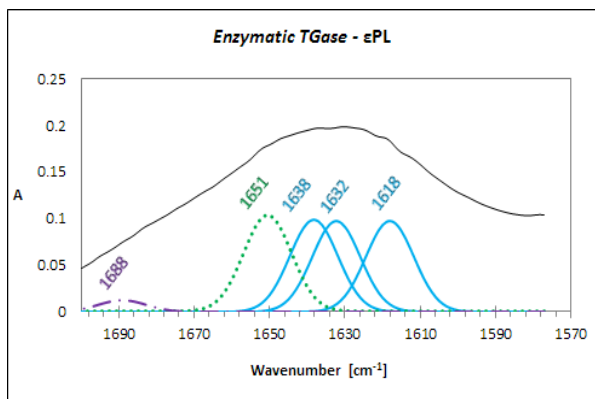
b)



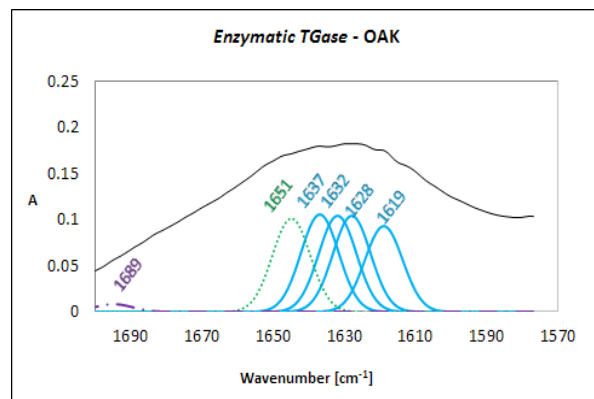
c)



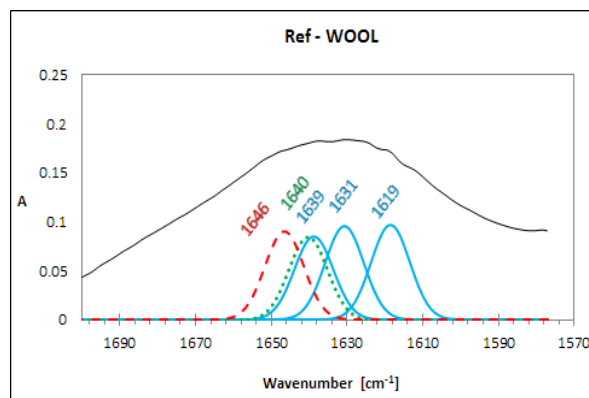
d)



e)



f)



g)

Positions [cm^{-1}]	Assignment	Relative area of Gaussian components [%]			
		<i>Grafting to</i> - ϵ PL	<i>Grafting from</i> - ϵ PL	<i>Enzymatic TGase</i> - ϵ PL	Ref WO
1617, 1618, 1619, 1627, 1628, 1630, 1631, 1632, 1633, 1636, 1637, 1638, 1639	β -sheet	67.05	66.43	71.87	59.31
1640, 1641	3_{10} helix	/	16.94	/	20.72
1645, 1646, 1647, 1648, 1649	random	28.61	17.64	/	19.97
1651	α -helix	/	/	25.25	/
1678, 1688, 1689, 1692	β -turn	4.34	/	2.89	/

Figure 5.4: Fourier self-deconvoluted FTIR spectra (shown as absorbance) of the amide I region ($1700\text{--}1570\text{ cm}^{-1}$, C=O stretching) with relative areas of assigned secondary structures for the reference and differently ϵ PL-functionalised wool samples.

EPR spectroscopy is a widely used spectroscopic technique for determining the structure-function correlations in protein macromolecules [147, 148]. As the mobility of a spin-label 3-maleimido PROXYL (MP), being covalently attached to ϵ PL is influenced by its micro environment, the analysis of the EPR spectra provides information on the orientation of site-specific immobilised ϵ PL-MP on wool. Presuming that all MP molecules (1000/1 molar excess of available groups over the amount of MP added) are covalently tethered to ϵ PL through their amino groups' availabilities, line-shape differences among samples thus yield information about their structural environments [164].

The rotational correlation time (τ_c , which may be viewed as the time taken for an axis of the nitroxide group of MPs to travel through one radian), is highly sensitive to the motion of the

chain [165]. In the fast tumbling limit ($10^{-11} < \tau_c < 10^{-9}$ s), the EPR spectrum of the MP's nitroxide consists of three anisotropic lines, the broadenings of which generally indicate MP immobilisation, whereas their sharpening indicates an increase in MP mobility. If the MP is thus attached to a molecule that is sufficiently small or flexible, it exhibits an isotropic EPR spectrum, as seen in Fig. 5.5, presenting a clean triplet signal of ϵ PL-MP being typical for nitroxide within the fast motional regime where τ_c is below 2ns. In contrast, if the mobility of the MP's nitroxide is restricted, a less isotropic EPR line-shape would be observed due to the unpaired electron of the MP residing in a molecular orbital 2p along the N–O bond [166].

The EPR spectra of the wool being functionalised with ϵ PL-MP by different approaches displayed different patterns of the characteristic MP's nitroxyl triplet signal. Rotational correlation times on ϵ PL-MP functionalised wool were significantly higher than those for ϵ PL-MP ($\tau_c \approx 0.11$ ns). In addition, the comparison between spectra shows a dramatic change in spectral line-shape, which can be associated with the modes of coupling chemistry and the mechanism (synthesis route) used. The MP attached to a molecule with a sufficient slow τ_c (> 0.1 ns) exhibits a broad EPR spectrum typical for a completely immobilised sample, as in the case of TGase grafted ϵ PL-MP ($\tau_c \approx 1.13$ ns). Depending on the degree of ϵ PL-MP immobilisation, partially broadened spectra may also be observed in the chemical *grafting-from* approach, indicating the mobility of an intermediate time scale ($\tau_c \approx 1.05$ ns). As the τ_c of the ϵ PL-MP functionalised wool by the *grafting-to* mechanism is lower ($\tau_c \approx 0.39$ ns), it suggests that a *grafted-to* ϵ PL-MP has higher mobility and thus indicates that ϵ PL molecules are linked to a wool surface within a highly-flexible (brush-like) structure. On the other hand, in the case of the *grafting-from* mechanism, the ϵ PL-MP may also be coupled to wool by ϵ PL side amino groups leading to a splitting of grafted ϵ PL chains into several parts forming loops or tails similar to the brush-like layer [130].

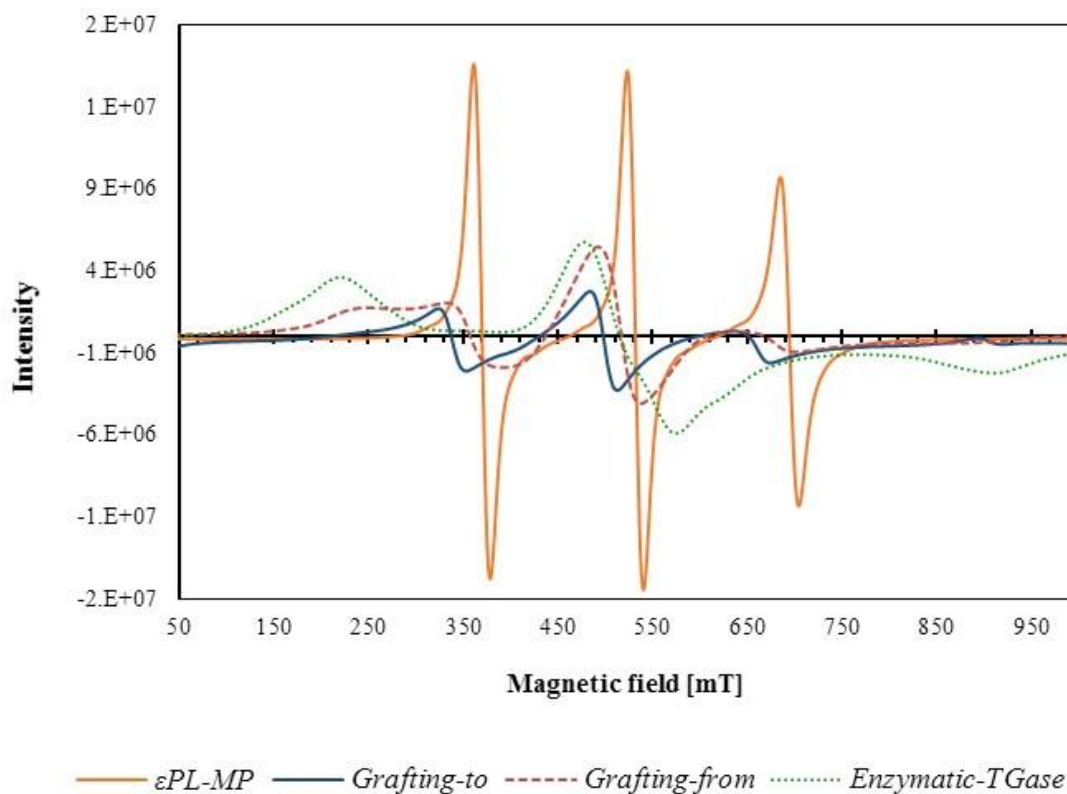


Figure 5.5: EPR spectra of 3-maleimido-proxyl spin-labelled ϵ PL (ϵ PL-MP) in comparison with the wool functionalised with ϵ PL-MP using different coupling approaches.

The results are well correlated with the FTIR spectra analysis, also indicating the fact that the conformation of ϵ PL onto the wool is affected not only by the coupling approach, but also by the pH used for the grafting. Namely, at lower pH values (pH 4.5), the ϵ PL possesses mainly the PII (polyproline II helical) and β structures [167], which are very likely to have been formed in the *grafting-to* approach where the highest flexibility was observed. In contrast, at higher pH values (pH 10) the α -helical conformation may also occur, leading to a more restricted motional regime, as there was in the case of the *grafting-from* and enzymatic coupling approaches.

5.1.3 Antibacterial activity of ϵ PL/OAK-functionalised wool

The results of the *in vitro* growth-inhibitory activities of differently treated wool substrates are shown in Fig. 5.6. For satisfactory antimicrobial activity the bacteria reduction should exceed 60 %, which is presented by the dashed line. As can be seen, all ϵ PL-functionalised

wool showed satisfactory bacteria reductions ($\geq 60\%$), being reached much faster kinetically (after 3 h) for Gram-positive *S. aureus* compared to Gram-negative *E. coli* bacteria, reaching this value after 6 h of inoculation. OAK-functionalised wool samples were tested only after 3 h or 24 h of inoculation. Results shown in Fig. 5.6 demonstrated that after three hours OAK-functionalised samples possessed a satisfactory antibacterial ability against *S. aureus*, while for *E. coli* the antibacterial rate based on the reduction of cell count reached 60 % only after 24-hour inoculation.

Specifically, there was no significant difference in inhibitory activity between ϵ PL- and OAK-functionalised samples, despite the fact, that the initial concentration of OAK was 100-times lower compared to ϵ PL, but nevertheless bring high antimicrobial activity, being related to OAKs electrostatic & hydrophobic interactions with bacteria. However, the functionalisation of wool by the *grafting-to* approach was the most effective, giving $\sim 99\%$ of both bacteria reductions, although the *grafting-from* and TGase-catalyzed approaches also gave satisfactory results with the reduction abilities of $\sim 74\%$ and $\sim 86\%$ for *E. coli* and even higher $\sim 92\%$ and $\sim 82\%$ for *S. aureus*, after 24 h of exposure. The apparent time-related viability decrease reflects on the higher resistance of Gram-negative *E. coli*, being attributed to its complex cell wall structure that is comprised with multiple layers in which an outer membrane layer containing long chain LPS in its outer leaflet and phospholipids in the inner leaflet, lies on top of a thin peptidoglycan layer (which is much thicker in Gram-positive bacteria). Such a thick cell wall structure restricts the penetrations of chemicals as well as antimicrobial agents. On the other hand, Gram-positive bacteria have a mesh-like peptidoglycan layer, being more accessible to permeation by the agents [168].

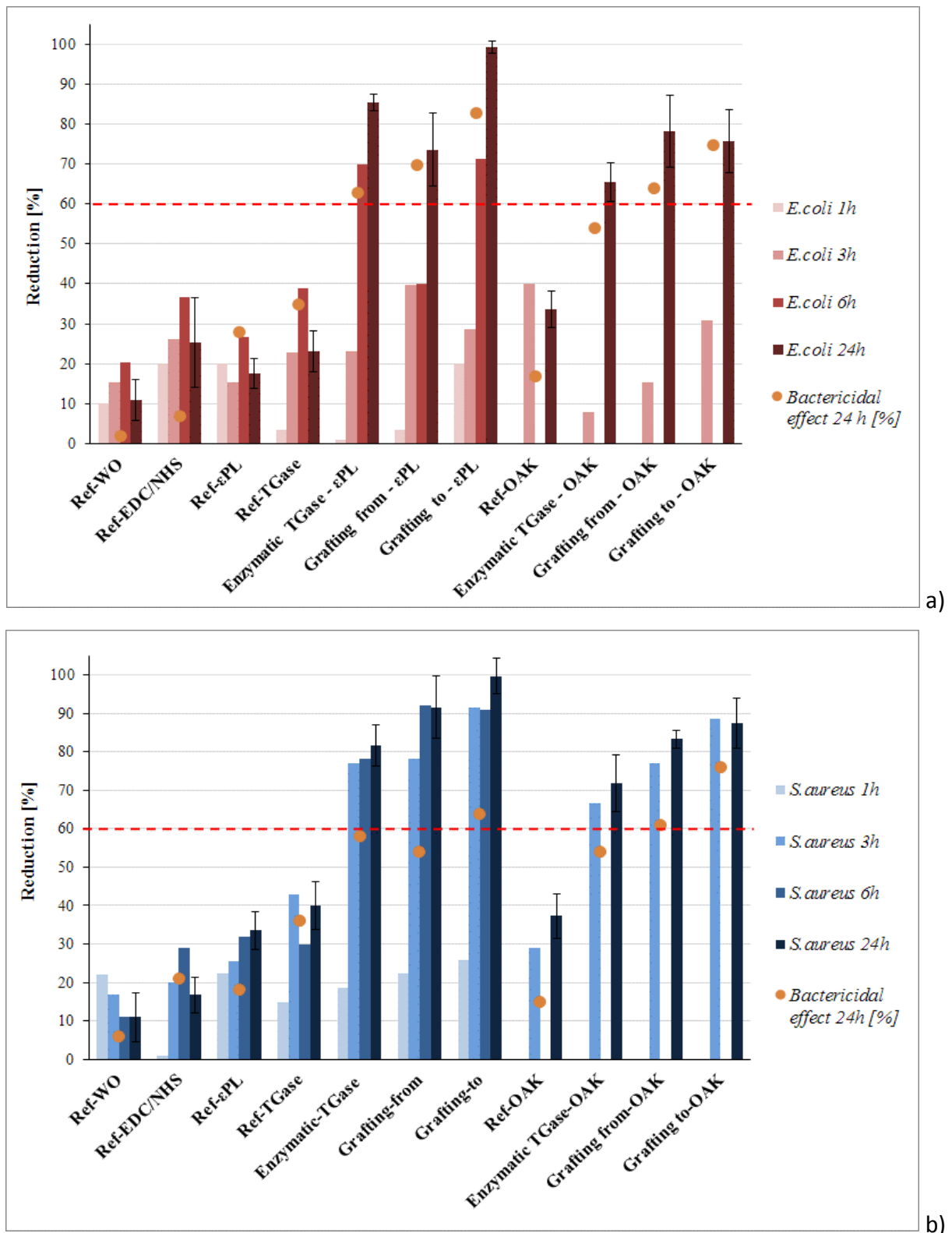


Figure 5.6: Time-dependent reduction of a) Gram-negative *E. coli* and b) Gram-positive *S. aureus* bacteria on the references and differently ϵ PL-functionalised wool samples, being evaluated by using the ASTM E2149-10 shake flask method [120], and corresponding bactericidal effect after 24 h of bacterial inoculation.

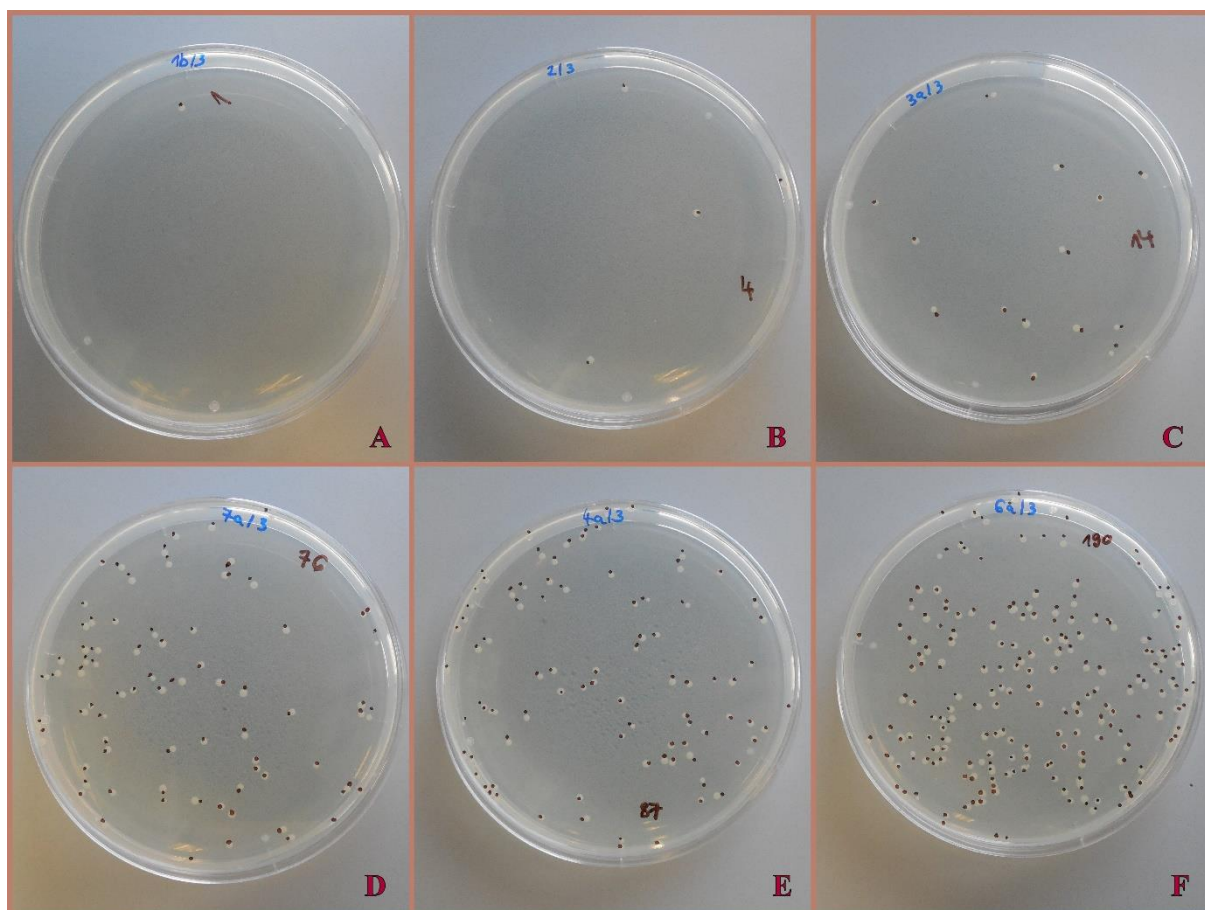


Figure 5.7: The colony forming units (CFU) of *E. coli* after 24 h incubation of wool samples, determined according to the dynamic shake flask test method ASTM E2149-10. A: *grafting to-εPL*, B: *grafting from-εPL*, C: *enzymatic TGase-εPL*, D: Ref-εPL, E: Ref WO, F: initial bacterial suspension.

As already described, the ϵ PL was initially described to show the analogical antimicrobial kinetics against different bacteria by causing irreversible changes in both the inner and outer cell membranes of pathogens. However, as all immobilised ϵ PL on the wool is bonded covalently, its good antibacterial activity can be attributed to its electrostatic interactions with the bacterial membrane, followed by stripping off the membrane and distribution of their cytoplasm [27]. For that purpose, the staining of bacteria after 24 h of inoculation was performed by using the Live/Dead BacLight bacterial viability staining test for detecting live cells with an intact membrane stained green by PI, and dead cells with a damaged membrane stained red by SYTO 9.

The data inserted in the graphs in Fig. 5.6 show an increase in bactericidal effect, as a result of the relative decrease in green fluorescence intensity when wool is functionalised with ϵ PL. These values for Gram-negative *E. coli* were comparatively higher and increased faster from enzymatic (~63 %) via *grafting-from* (~70 %) to *grafting-to* (~83 %) coupled ϵ PL as those for Gram-positive *S. aureus* (~58 % vs. ~54 % vs. ~64 %). However, there is a clear need for critical evaluation of the results obtained from combined staining, as previous studies have shown that SYTO 9 could not be effective in staining some intact Gram-negative bacteria, being related to its permeability problems through the double-membrane layer or its exporting from the bacteria cytoplasm [125], while a decrease in green fluorescence intensity can be related to the entrance of PI [169]. The confocal fluorescence microscopy imaging of the samples was performed despite the fact, that the combined fluorescent staining may lead to results with some deviations.

On Fig. 5.8 presented representative fluorescence images after exposure to the bacterial strain show green labelled cells on the surface of all the tested samples, being much more intensive on the Ref WO when compared to the other modified wool samples, where the presence of red bacteria indicates that ϵ PL may destroy the cytoplasmic membranes of bacterial cells before lysis. Similar observations were reported recently by Zhou et al. [170], where various damage to the *E. coli* cell envelope by ϵ PL demonstrated detachment of the outer membrane, swelling of the inner membrane, apical bursting of cells and leakage of cytosol at a minimal inhibitory concentration. This hypothesis may also be supported by the already approved bactericidal effect of ϵ PL by the US FDA [171], indicating that the bactericidal action of ϵ PL against both bacteria is mediated by physical ionic interactions with the microbial cell wall inducing on pore formation and/or disintegrating the cell membrane. Cytoplasmic membrane damage and cell permeabilization caused by ϵ PL would thus be responsible for PI entry and cell staining. Furthermore, the Live/Dead confocal micrographs confirmed the highest cell density on the wool being ϵ PL-functionalised by the *grafting-to* approach as compared to the other two mechanisms used. In addition, the ratio between the green (living) and red (dead) cells (*i.e.* cell viability) varied proportionally with the quantity of bound ϵ PL, being the highest for the sample functionalised by the *grafting-to* coupling approach.

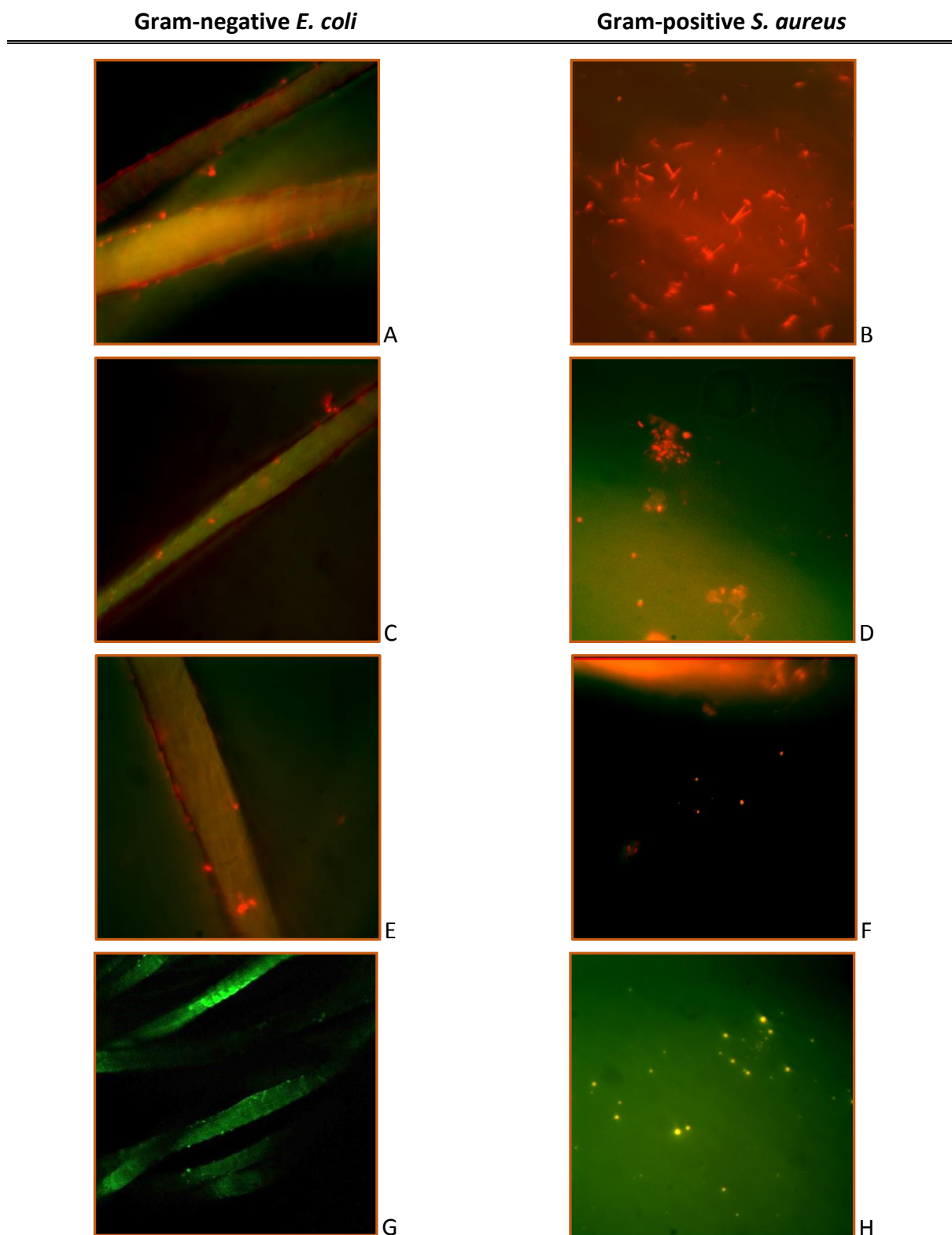


Figure 5.8: Confocal microscopy images of the ϵ PL-functionalised wool samples by *grafting-to* (A and B), *grafting-from* (C and D) and *enzymatic TGase* - catalyzed (E and F) coupling approaches in comparison with the reference sample (Ref WO, G and H), after exposure to a media inoculated with Gram-negative bacteria *E. coli* (A, C, E, G) or

Gram-positive bacteria *S. aureus* (B, D, F, H) for 24 h, and a Live/Dead BacLight bacterial viability staining test. Representative scans were taken at 60 x magnification showing green colour for Live and red colour for Dead bacterial cells.

5.1.4 Durability of wool's antibacterial activity to washing

The ϵ PL-functionalised wool substrates were washed according to the standard ISO 105-D01:2010 test method to evaluate the durability of the wool's antibacterial effect. As seen in Fig. 5.9, the wool functionalised by the *grafting-to* approach still provided ~86 % reduction of Gram-negative *E. coli* after 5 washing cycles, being slightly lower for ϵ PL coupled by the *grafting-from* approach but still satisfactory, while showing minimal but still sufficient effect in the case of *enzymatic-TGase* functionalised wool. However, although the ϵ PL was immobilised covalently, an increased number of washes (20 washing cycles) caused progressively reduced antimicrobial efficacy. As the presence of residues of non-ionic surfactant after washing may reduce the antimicrobial activity of the wool [172], the samples were extracted by Soxhlet extraction using dichloromethane as the extraction solvent, and the non-ionic detergent measured gravimetrically as solvent extractable material after removing the solvent using a rotary evaporator under vacuum. The results presented in Table 5.3 showed that wool adsorbed appreciable quantities of surfactant (*i.e.* ~0.016 g/ g of wool and ~0.027 g/ g of wool, submitted to 5 and 20 washing cycles, respectively), which was in accordance with the previous studies showing that non-ionic surfactants are adducts that can form complexes with wool protein by means of hydrophobic interaction between hydrophobic sites [173], thus blocking the functional groups of wool. In addition, the ϵ PL-functionalised wool washed with 20 cycles without the surfactant, showed good wash fastness properties, indicating that ϵ PL continuously inhibits the growth of bacteria in contact with the surface [77]. *Grafting-to* approach was the most effective, providing ~98 % reduction against *E. coli* and ~79 % against *S. aureus*. The influence of the surfactant chosen for washing seems to be crucial for both the effectiveness of the finishing (in our case antibacterial activity) as well as the durability evaluation, requiring additional studies.

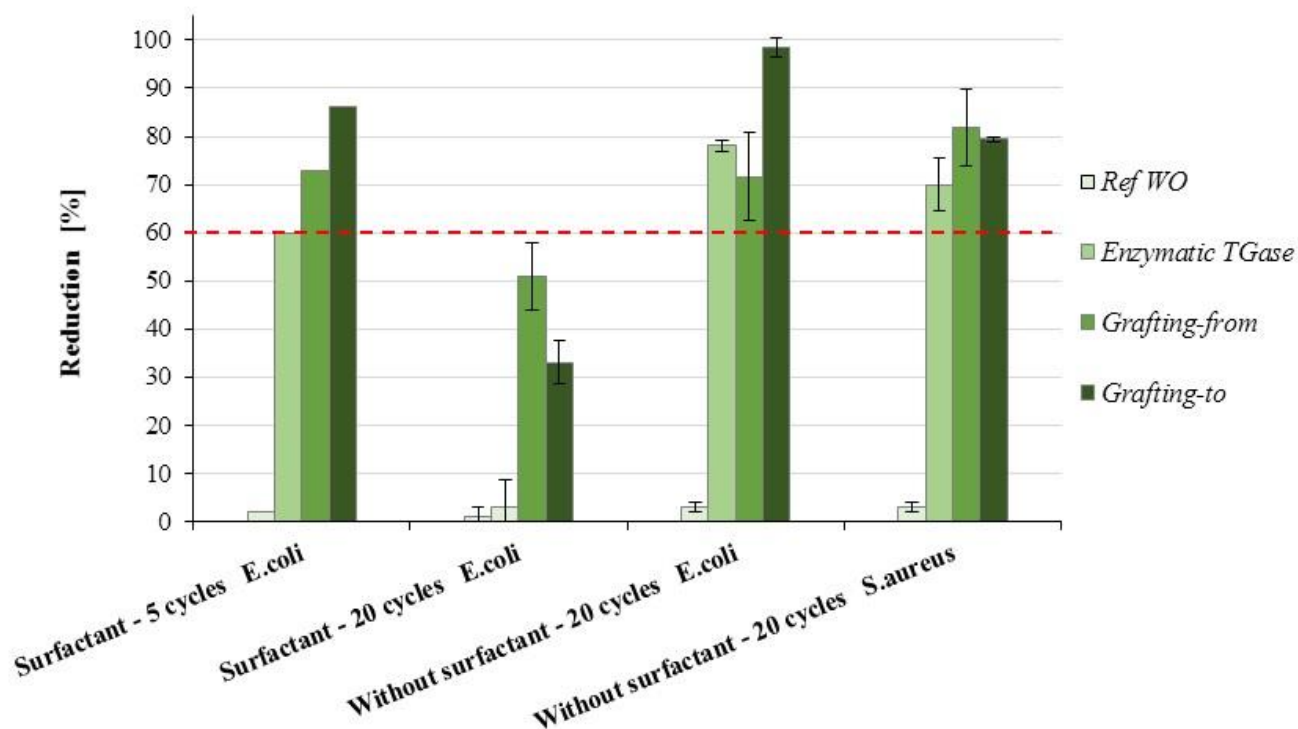


Figure 5.9: The reduction of Gram-negative *E. coli* and Gram-positive *S. aureus* on the reference and differently ϵ PL-functionalised wool samples, being washed with and without non-ionic surfactant according to ISO 105-D01:2010 for 5 and 20 cycles, evaluated by using the ASTM E2149-10 shake flask method [120].

Table 5.3: The amount of non-ionic surfactant extracted from ϵ PL-functionalised wool by the *grafting-to* coupling approach and submitted to 5 and 20 washing cycles

Solvent and conditions	Mass of the extracted detergent [g]		% of non-ionic detergent [w/w]	
	5 cycles	20 cycles	5 cycles	20 cycles
CH ₂ Cl ₂ & Soxhlet, 24h	0.016 ± 0.005	0.027 ± 0.011	1.6 ± 0.5	2.7 ± 1.1

5.2 The effect of ϵ PL/OAK binding on the antimicrobial activity and biocompatibility of GEL

5.2.1 Evaluation of the coupling efficacy of ϵ PL/OAK onto GEL

The coupling of low molecular weight peptides (as ϵ PL and OAK) onto high-MW protein-based polymer (as GEL) can be achieved relatively easily, but the characterization of the resulting conjugate products could be more difficult due to their structural similarities and high potential for physical interactions. The potential for side products is also high, leading to inter- and intra- molecular cross-linking and inactivation of the peptide's antimicrobial activity, which makes the characterization of such modified biopolymers highly challenging. Accordingly, various spectrophotometric evaluations of differently stained (with TNBS and Coomassie Brilliant Blue G-250 dyes) samples were used, followed by zeta-potential measurements and chromatographic vs. electrophoretic separation techniques, for quantitative and qualitative determination of the ϵ PL or OAK immobilised to the GEL.

The quantification of free and available side amino (ϵ -NH₂) groups on the reference and ϵ PL/OAK-treated GEL solutions after the reaction with TNBS was determined based on the spectroscopic method and using Eq. 4.1. The highest reduction of ϵ -NH₂ groups (Table 5.4, first column) was identified in GEL samples functionalised by the enzymatic (~90.6 % for ϵ PL and ~88.8 % for OAK) approach, being followed by chemical *grafting-to* (~87.9 % for ϵ PL and ~86.2 % for OAK) and chemical *grafting-from* (~84.2 % for ϵ PL and ~85.5 % for OAK) approaches, indicating on the highest interactions of reactive ϵ -NH₂ groups of GEL with ϵ PL/OAK by enzymatic mediated reaction using TGase. The observed decrease of ϵ -NH₂ groups in the case of reference GEL samples (Ref GEL compared to Ref GEL+TGase vs. Ref GEL+EDC/NHS), being higher for the Ref GEL+TGase (~49.3 % reduction: from 1072 ± 78.2 μ mol/g to 544 ± 16.3 μ mol/g) than for the Ref GEL+EDC/NHS (~37.3 % reduction: from 1072 ± 78.2 μ mol/g to 671 ± 40.3 μ mol/g) indicate also the GEL self-cross-linking by both reagents (enzyme TGase and EDC/NHS crosslinkers), being well in agreement with previous studies [79, 154, 174, 175]. Both reagents also induce the cross-linking of ϵ PL, as well as OAK itself, being evident by the reduction of ϵ -NH₂ groups by ~59.3 % (from 4850 ± 390 μ mol/g at Ref ϵ PL to 1975 ± 64 μ mol/g at Ref ϵ PL+EDC/NHS) and by ~15.6 % (from 3733 ± 226 μ mol/g at Ref OAK to 3151 ± 92 μ mol/g at Ref OAK+EDC/NHS) in the case of ϵ PL and OAK,

respectively, which was higher than expected. This may also be due to the concealment of non-cross-linked ϵ -NH₂ groups in polymerised ϵ PL/OAK peptides which, thus, may not be available for the reaction with the TNBS reagent due to possible steric hindrance [176]. Nevertheless, as the amounts of ϵ -NH₂ groups in the case of Ref GEL+ ϵ PL (being prepared without the crosslinking reagents EDC and NHS) did not change significantly (9.7 % increase), it may be concluded that ϵ PL/OAK peptides were bound successfully onto the GEL macromolecule. Besides, the cross-linking of GEL, as well as the ϵ PL/OAKs, may also occur simultaneously, being, however, less significant in the case of using EDC/NHS reagents than TGase. The coupling catalyzed by TGase, namely, based predominantly on the reaction between the γ -carboxamide group of glutamyl residues (from GEL, as a residue of glutamic acid) and the ϵ -NH₂ group of lysine residues (which may be from ϵ PL/OAKs, as well as the GEL) resulting in a ϵ -(γ -glutamyl)-lysine linkage [177], and secondly by deamidation of the γ -carboxamide groups of Gln to glutamate, by water molecules acting as the acyl acceptor. The TGase can thus, modify proteins by catalysing the amine incorporation, cross-linking and deamination [178, 179, 180], all of the reactions being responsible for the reduction of ϵ -NH₂ groups. TGase show high activity in a wide pH-range, *i.e.* between pH value 5 and 8 but, nevertheless, protonation of ϵ PL/OAK's amino groups (with pKa \geq 9) is possible at pH \sim 7, which was used through the enzymatic grafting, making them inaccessible for the reaction with the analytical reagent (GEL or TNBS).

It may be concluded that the chemical *grafting-to* approach was quantitatively the most successful related to the immobilization of both ϵ PL and OAK to GEL, followed by the *grafting-from* approach, where the simultaneously present self-cross-linking of ϵ PL was more significant compared to OAK. In the case of TGase grafting, the self-crosslinking of both GEL and ϵ PL/OAK affected its lower immobilization efficacy.

Total protein concentrations of the reference and differently ϵ PL/OAK-treated GEL samples were determined according the Bradford method using Coomassie Brilliant Blue G-250 dye that binds strongly to the all basic amino acids (primarily arginine, lysine and histidine, but also to tryptophan, tyrosine and phenylalanine residues, being available in GEL macromolecules or lysine, in ϵ PL/OAK). In GEL macromolecules, the amino acids are joined together by the peptide bonds between the carboxyl and amino groups of adjacent amino acid residues and, since the GEL structure is a stick-shaped molecule, it is reasonable that

the ϵ PL has a higher amount of available amino groups. An increased value for all ϵ PL/OAK-treated GEL samples (Table 5.4, second column) was obtained compared to the reference GEL sample, among which the EDC/NHS treatment resulted in the most intensive colouration in the case of the *grafting-to* approach, indicating the highest values of proteins (5.74 ± 0.23 mg/mL for ϵ PL and 2.74 ± 0.08 mg/mL for OAK), compared to the *grafting-from* (4.89 ± 0.15 mg/mL for ϵ PL and 2.73 ± 0.07 mg/mL for OAK) mechanism and the enzymatic approach using TGase (4.14 ± 0.12 mg/mL for ϵ PL and 1.62 ± 0.08 mg/mL for OAK), being again significantly higher compared to all the references showing content of proteins between 1.58 and 2.05 mg/mL for ϵ PL and between 0.041 and 2.730 mg/mL for OAK. The exception is the starting concentration (5 mg/mL) of the ϵ PL, with many available charged amino groups, which resulted in higher absorbance intensity and, thereby, protein content, in a solution of 6.79 ± 0.11 mg/mL (Ref ϵ PL). The concentration of the OAK (Ref OAK) was equivalent to its starting concentration (0.05 mg/mL).

By subtracting the supernatant concentration in the solution after the GEL treatment from the starting concentration of ϵ PL/OAK, **the quantity of ϵ PL/OAK immobilised on the GEL** was determined (Table 5.4, third column). The highest quantity of ϵ PL/OAK coupling was accessed for the GEL treated by the chemical *grafting-to* approach (~ 10.65 mg of ϵ PL and ~ 0.026 mg of OAK per mg of GEL). The *grafting-from* approach showed a somewhat lower grafting efficacy (~ 5.40 mg of ϵ PL and ~ 0.025 mg of OAK per mg GEL), being additionally reduced to ~ 3.53 mg of ϵ PL and ~ 0.008 mg of OAK by using the enzymatic coupling.

The fluorescence spectroscopy of the reference and differently ϵ PL-treated GEL samples using FITC-labelled ϵ PL (ϵ PL-FITC) was also performed to be more sensitive in quantification [181] of the immobilised ϵ PL on the GEL, although the control sample (Ref GEL, Table 5.4, fourth column) exhibited some fluorescence already by itself due to the presence of the fluorescent constituent pyridinoline and the pentosidine cross-links [182]. The significant increase in fluorescence intensity for all GEL samples treated with ϵ PL-FITC can be observed compared to the Ref GEL (~ 350 FU), indicating the highest immobilization of ϵ PL-FITC in the case of *grafting-to* ($\sim 19\,200$ FU), and followed by the *grafting-from* ($\sim 18\,000$ FU) and enzymatic ($\sim 13\,300$ FU) coupling approaches. The results are in good agreement with the other spectrophotometrically-evaluated results.

Table 5.4: The quantity of side ϵ -NH₂ groups [$\mu\text{mol/g}$ sample], the total protein content [mg/mL] and the fluorescence intensity [FU] of the references and $\epsilon\text{PL/OAK}$ -functionalised GEL samples, being evaluated through their staining with TNBS and Coomassie Brilliant Blue G–250, as well as by using unlabelled and FITC-labelled ϵPL

Samples	By using $\epsilon\text{PL/OAK}$			By using FITC-labelled ϵPL
	<u>$\mu\text{mol of } \epsilon\text{-NH}_2$ per g of sample</u> by staining of $\epsilon\text{-NH}_2$ groups of samples with TNBS at $\text{pH} \sim 8.5$	<u>mg protein per mL of sample solution</u> by staining of all primary NH ₂ groups with Coomassie Brilliant Blue G– 250 at $\text{pH} \sim 3$	<u>mg $\epsilon\text{PL/OAK}$ per mg of GEL</u> by subtracting the supernatant concentration in the solution after the GEL treatment from the starting $\epsilon\text{PL/OAK}$ concentration	Measurement of fluorescence intensity [FU] of sample solutions ($\text{Ex}=492 \text{ nm}$, $\text{Em}=522 \text{ nm}$)
Ref GEL	$1\,072 \pm 37$	1.58 ± 0.02	/	349 ± 18
Ref GEL+EDC/NHS	671 ± 15	2.73 ± 0.03	n.d.	$1\,211 \pm 28$
Ref ϵPL	$4\,850 \pm 153$	6.79 ± 0.11	/	$7\,382 \pm 179$
Ref $\epsilon\text{PL+EDC/NHS}$	$1\,975 \pm 45$	1.48 ± 0.04	n.d.	$10\,899 \pm 291$
Ref GEL+ ϵPL	$1\,176 \pm 25$	2.05 ± 0.05	n.d.	$7\,903 \pm 322$
Ref OAK	$3\,733 \pm 79$	0.05 ± 0.004	/	n.d.
Ref OAK+EDC/NHS	$3\,151 \pm 113$	0.04 ± 0.001	n.d.	n.d.
<i>Enzymatic</i> ϵPL	224 ± 34	4.14 ± 0.12	3.53 ± 0.12	$13\,285 \pm 923$
<i>Grafting-from</i> ϵPL	377 ± 26	4.89 ± 0.15	5.40 ± 0.40	$17\,975 \pm 979$
<i>Grafting-to</i> ϵPL	287 ± 15	5.74 ± 0.23	10.65 ± 0.51	$19\,167 \pm 843$
<i>Enzymatic</i> OAK	354 ± 27	1.62 ± 0.08	0.0083 ± 0.0001	n.d.
<i>Grafting-from</i> OAK	457 ± 30	2.73 ± 0.07	0.0251 ± 0.001	n.d.
<i>Grafting-to</i> OAK	435 ± 34	2.74 ± 0.08	0.0257 ± 0.001	n.d.

The ZP curves of the reference and ϵ PL/OAK-treated GEL solutions were performed in the pH range of 2–11 to obtain more information on the ϵ PL/OAK immobilization onto the GEL macromolecules, as well as to identify possible physical adsorption. As seen from Fig. 5.10, the hyperbranched ϵ PL (Ref ϵ PL) [183] with high amounts of amino groups, shows a highly positive ZP value of around +21 mV at pH 2, being reduced to -25 mV at pH 10 due to the dissociated end-carboxylic groups, by passing the x-axis at $\text{pH} \sim 7.9$. On the other hand, the lines for the Ref GEL+ ϵ PL and differently ϵ PL-functionalised GEL samples shows a similar trend to that for the pure GEL (Ref GEL), however, with slightly lower ZP values in the pH range of 2–5 and the pI shifting to higher pH (from $\text{pH} \sim 5$ at GEL to $\text{pH} \sim 5.8$ at Ref GEL+ ϵ PL, to $\text{pH} \sim 6.8$ in samples prepared by *grafting-from* and TGase induced coupling chemistry, and to $\text{pH} \sim 7.9$ in samples prepared by the *grafting-to* approach). Changes in the ZP in the presence of peptide may be caused by the following three different effects occurring simultaneously: i) The displacement of the counter-ions in the Stern layer due to polymer adsorption, ii) The blockade of solid active sites by the previously adsorbed polymer chains, or iii) The presence of functional groups in macromolecules [106, 184]. This may indicate that some part of ϵ PL is immobilised (adsorbed) physically on the GEL (*i.e.* being not removed entirely during the washing process) and that the chemical *grafting-to* approach is the most effective related to the ϵ PL coupling. In addition, the relatively gradual slope of the zeta-potential titration curve for pure GEL may indicate its tight hydrogel structure, which slope however is not changed by the presence of highly branched and charged ϵ PL as would be expected. On the contrary, the amount of displaced counter-ions was reduced significantly than that in the case of ϵ PL, which may indicate ϵ PL self-crosslinking and coupling to the GEL surface by possibly forming structure rich in numerous loops and tails [185].

A much different course of the ZP curve was observed for the OAK and OAK-functionalised GEL, compared to the ϵ PL-related samples, reflecting the difference in the structure of grafted peptides. OAK-functionalised GEL samples show the positive ZP values (≥ 15 mV) in all pH ranges, which may be attributed to the hydrophobic effects of its alkyl chains, which can easily induce OAK self-aggregation [80]. The zeta potential is reduced at pH 7 due to the branched architecture of the available surface charges on the OAK. In differently prepared OAK-functionalised GEL samples, small changes of ZP values are observed at low ($\text{pH} < 4$)

and high ($\text{pH} > 9$) pH values with an equivalent drop at pH 7, being related to the type of coupling chemistry and the conformation phenomena of the OAK [186].

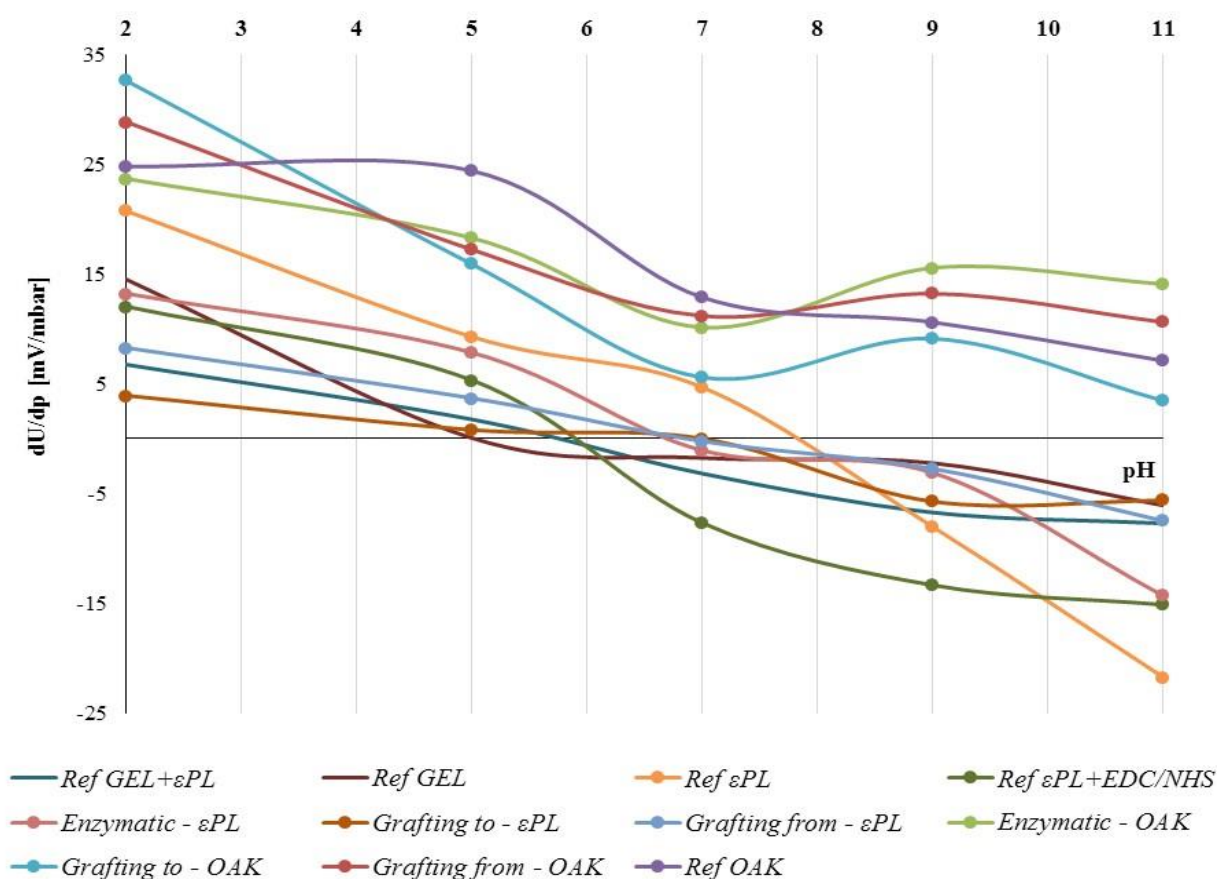


Figure 5.10: ZP curves of the reference and differently ϵ PL/OAK-functionalised GEL samples as a function of pH. Each value of the zeta-potential at a given pH value represents an average value over at least three individual measurements, where the standard deviation was less than 3 %, respectively.

Size-exclusion chromatography (SEC) was used to evaluate both the efficacy and structure of ϵ PL-treated GEL macromolecules (Fig. 5.11 a), based on their separation followed by differences in their hydrodynamic volumes being related to both the MWs and chemical composition of both components [145]. In order to improve the sensitivity and selectivity of detection, FITC-labelled ϵ PL (ϵ PL-FITC) was used and the SEC was performed by using the VWD and FLD detectors. In addition, as the sample can be affected strongly by repulsive/attractive inter/intra-molecular interactions within the column and other solution effects such as molecule associations, the phosphate buffer and sodium azide solution of

pH 7.5 as a mobile phase was used to put them on a minimum. Reaction products of GEL-OAK could not be analysed by SEC, due to the very weak signals identified, which we assume is caused by the 100-fold lower initial concentration of OAK compared to the ϵ PL.

By using the **UV detection** (Fig. 5.11 a), the control GEL sample (Ref GEL) displayed one broad peak with a max at ~ 6.9 min, corresponding to an average MW of 77 kDa, determined from the calibration curve estimated by using Pullulan standards with known MWs in the range between 1000 – 380 000 g/mol [187]. An increase in MW was observed for all ϵ PL-FITC functionalised GEL solutions that corresponded to shorter elution times eluting as broad asymmetrical peaks with the maximum at ~ 6.3 min, ~ 6.7 min and ~ 6.9 min for samples prepared by *grafting-from*, *grafting-to* and enzymatic coupling approaches, respectively, their increase and broadening, which suggest an increase of its hydrodynamic volume due to the immobilised ϵ PL-FITC. As the amount of bound ϵ PL-FITC with the *grafting-to* approach is the highest (based on the previously presented spectrophotometric and ZP evaluation methods), the formation of ϵ PL-FITC+GEL products with the highest hydrodynamic volume than either of the other two products is evidenced by a twice-larger peak area with two maximums at ~ 6.7 min and ~ 7.9 min, which may indicate a flexible hyper-branched structure. In addition, as the Ref GEL+ ϵ PL sample displayed a significant difference, *i.e.* reduction in peak area and elution at ~ 7.1 min compared to the Ref GEL, an increase in hydrodynamic volumes and their shifting to lower elution times of ϵ PL-GEL products may provide additional evidence for the formation of strongly interacting GEL with ϵ PL molecules. Besides, an obvious peak shifting from ~ 8.4 min to one broad peak with two maximums at ~ 7.2 min and ~ 7.7 min for ϵ PL and ϵ PL treating with EDC/NHS, respectively, indicates ϵ PL self-cross-linking (the formation of amide bonds between the free amino and carboxylic groups of the ϵ PL polypeptide chain may occur). Two additional peaks that appear at around ~ 11 min and ~ 12.7 min are legitimate system peaks, resulting from the mobile phase components (phosphate buffer) due to their absence in the injected sample [188, 189]. A decrease in the elution time was consistent with an increase in the MWs, which revealed wide distributed ϵ PL-GEL products with average MWs of ~ 486 kDa, ~ 103 kDa and ~ 300 kDa corresponding to *grafting-to*, *grafting-from* and *enzymatic* coupling approaches, respectively.

By **fluorescence detection** evaluated sample solutions (Fig. 5.11 b) show a similar trend. The apparent MW's of products increases with increasing of the grafting density and ϵ PL content, being the largest using the *grafting-to* approach. An increase in MW was observed that corresponded to the expected products. The ϵ PL-GEL product functionalised using the *grafting-to* approach showed the greatest shift with a broad peak containing two maximums at ~ 6.5 min and ~ 7.1 min, whereas samples prepared by the *grafting-from* approach displayed a peak with the maximum at the same time as Ref GEL (~ 6.9 min), but with broader molar mass distribution. The enzymatically functionalised GEL appeared midway between the other ϵ PL-GEL conjugate products (~ 6.8 min) as expected.

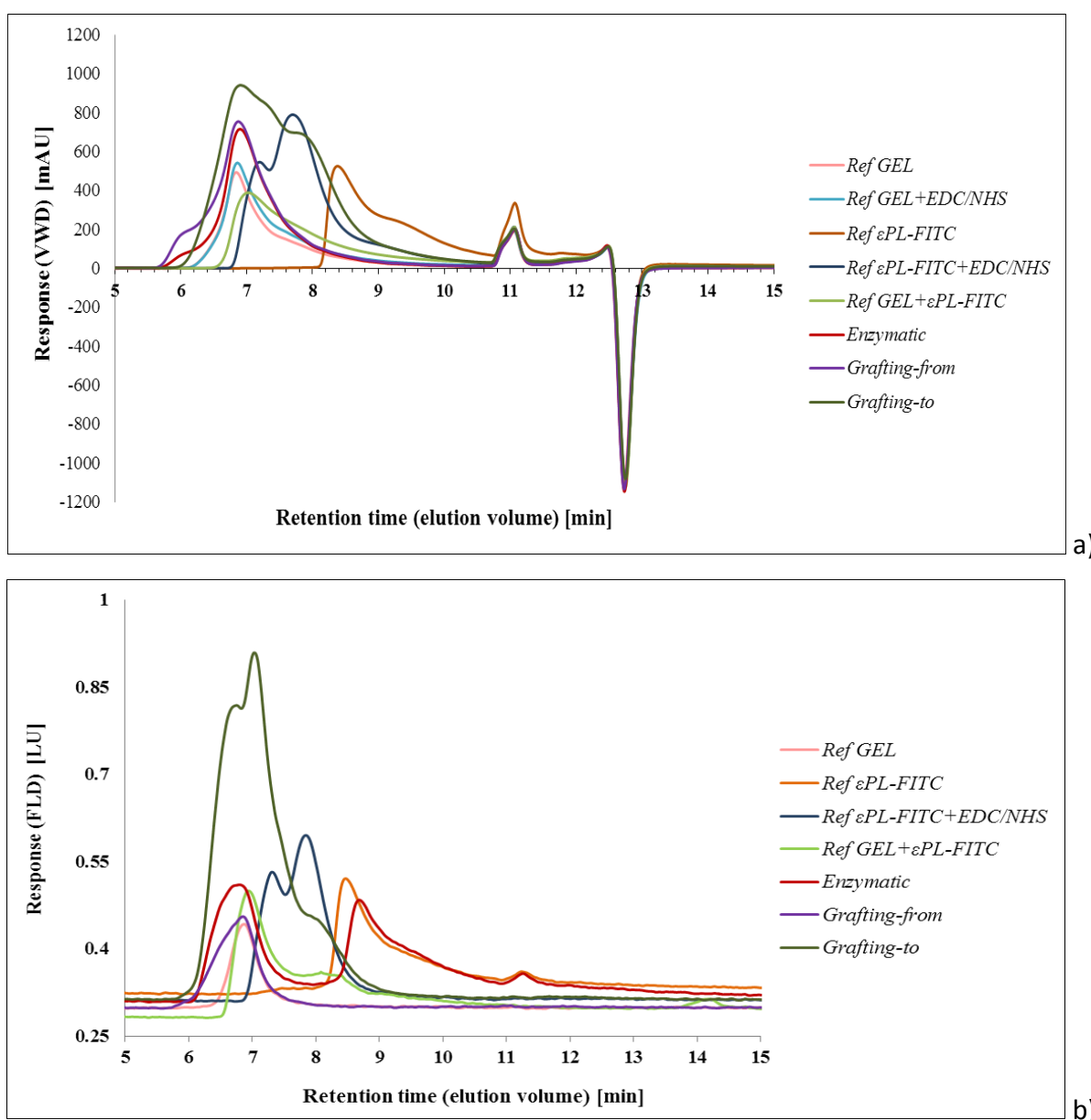


Figure 5.11: HPLC-SEC chromatograms of the reference and differently ϵ PL-FITC functionalised GEL samples being separated by 150 mM phosphate buffer and 5 mM sodium

azide solution of pH 7.5 as the mobile phase and evaluated by a) UV detection (at 210 nm) and b) fluorescence detection (Ex at 492 nm and Em at 522 nm). All displayed spectra are the accumulation of at least two scans.

High-sensitive **CZE** was used as a more advanced separation technique to identify the unbound ϵ PL and OAK from their bound (to GEL) or self-crosslinked form, based on differences in electrophoretic mobility [190] of the reference and differently ϵ PL/OAK treated GEL samples, being related to their differences in molecular size and surface charge. As seen in Fig. 5.12, successful separation of products by CZE provided a three-step profile in which the starting Ref GEL is followed by the zone of ϵ PL/OAK-functionalised GEL products and the profiles terminated by a plateau corresponding to the Ref ϵ PL and Ref OAK, respectively. GEL with a higher ϵ PL/OAK grafting yield possesses a lower extent of carboxylic groups and, thus, exhibits lower negative charges (and, thus, more negative zeta potential, Fig. 5.10) in the carrier electrolyte buffer with a pH of 9.3 used in the present study. The stronger the negative charge of the electrolyte, the slower is the observed mobility of the electrolyte toward a cathode due to the presence of strong electroosmotic flow [191]. Since in the presence of EDC/NHS, the coupling or crosslinking of ϵ PL/OAK itself can be a competitive reaction with the grafting to GEL-macromolecules, all the reference samples were also analysed. The analysis indicated that EDC/NHS changed ϵ PL molecules to larger and less charged ones (being seen in an increase of ϵ PL peak area and its shifting from ~ 5.9 min to one broader peak consisting of two maximums at ~ 6.2 and ~ 7.0 min), which may be related to the ϵ PL self-cross-linking and formation of differently structured aggregates, being well in correlation with the highly negative ZP value of around -14 mV at pH 9 (Fig. 5.10) and SEC analysis (Fig. 5.11), indicating a flexible structure, forming loops or tails. However, since all control samples (Ref GEL, Ref GEL+ ϵ PL, Ref GEL+EDC/NHS, Ref ϵ PL+EDC/NHS, Ref GEL+TGase) migrated with different electrophoretic mobility compared to the ϵ PL/OAK functionalised GEL samples, eluting at $\sim 7.8/\sim 6.5$ min for the *grafting-to* approach, at $\sim 4.6/\sim 6.0$ min for the *grafting-from* approach and at $\sim 4.6/\sim 7.2$ min for the enzymatic approach, respectively, we can conclude, that the coupling of both ϵ PL and OAK onto GEL molecules was performed successfully. It was also observed that samples with higher ϵ PL grafting yield exhibited longer migration time, being related to their larger molecular sizes and multiplier charges (*i.e.* numbers and pKa values of their weak base

protonated groups and carboxylic acid groups). Cations elute first in an order corresponding to their electrophoretic mobilities, with small, highly charged cations eluting before larger cations possessing high ϵ PL density. Finally, anions are the last components to elute, with smaller, highly charged anions having the longest elution time (as the Ref OAK).

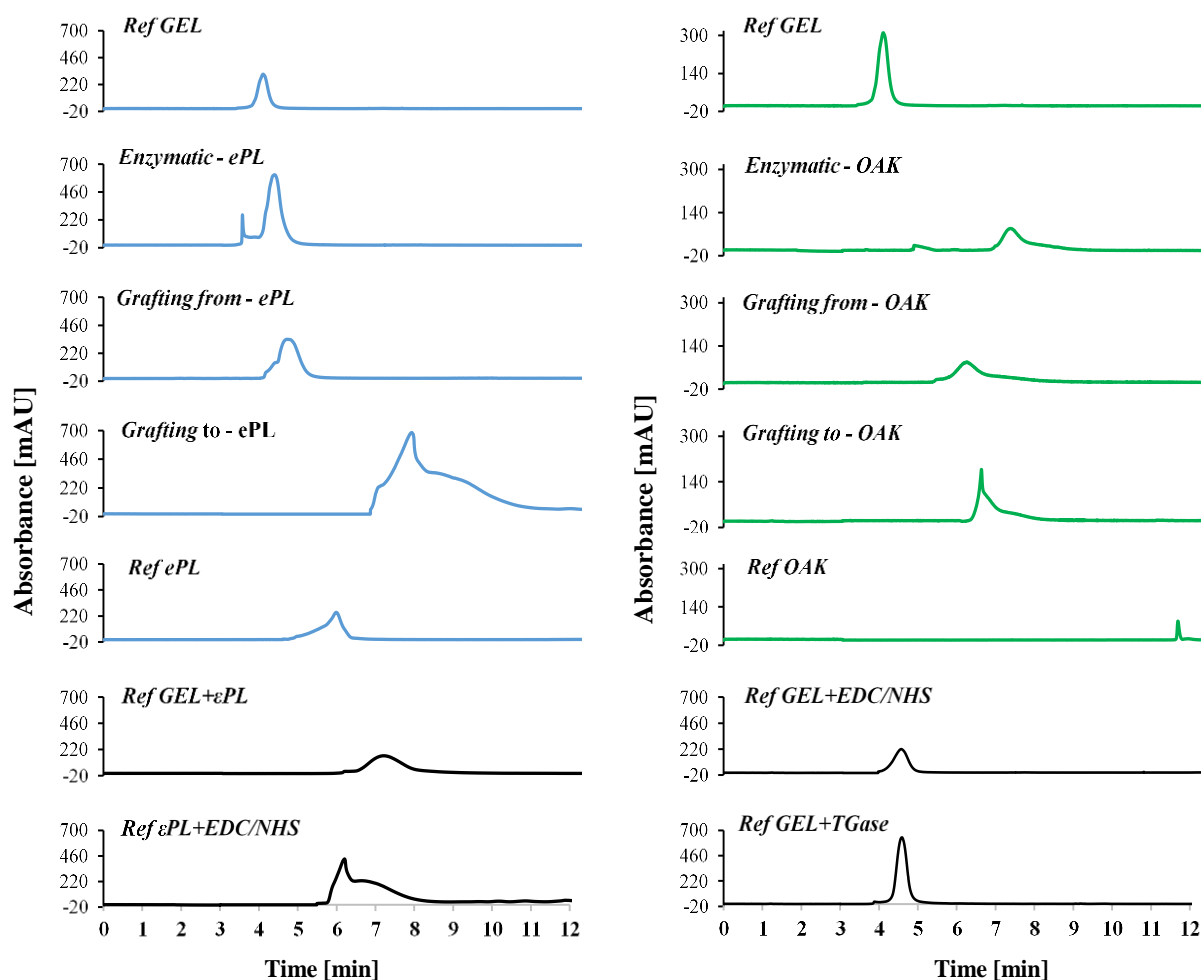


Figure 5.12: Capillary electropherograms of the reference and differently ϵ PL/OAK-functionalised GEL samples. The samples were analysed at pH 9.3 using a 100 mM borate buffer as the mobile phase. All spectra are displayed as the accumulation of three scans.

5.2.2 Orientation and localization of ϵ PL/OAK on GEL macromolecules

In order to evidence the information about conformational dynamics and binding of polypeptide ϵ PL onto complex GEL macromolecules, which may have a significant role on the antimicrobial activity of the coupling product, the **EPR spectroscopy** was implemented [147, 148].

The ϵ PL was labelled with the 3-maleimido-proxyl (MP) molecule, which possesses an unpaired electron (*i.e.* a stable nitroxide radical) being used to determine its potential mobility changes in its micro environment and different ϵ PL-MP containing samples, thus, the information on the orientation of site-specific immobilised ϵ PL-MP on GEL. Presuming that all MP molecules are tethered covalently to ϵ PL through their amino groups' availabilities, line-shape differences among samples thus yield information about their structural environments. In the fast tumbling limit ($10^{-11} < \tau_c < 10^{-9}$ s), the EPR spectrum of the MP's nitroxide namely consists of three anisotropic lines, the broadenings of which generally indicate MP immobilisation, whereas their sharpening indicates an increase in MP mobility. If the MP is, thus, attached to a molecule that is sufficiently small or flexible, it exhibits an isotropic EPR spectrum, as seen in Fig. 5.13, presenting a clean triplet signal of ϵ PL-MP being typical for nitroxide within the fast-motional regime where τ is below 1 ns. In contrast, if the mobility of the MP's nitroxide is restricted, a less isotropic EPR line-shape would be observed due to the unpaired electron of the MP residing in a molecular orbital 2p along the N–O bond [166].

The EPR spectra of the GEL being functionalised with ϵ PL-MP by different approaches displayed different patterns of the characteristic MP's nitroxyl triplet signal, as well as different rotational correlation times, which can be associated with the modes of coupling chemistry and the approach used. Rotational correlation times on ϵ PL-MP functionalised GEL were significantly higher than those for ϵ PL-MP ($\tau \approx 0.11$ ns), that may be attributed to a gain of rigidity arising from its grafting onto GEL molecules. The MP attached to a molecule with sufficient slow rotational correlation times ($\tau \approx 1.60$ ns) exhibits a broader EPR spectrum typical for a completely immobilised sample, as in the case of the chemical *grafting-from* approach. Depending on the degree of ϵ PL-MP immobilisation, partially broadened spectra may also be observed in the enzymatic TGase grafted ϵ PL-MP, indicating the mobility of an intermediate time scale ($\tau \approx 1.24$ ns). As the τ of the ϵ PL-MP functionalised GEL by the *grafting-to* mechanism is the lowest ($\tau \approx 0.27$ ns), it suggests that a *grafted-to* ϵ PL-MP has higher mobility and, thus, indicates that ϵ PL molecules are linked to the GEL within a highly-flexible (brush-like) structure. On the other hand, in the case of the *grafting-from* approach, the ϵ PL-MP may also be coupled to GEL by ϵ PL side amino groups leading to a splitting of grafted ϵ PL chains into several parts forming loops or tails similar to

the brush-like layer [130], being already observed by ZP, SEC and CZE analysis. In the case of TGase grafted ϵ PL-MP a broad EPR spectrum is exhibited, typical for a partially immobilised sample, since the α -helical conformation may also occur.

Reaction products of OAK-MP could not be analysed by EPR, due to the very weak signals identified, which we assume is caused by low coupling efficiency of MP spin-label to OAK being related to higher reactivity of the maleimide group of MP with sulfhydryl residues than the amine [192], which was used as a consequence of the absence of Cys residues.

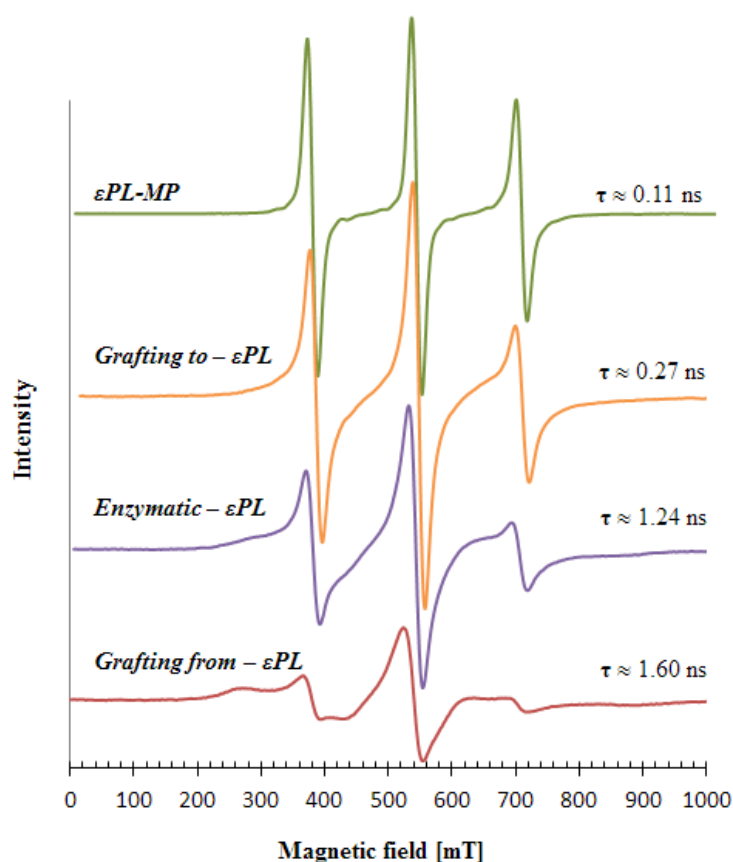


Figure 5.13: EPR spectra of 3-maleimido-proxyl (MP) spin-labelled ϵ PL (ϵ PL-MP) in comparison with the GEL- ϵ PL-MP products prepared by different coupling approaches. All displayed EPR spectra are the accumulation of three scans.

5.2.3 Antibacterial activity of ϵ PL/OAK-functionalised GEL

The driving physical forces behind antibacterial activity of cationic AMPs have been well studied [193, 194, 195] and include net positive charge (enhancing interaction with anionic lipids and other bacterial targets), hydrophobicity (required for membrane insertion and

often driven by this process), and flexibility (permitting the peptide to transition from its solution conformation to its membrane-interacting conformation). Each of these characteristics can vary substantially over particular range, but are essential for the function of the AMPs and allow them to interact with bacterial membranes, which is critical to their exertion of antimicrobial effects.

The results of the *in vitro* growth-inhibitory activities of the reference and ϵ PL/OAK-functionalised GEL samples are shown in Fig. 5.14. ϵ PL-functionalised GEL showed a significant level of bacterial reduction, among which the ϵ PL-functionalised sample using the *grafting-to* approach exhibits the highest reduction ability to both bacteria (~ 96 % to Gram-positive *S. aureus* and ~ 81 % to Gram-negative *E. coli*), followed by *grafting-from* and *enzymatic* approaches with the reduction abilities of ~ 72 % and ~ 63 % for *E. coli* and ~ 85 % and ~ 76 % for *S. aureus*, respectively, after 24 h of exposure. In comparison, OAK-functionalised GEL using the *grafting-to* approach also showed significant reduction of both bacteria (~ 82 % for *S. aureus* and ~ 77 % for *E. coli*), despite the fact, that the initial concentration of OAK was 100-fold lower as compared to the ϵ PL (0.05 g/L vs. 5 g/L) and 400-fold lower immobilization efficacy (Table 5.4, ~ 0.0257 vs. ~ 10.65 mg/g), evaluated by the Bradford method.

While the antibacterial activity of ϵ PL depends on its cationic character and can be achieved by containing at least ten monomeric lysine residues [27, 74] and concentrations less than 0.1 mg/mL [25, 197], the OAK (K-7 α_{12} -OH) with eight Lys residues and hydrophobic chains exhibits even more effective antibacterial activity. To explain the observed differential activities, it is tempting to implicate the peptides' differential structural features. Thus, due to its extra acyl moieties, the OAK may be able to employ both the charge and hydrophobic attributes for enhancing its interactions with bacteria. Consequently, the OAK might be more efficient in affecting bacterial viability than the less hydrophobic ϵ PL. Support for this view can be drawn from previous findings comparing bacterial capture capacities of this specific OAK and a 15-residue ϵ PL when each peptide was conjugated to polystyrene beads. In this configuration, the OAK-linked bead was shown to inhibit ~ 1000 -fold more bacteria than its ϵ PL-based counterpart [38].

However, the reduction of Gram-positive *S. aureus* was again higher and further reduced from the *grafting-from* (~ 80 %) to *enzymatic* (~ 67 %) coupling approach compared to those

obtained for Gram-negative *E. coli* showing ~53 % and ~40 % bacteria reduction, respectively. Indeed, since acylated Lys of OAK is arranged to create an optimal molecular amphipathic structure, it means having both a cationic region and a hydrophobic region, which associate with one another to protect the hydrophobic side and expose the cations to interact with the bacterial membrane [81], their interaction with bacteria is enhanced [80].

The apparent decrease of bacteria viability reflects the higher resistance of Gram-negative *E. coli* with ZP from -4 mV to -44 mV [198, 199, 200], depending on its physiological state or growing conditions, as well as buffer additives whose factors influence the electrophoretic behaviour. The presence of an additional layer of negatively charged LPS in Gram-negative bacteria as compared to Gram-positive bacteria, leads to the higher negative potential of *E. coli* than that of *S. aureus* [199], being attributed to its complex cell wall structure that is comprised with multiple layers in which an outer membrane layer containing long chain LPS in its outer leaflet and phospholipids in the inner leaflet which lie on top of a thin peptidoglycan layer (which is much thicker in Gram-positive bacteria). Such a thick cell wall structure restricts the penetrations of chemicals as well as antimicrobial agents. On the other hand, Gram-positive bacteria with surface potentials ranging from ~ -14.7 to ~ -20.6 mV have a mesh-like peptidoglycan layer, being more accessible to permeation by the agents [168].

The cationic and hydrophobic nature of an AMP provides initial interaction with the negatively-charged LPS of the Gram-negative cell surface, [201, 202] as well as with the teichoic and teichuronic acids in Gram-positive bacteria [203] and, as such, create stress, leading to enhancement of cell permeability [200]. In addition, although the likely mechanism of material' bactericidal activity is in its direct contact with bacteria [204], highly dispersed solutions have more chances to interact with bacterial cells directly than aggregated ones. From that point of view, although the cell wall of *E. coli* is more negatively charged, ϵ PL-functionalised GEL by the *grafting-to* approach (and ZP of ~0.02 mV at pH 7) induced a significant loss of viability on *E. coli* (~81 %) and the OAK-functionalised GEL with ZP of -38 mV at pH 7 showed satisfactory bacteria reduction (> 60 %).

The zone of inhibition after overnight incubation of the samples with relevant bacteria (the data are inserted in the graphs in Fig. 5.14) indicate larger zones of inhibition growth for *S. aureus* (zone diameters between ~1.1 and ~1.9 mm) in comparison with growth for *E. coli*

(producing zone diameters between ~ 0.5 and ~ 0.8 mm), being again the largest for the ϵ PL-functionalised GEL product prepared by the *grafting-to* approach. The testing of OAK-functionalised GEL samples was not possible due to insufficient amounts of samples.

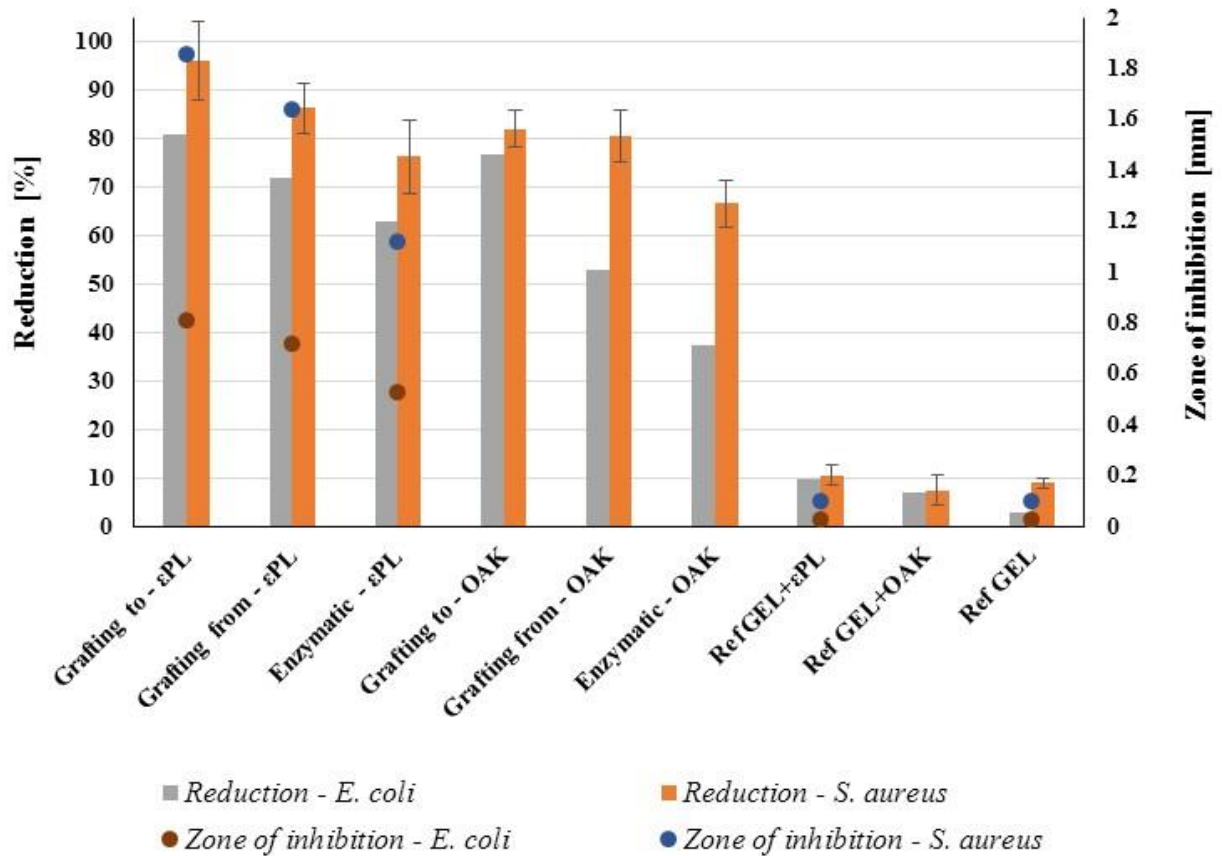


Figure 5.14: Reduction of CFU number of Gram-negative bacteria *E. coli* and Gram-positive bacteria *S. aureus* and zone of inhibition after 24 h of exposure to the reference and differently ϵ PL/OAK-functionalised GEL samples determined by modified broth-dilution and agar-diffusion assays.

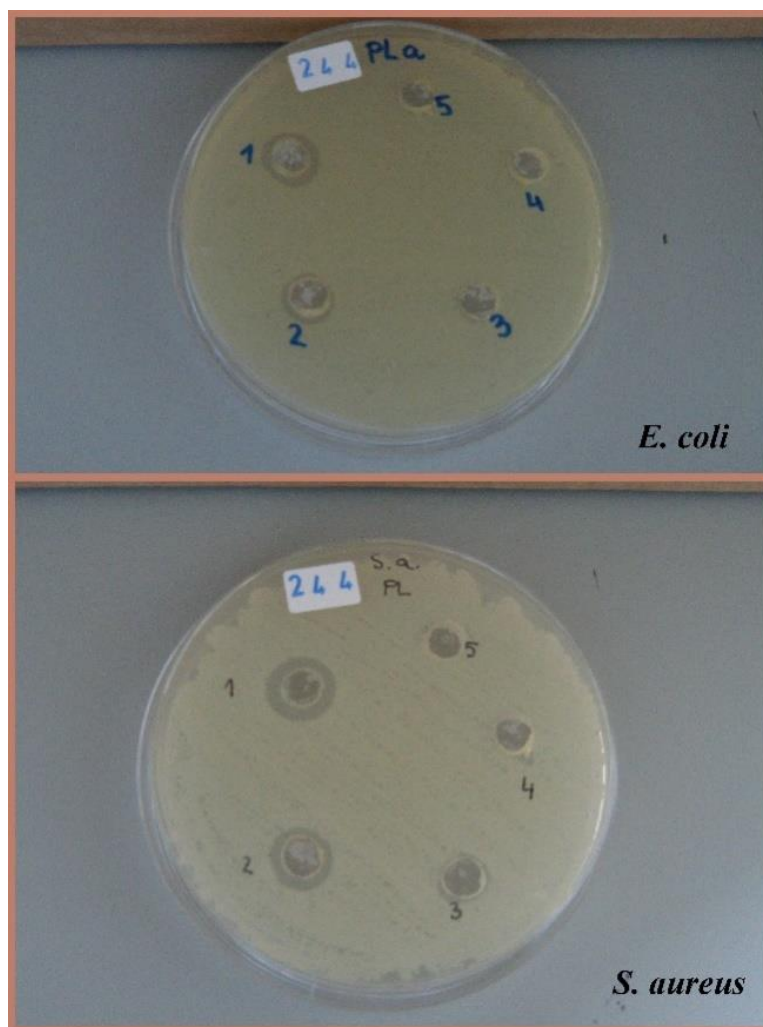


Figure 5.15: The zone of inhibition after modified agar diffusion test used for determination of antibacterial efficacies of GEL samples against Gram-negative bacteria *E. coli* (top image) and Gram-positive bacteria *S. aureus* (bottom image).

1: grafting to- ϵ PL, 2: grafting from- ϵ PL, 3: enzymatic TGase- ϵ PL, 4: Ref- ϵ PL, 5: Ref-GEL

5.2.4 Cytotoxicity of ϵ PL/OAK-functionalised GEL

The *in vitro* osteoblasts (hFOB) viability testing were performed on the GEL and ϵ PL/OAK-functionalised GEL samples prepared according to the chemical *grafting-from* approach to assess the cytotoxic/citostatic influence of the materials and functional response of the cells. The results presented in Fig. 5.16 revealed that OAK-functionalised GEL (GEL-OAK) induced no distinct cytotoxic impact on the cell growth, and no zone of inhibition was visible after 24 h of incubation in culture media. In contrast, the presence of ϵ PL-functionalised GEL (GEL- ϵ PL) expressed a low level of stress to the cells, visible through lower cell density than in the non-cytotoxic control, as well as irregular sizes, withered, and coarse surfaces, forming aggregations that caused ~ 72.1 % lysis of hFOB cells at concentrations corresponding to ~ 25 -fold of ϵ PL's MIC values, ranging from 2 to 12.5 $\mu\text{g}/\text{mL}$ [197, 205, 206].

Further dilution of the initial solutions improved the viability of the ϵ PL-functionalised GEL sample indicating recovery of the cell metabolic activity for concentrations under ~ 0.27 mg/mL (1:8 dilution), and exhibited a normal morphology, similar to the negative control, and incubation with 0.135 mg/mL (1:16 dilution), as evident from Fig. 5.17. Similar results are obtained by [80] that reported cationic lipopeptides with saturated fatty acid chain length to be more lytic as compared to their unsaturated counterparts. Considering that a sample has a cytotoxic potential if its metabolic activity is reduced to less than 70 % compared to the negative control for metabolic activity decrease [207], it can be concluded that both ϵ PL- and OAK-functionalised GEL are potentially nontoxic up to a concentration of ~ 0.27 mg/mL of ϵ PL grafted (1:8 dilution) or 5 $\mu\text{g}/\text{mL}$ of OAK grafted in GEL-OAK, which is ~ 25 -fold higher than their MIC. The data also indicated no significant difference in cell viability among different concentrations of OAK (5 $\mu\text{g}/\text{mL}$, 2.5 $\mu\text{g}/\text{mL}$, 1.25 $\mu\text{g}/\text{mL}$ and 0.625 $\mu\text{g}/\text{mL}$), which is comparable to the findings for the control (Ref GEL). The result suggests that OAK does not have any effect on the viability of human cell lines, which is in accordance with previous studies [208], suggesting no or minimal physiological toxicity.

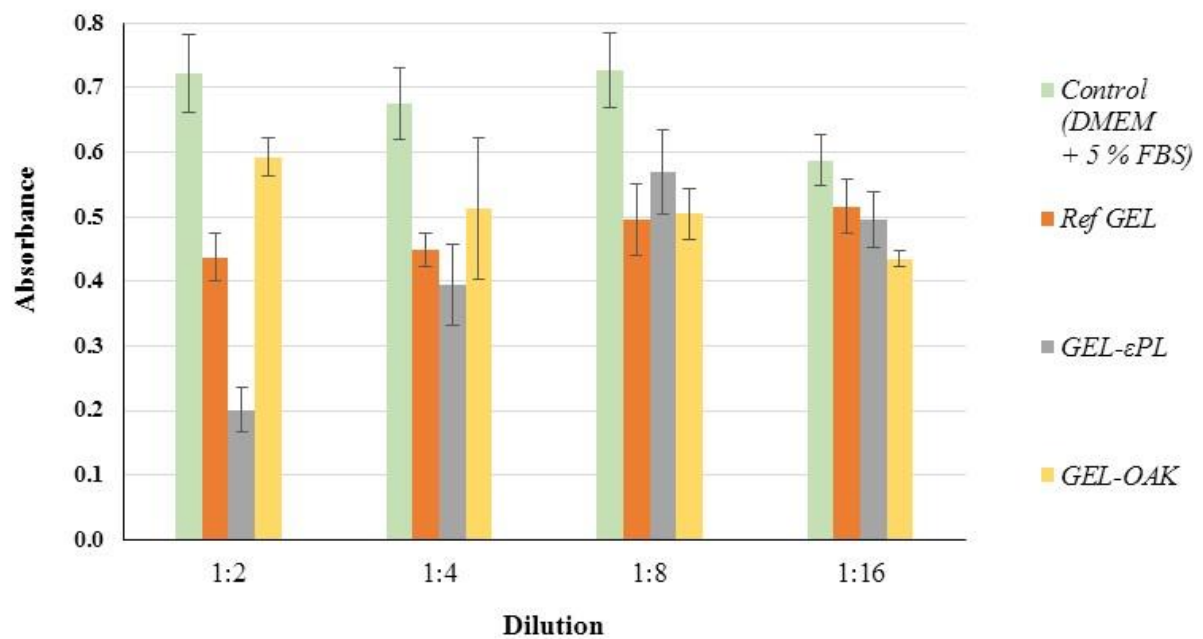


Figure 5.16: Absorbance of MTT-stained human osteoblast cells (hFOB) after 24 h of cultivation onto negative (non-cytotoxic) control and 2.5 % v/w solutions of the GEL (Ref GEL) and εPL/OAK-functionalised GEL according to the *grafting-from* approach, being diluted to concentrations of 1.250 % v/w (1:2), 0.625 % v/w (1:4), 0.313 % v/w (1:8) and 0.156 % v/w (1:16) in DMEM with 5 % fetal bovine serum (FBS) before incubation.

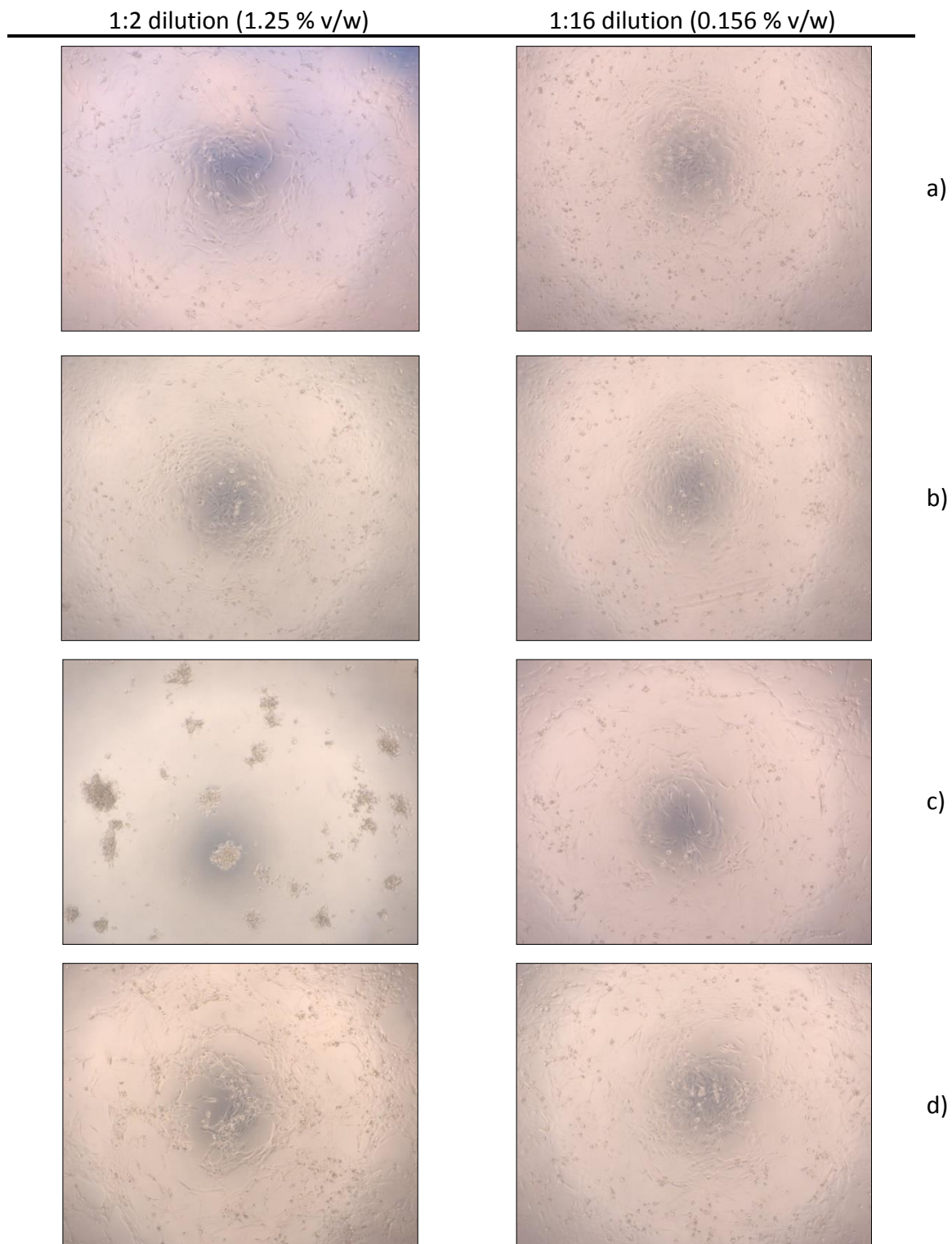


Figure 5.17: Optical micrographs (taken at 50 x magnification) of human osteoblast cells (hFOB) after 24 h of cultivation with a) Negative (non-cytotoxic) control, and 2.5 % v/w solution of b) GEL (Ref GEL) and GEL functionalised with c) ϵ PL or d) OAK according to the *grafting-from* approach and after 1:2 (to 1.25 % v/w) and 1:16 (to 0.156 % v/w) dilutions.

The differences in toxic concentrations observed for GEL grafted ϵ PL and OAK against the hFOB tested may be related to the differences in peptides' structure, the composition of the cell membrane, the metabolic activity of the cells and their exposure time to the peptides [209]. Above all, the differences in the cell surface hydrophobicity on one side and peptide structure on the other, may influence the effective binding and cytotoxic action of peptides, although the exact mechanism by which toxicity differs among different cell types is not completely elucidated [210]. The OAK's bactericidal mode of action is associated with rapid membrane depolarization and cell permeabilization, suggesting that the inner membrane is the primary target [211], while ϵ PL's bactericidal mode of action is most likely a carpet-like mechanism that causes disruption by imposing negative curvature. The ϵ PL is composed of cationic residues, and cannot interact directly with the hydrophobic parts of membranes [212].

6 SUMMARY AND OUTLOOK

The scope of this work was to examine the possibility of antimicrobially active ϵ -poly-L-lysine (ϵ PL) and oligo-acyl-lysyl (OAK) peptides to immobilize on protein-based substrates (wool fibers and gelatine macromolecules) in a way to interfere with bacteria in a different and/or specific mode (related to Gram-negative *E. coli* and Gram-positive *S. aureus* bacteria; a biocidal or biostatic way, and/or by different time-scale), and a long-lasting microbial resistant without cytotoxic effect. The results of these hypotheses can be summarized as follows:

- Bacterial minimum inhibitory (MIC) concentration of amphiphilic OAK with eight Lys residues and hydrophobic alkyl moieties is ~ 100 -times lower compared to cationic ϵ PL of approximately 70 Lys residues.
- Both ϵ PL and OAK can be covalently attached to wool fibers and GEL macromolecules by carbodiimide chemistry using *grafting-to* and *grafting-from* mechanisms as well as enzymatic by transglutaminase (TGase).
- The immobilization of ϵ PL/OAK is confirmed by different spectroscopic and separation methods, including colorimetric UV-Vis, HPLC-SEC and CZE, FTIR spectroscopy and, for the first time, EPR spectroscopy using spin-labelled ϵ PL by which the conformational dynamic of immobilised peptides is also estimated.
- The considerable difference in both the structure (hydrophilic and hydrophobic behaviour) and conformation (i.e. flexible brush-like vs. rigid layered form) of the peptides at the immobilised stage is observed, influencing on their antimicrobial activity.
- **In the case of wool**, the highest (~ 99 % against *E. coli* vs. ~ 92 % against *S. aureus*) and kinetically the fastest (3 h) antibacterial activity with ~ 83 % for *E. coli* vs. ~ 64 % for *S. aureus* bactericidal effect was determined for the wool functionalised by chemical *grafting-to* approach. Such an effect may be related to both quantitatively the highest (~ 62 g $_{\epsilon$ PL}/kg $_{\text{wool}}$) grafting yield of ϵ PL and conformationally its highly-flexible (brush-like) orientate linkage. Comparably, the enzymatic coupling (~ 50 g $_{\epsilon$ PL}/kg $_{\text{wool}}$) giving ~ 95 % and

~82 % reductions of *E. coli* and *S. aureus* respectively, being additionally reduced to ~74 % and ~78 % by using the *grafting-from* approach (~34 g_{εPL}/kg_{wool}), was identified as the less bactericidally effective (~63 % vs. ~58 %).

- A non-ionic surfactant being used in the durability testing of functionalised wool to washing, adheres strongly onto the fibres, thus blocking the amino groups of εPL, and, as such, decreases the antibacterial efficiency of the wool, being not affected in the case when the washing was carried out without surfactant.
- **In the case of GEL**, the highest level of bacterial reduction (~81 % and ~77 % against *E. coli* vs. ~96 % and ~82 % against *S. aureus*) was also achieved with GEL functionalised by the chemical *grafting-to* approach. This effect correlated again with both the highest grafting yield (~10.65 mg of εPL and ~0.026 mg of OAK per mg of GEL) and the highly-flexible (brush-like) orientation of peptides, implicating the highest amount of accessible amino groups for interaction with bacteria. The *grafting-from* approach (~5.40 mg of εPL and ~0.025 mg of OAK per mg GEL) yielded ~72 % and ~75 % reduction of *E. coli*, and was reduced further to ~63 % and ~38 % by using the enzymatic coupling chemistry (~3.53 mg of εPL and ~0.008 mg of OAK per mg of GEL).
- The up to 400-fold lower yield of OAK being grafted on GEL compared to εPL may be related to its amphiphilic structure (the cationic amino residues and hydrophobic alkyl chains), enabling its targeted and rapid interactions with bacteria membrane compared to the more hydrophilic εPL, easily causing random polymerization and self-conjugation.
- εPL/OAK-functionalised GEL did not induce toxicity in human osteoblast cells, even at ~25-fold higher concentration than bacterial MIC.
- Both εPL- and OAK-functionalised GEL may be a promising antimicrobial and bioactive coating material, used in bacteria-associated infections caused by medical devices' implantation.
- This work brought new knowledge into the designing of antimicrobially active biomaterials and offers the potential for creating multifunctional and specific antimicrobial protection, without affecting mammalian cells.

7 REFERENCES

- [1] Tachibana A., Furuta Y., Takeshima H., Tanabe T., Yamauchi K. Fabrication of wool keratin sponge scaffolds for long-term cell cultivation. *J Biotechnol* 2002; 93(2):165–70. doi:10.1016/S0168-1656(01)00395-9
- [2] Crawshaw G.H., Simpson W.S. *Wool: Science and technology*. Woodhead Publishing Ltd; USA, 2002
- [3] Kazunori K., Mikio S., Toshizumi T., Kiyoshi Y. Preparation and physicochemical properties of compression-molded keratin films. *J Biomaterials* 2004; 25(12):2265–2272. doi:10.1016/j.biomaterials.2003.09.021
- [4] Yamauchi K., Maniwa M., Mori T. Cultivation of fibroblast cells on keratin-coated substrata. *J Biomater Sci Polymer* 1998; 9(3):259–70. doi :10.1163/156856298X00640
- [5] Tachibana A., Nishikawa Y., Nishino M., Kaneko S., Tanabe T., Yamauchi K. Modified keratin sponge: binding of bone morphogenetic protein-2 and osteoblast differentiation. *J Biosci Bioeng* 2006; 102(5):425–9. doi:10.1263/jbb.102.425
- [6] Yamauchi K., Yamauchi A., Kusunoki T., Kohda A., Konishi Y. Preparation of stable aqueous solution of keratins, and physicochemical and biodegradational properties of films. *J Biomed Mater Res* 1996; 31(4):439–444. doi:10.1002/(SICI)1097-4636(199608)31:4<439::AID-JBM1>3.0.CO;2-M
- [7] Zhu P., Sun G. Antimicrobial finishing of wool fabrics using quaternary ammonium salts. *J Appl Polym Sci* 2004; 93:1037–1041. doi:10.1002/app.20563
- [8] Panáček A., Kvítek L., Prucek R., Kolář M., Večeřová R., Pizúrová N., K. Sharma V., Nevěčná T., Zbořil R. Silver colloid nanoparticles: Synthesis, characterization and their antibacterial activity. *J Phys Chem B* 2006; 110(33):16248–16253. doi:10.1021/jp063826h
- [9] Meade S.J., Caldwell J.P., Hancock A.J., Coyle K., Dyer J.M., Bryson W.G. Covalent modification on the wool fiber surface: The attachment and durability of model surface treatments. *Text Res J* 2008; 78(12):1087–1097. doi:10.1177/004051750708785

- [10] Dastjerdi R., Montazer M. A review on the application of inorganic nano-structured materials in the modification of textiles: focus on anti-microbial properties. *Colloids Surf B* 2010; 79(1):5–18. doi:10.1016/j.colsurfb.2010.03.029
- [11] Gao Y., Cranston R. Recent advances in antimicrobial treatments of textile, *Text Res J* 2008; 78:60–72. doi:10.1177/0040517507082332.
- [12] Beyth N., Hourri-Haddad Y., Baraness-Hadar L. Surface antimicrobial activity and biocompatibility of incorporated polyethylenimine nanoparticles. *J Biomaterials* 2008; 29(31):4157–4163; 2008. doi:10.1016/j.biomaterials.2008.07.003
- [13] Saha N., Saarai A., Roy N., Kitano T., Saha P. Polymeric biomaterial based hydrogels for biomedical applications. *Journal of Biomaterials and Nanobiotechnology* 2011; 2:85–90. doi:10.4236/jbnt.2011.21011
- [14] Anand S.C., Kennedy J.F., Miraftab M. and Rajendran S. Medical textiles and biomaterials for healthcare; Woodhead Publishing Ltd, Cambridge, 2006
- [15] Dumitriu S. Polymeric Biomaterials, 2nd Ed, Marcel Dekker publisher, New York, 2002
- [16] Mariod A.A., Adam H.F. Review: Gelatin, source, extraction and industrial applications. *Acta Sci Pol, Technol. Aliment.* 2013; 12(2):135–147
- [17] Vlierberghe S.V., Cnudde V., Dubruel P., Masschaele B., Cosijns A., Paepe I.D., Jacobs P.J., Hoorebeke L.V., Remon J.P., Schacht E. Porous gelatin hydrogels: 1. Cryogenic formation and structure analysis. *Biomacromolecules* 2007; 8(2):331–337. doi:10.1021/bm060684o
- [18] Jeevithan E., Qingbo Z., Bao B., Wu W. Biomedical and pharmaceutical application of fish collagen and gelatin: A review. *Journal of Nutritional Therapeutics* 2013; 2(4):218–227
- [19] Stimuli-Responsive Structures from Cationic Polymers for Biomedical Applications. In *Cationic Polymers in Regenerative Medicine*, Samal S.K., Dubruel P., p.149–177. RSC Polymer Chemistry; vol. 13. Royal society of chemistry. doi:10.1039/9781782620105-00149
- [20] Gorgieva S., Kokol V. Collagen- vs. gelatine-based biomaterials and their biocompatibility: review and perspectives, in: Biomaterials applications for nanomedicine, Pignatello R. (Ed.). InTech, cop. 2011: 17–52. doi:10.5772/24118

- [21] Gorgieva S., Štrancar J., Kokol V. Evaluation of surface/interface-related physicochemical and microstructural properties of gelatin 3D scaffolds, and their influence on fibroblast growth and morphology. *Journal of biomedical materials research. Part A* 2014; 102(11):3986–3997
- [22] Goldfeder Y., Zaknoon F., Mor A. Experimental conditions that enhance potency of an antibacterial oligo-acyl-lysyl. *Antimicrob Agents Chemother* 2010; 54(6):2590–2595. doi:10.1128/AAC.01656-09
- [23] Bell G., Gouyon P. H. Arming the enemy: the evolution of resistance to self-proteins. *Microbiology* 2003; 149:1367–1375. doi:10.1099/mic.0.26265-0
- [24] Perron G.G., Zasloff M., Bell G. Experimental evolution of resistance to an antimicrobial peptide. *Proc Biol Sci* 2006; 273:251–256
- [25] Yoshida T., Nagasawa T. ϵ -Poly-L-lysine: microbial production, biodegradation and application potential. *Appl Microbiol Biotechnol* 2003; 62:21–26. doi:10.1007/s00253-003-1312-9
- [26] Chheda A. H., Vernekar M. R. A natural preservative ϵ -poly-L-lysine: fermentative production and applications in food industry. *Int Food Res J* 2015; 22(1):23–30
- [27] Shima S., Matsuoka H., Iwamoto T., Sakai H. Antimicrobial action of epsilon-poly-L-lysine. *J Antibiot* 1984; 37:1449–1455. doi:10.7164/antibiotics.37.1449
- [28] Chang J., Zhong Z., Xu H. Multifunctional wool fiber treated with ϵ -polylysine. *Korean J Chem Eng* 2012; 29(4):507–512. doi:10.1007/s11814-011-0194-2
- [29] Wang Q., Fan X., Hu Y., Yuan J., Cui L., Wang P. Antibacterial functionalization of wool fabric via immobilizing lysozymes. *Bioprocess Biosyst Eng* 2009; 32(5):633–639. doi:10.1007/s00449-008-0286-5
- [30] Li X., Wang Q., Sun X., Fan X., Han X. The hydrophilic finishing of wool fabric via mTGase-catalyzed grafting of ϵ -PL. *Int J Cloth Sci Tech* 2012; 24(5):317–327. doi:10.1108/09556221211258975
- [31] Wang Q., Jin G., Fan X., Zhao X., Cui L., Wang P. Antibacterial functionalization of wool via mTGase-catalyzed grafting of ϵ -Poly-L-lysine. *Appl Biochem Biotechnol* 2010; 160:2486–2497. doi:10.1007/s12010-009-8708-7
- [32] Amram M. Host defense peptides and their potential as therapeutic agents, © Springer International Publishing Switzerland 2016 R.M. Epand (ed.), doi:10.1007/978-3-319-32949-9_8

- [33] Radzishevsky I.S., Rotem S., Bourdetsky D., Navon-Venezia S., Carmeli Y., Mor A. Improved antimicrobial peptides based on acyl-lysine oligomers. *Nat Biotechnol* 2007; 25(6):657–659. doi:10.1038/nbt1309
- [34] Rotem S., Radzishevsky I.S., Bourdetsky D., Navon-Venezia S., Carmeli Y., Mor A. Analogous oligo-acyl-lysines with distinct antibacterial mechanisms. *Faseb J* 2008; 22(8):2652–2661. doi:10.1096/fj.07-105015
- [35] Sarig H., Livne L., Held-Kuznetsov V., Zaknoon F., Ivankin A., Gidalevitz D., Mor A. A miniature mimic of host defense peptides with systemic antibacterial efficacy. *Faseb J* 2010; 24:1904–1913
- [36] Livne L., Kovachi T., Sarig H., Epanand R.F., Zaknoon F., Epanand R.M., Mor A. Design and characterization of a broad-spectrum bactericidal acyl-lysyl oligomer. *Chem Biol* 2009; 16(12):1250–1258. doi:10.1016/j.chembiol.2009.11.012
- [37] Costa F., Carvalho I.F., Montelaro R.C., Gomes P., Martins M.C. Covalent immobilization of antimicrobial peptides (AMPs) onto biomaterial surfaces. *Acta Biomater* 2011; 7(4):1431–1440. doi:10.1016/j.actbio.2010.11.005
- [38] Rotem S., Raz N., Kashi Y., Mor A. Bacterial capture by peptidomimetic oligoacyllysine surfaces. *Appl Environ Microbiol* 2010; 76(10):3301–3307. doi:10.1128/AEM.00532-10.
- [39] Marjeh I., Meir O., Zaknoon F., Mor A. Improved bacterial detection using immobilised acyl-lysyl oligomers. *Appl Environ Microbiol* 2015; 81(1):74–80. doi:10.1128/AEM.02537-14
- [40] Mckinnon J. Chemistry of the wool Industry scouring and Yarn production. *Wool Research organisation of New Zealand; Animal product F, Wool*: p.1–30
- [41] Lewis D.M., Rippon J.A. The coloration of wool and other keratin fibres; John Wiley & Sons Inc.: Hoboken, NJ, USA, 2013
- [42] Chen J., Vongsanga K., Wang X., Byrn N. What Happens during Natural Protein Fibre Dissolution in Ionic Liquids. *Materials* 2014; 7:6158–6168. doi:10.3390/ma7096158
- [43] Leeder J.D. The Cell Membrane Complex and its Influence on the Properties of the Wool Fibre. *Wool Sci Rev* 1986; 63:3–35
- [44] Bradbury J.H., Chapman G.V., Hambly A.N., King N.L.R. Separation of chemically unmodified histological components of keratin fibers and analyses of cuticle. *Nature* 1966; 210(5043):1333–1334. doi:10.1038/2101333a0

- [45] Leon N.H. Structural aspects of keratin fibers. *J Soc Cosmet Chem* 1972; 23:427–445.
- [46] Block R.J., Bolling D. The composition of keratin. The amino acid composition of hair, wool, horn and other eukeratins. *J Biol Chem* 1939; 128:181–186
- [47] Chapter 3: Fibre morphology. Höcker H. // *Wool: Science & Technology*; 2002, p.60–79
- [48] Rippon J.A. The structure of wool. In *Wool Dyeing*; Lewis D.M. (Ed.); Society of Dyers and Colourists: Bradford, UK, 1992; p.1–51
- [49] Ivanova E.P., Pham D.K., Brack N., Pigram P., Nicolau D.V. Poly(l-lysine)-mediated immobilisation of oligonucleotides on carboxy-rich polymer surfaces. *Biosens Bioelectron* 2004; 19(11):1363–1370. doi:10.1016/j.bios.2003.12.030
- [50] Chang Y., McLandsborough L., McClements D.J. Interactions of a cationic antimicrobial (ϵ -Polylysine) with an anionic biopolymer (Pectin): An isothermal titration calorimetry, microelectrophoresis and turbidity study. *J Agric Food Chem* 2011; 59:5579–5588. doi:10.1021/jf104299q
- [51] Crompton K.E., Goud J.D., Bellamkonda R.V., Gengenbach T.R., Finkelstein D.I., Horne M.K., Forsythe J.S. Polylysine-functionalised thermoresponsive chitosan hydrogel for neural tissue engineering. *Biomaterials* 2007; 28(3):441–449. doi:10.1016/j.biomaterials.2006.08.044
- [52] Besheer A., Hertel T.C., Kressler J., Mäder K., Pietzsch M. Enzymatically catalyzed conjugation of a biodegradable polymer to proteins and small molecules using microbial transglutaminase. *Methods Mol Biol* 2011; 751:17–27. doi:10.1007/978-1-61779-151-2_2
- [53] Cortez J., Anghieri A., Bonner P.L.R., Griffin M., Freddi G. Transglutaminase mediated grafting of silk proteins onto wool fabrics leading to improved physical and mechanical properties. *Enzyme and Microb Technol* 2007; 40(7):1698–1704
- [54] Jones R.T. Gelatin: manufacture and physico-chemical properties, p.23–61 In: Podczek F., Jones B.E. *Pharmaceutical Capsules*. Pharmaceutical Press, London, 2004
- [55] Morrison N.A., Clark R.C., Chen Y.L., Talashek T., Sworn G. Gelatin alternatives for the food industry. *Prog Colloid Polym Sci* 1999; 114:127–131
- [56] Djabourov M., Lechaire J.P., Gaill F. Structure and rheology of gelatin and collagen gels. *Biorheology* 1993; 30(3-4):191–205

- [57] Gómez-Guillén M.C., Turnay J., Fernández-Díaz M.D., Ulmo N., Lizarbe M.A., Montero P. Structural and physical properties of gelatin extracted from different marine species: a comparative study. *Food Hydrocol* 2002; 16:25–34
- [58] Asghar A., Henrickson R.L. Chemical, biochemical, functional, and nutritional characteristics of collagen in food systems. *Advances in Food Research* 1982; 28:231–372. doi:10.1016/S0065-2628(08)60113-5
- [59] Jamilah B., Harvinder K.G. Properties of gelatins from skins of fish: black tilapia (*Oreochromis mossambicus*) and red tilapia (*Oreochromis nilotica*). *Food Chemistry* 2002; 77:81–84. doi:10.1016/S0308-8146(01)00328-4
- [60] Chapman and Hall. Thickening and gelling agents for food. 2nd edition, Blackie Academic and Professional, London, 150-153, 1997
- [61] Farris S., Song J., Huang Q. Alternative reaction mechanism for the cross-linking of gelatin with glutaraldehyde. *J. Agric. Food Chem.* 2010; 58(2):998–1003
- [62] Chang M.C., Douglas W.H. Cross-linkage of hydroxyapatite/gelatin nanocomposite using imide-based zero-length cross-linker. *J Mater Sci Mater Med* 2007; 18(10):2045–2051
- [63] Zeeman R., Dijkstra P.J., Van Wachem P.B., Van Luyn M.J., Hendriks M., Cahalan P.T., Feijen J. Crosslinking and modification of dermal sheep collagen using 1, 4-butanediol diglycidyl ether. *J Biomed Mater Res* 1999 Sep 5;46(3):424–433
- [64] Everaerts F., Torrianni M., Hendriks M., Feijen J. Quantification of carboxyl groups in carbodiimide cross-linked collagen sponges. *J Biomed Mater Res A* 2007; 83:1176–1183.
- [65] Kuijpers A.J., Engbers G.H., Krijgsveld J., Zaat S.S., Dankert J., Feijen J. Cross-linking and characterisation of gelatin matrices for biomedical applications. *J Biomater Sci Polym Ed* 2000; 11(3):225–43
- [66] Van Vlierberghe S., Vanderleyden E., Boterberg V., Dubruel P. Gelatin functionalization of biomaterial surfaces: Strategies for immobilization and visualization. *Polymers* 2011; 3(4):114–130. doi:10.3390/polym3010114
- [67] Nomura Y., Toki S., Ishii Y., Shirai K. Improvement of material property of shark type I collagen by composing with porcine type I collagen. *J Agric Food Chem* 2000; 48:6332–6336

- [68] Balada E., Taylor M.M., Phillips J.G., Marmer W.N., Brown E.M. Properties of biopolymers produced by transglutaminase treatment of whey protein isolate and gelatin. *Bioresour Technol* 2009; 100(14):3638–3643. doi:10.1016/j.biortech.2009.02.039
- [69] Muguruma M., Tsuruoka K., Fujino H., Kawahara S., Yamauchi K., Matsumura S., Soeda T. Gel strength enhancement of sausages by treating with microbial transglutaminase. Proceedings of the 45th International Congress of Meat Science and Technology, 1999. Yokohama, Japan; 1:138–139
- [70] Alting A.C., Hamer R.J., De Kraif C.G., Visschers R.W. Formation of disulfide bonds in acid induced gels of preheated whey protein isolate. *J Agric Food Chem* 2000; 48:5001–5007
- [71] Jayapriya S., Bagyalakshmi G. Textile Antimicrobial Testing and Standards. *International Journal of Textile and Fashion Technology (IJTFT)* 2013; 4(1):1–10
- [72] El-Sersy N.A., Abdelwahab A.E., Abouelkhiir S.S., Abou-Zeid D.M., Sabry S.A. Antibacterial and anticancer activity of ϵ -poly-L-lysine (ϵ -PL) produced by a marine *Bacillus subtilis* sp. *J Basic Microbiol* 2012; 52(5):513–522. doi:10.1002/jobm.201100290
- [73] Geornaras I., Yoon Y., Belk K.E., Smith G.C., Sofos J.N. Antimicrobial activity of epsilon-polylysine against *Escherichia coli* O157:H7, *Salmonella* Typhimurium, and *Listeria monocytogenes* in various food extracts. *J Food Sci* 2007; 72(8):330–334. doi:10.1111/j.1750-3841.2007.00510.x
- [74] Takehara M., Hibino A., Saimura M., Hirohara H. High-yield production of short chain length poly(ϵ -l-lysine) consisting of 5–20 residues by *Streptomyces aureofaciens*, and its antimicrobial activity. *Biotechnol Lett* 2010; 32(9):1299–1303. doi:10.1007/s10529-010-0294-9
- [75] Hyldgaard M., Mygind T., Vad B.S., Stenvang M., Otzen D., Meyer R.L. The antimicrobial mechanism of action of epsilon-poly-L-Lysine. *Appl Environ Microbiol* 2014; 80(24):7758–7770. doi:10.1128/AEM.02204-14
- [76] Vaara M. Agents that increase the permeability of the outer membrane. *Microbiol Rev* 1992; 56:395–411

- [77] Ye R., Xu H., Wan C., Peng S., Wang L., Xu H., Aguilar Z.P., Xiong Y., Zeng Z., Wei H. Antibacterial activity and mechanism of action of ϵ -poly-L-lysine. *Biochem Biophys Res Commun* 2013; 439(1):148–153. doi:10.1016/j.bbrc.2013.08.001
- [78] Zhao R., Wang H., Ji T., Anderson G., Nie G., Zhao Y. Biodegradable cationic ϵ -poly-L-lysine-conjugated polymeric nanoparticles as a new effective antibacterial agent. *Sci Bull* 2015; 60(2):216–226. doi:10.1007/s11434-014-0704-9
- [79] Parenteau-Bareil R., Gauvin R., Berthod F. Collagen-based biomaterials for tissue engineering applications. *Materials* 2010, 3(3):1863–1887; doi:10.3390/ma3031863
- [80] Sarig H., Rotem S., Ziserman L., Danino D., Mor A. Impact of self-assembly properties on antibacterial activity of short acyl-lysine oligomers. *Antimicrob Agents Chemother* 2008; 52(12):4308. doi: 10.1128/AAC.00656-08
- [81] Zasloff M. Antimicrobial peptides of multicellular organisms. *Nature* 2002; 415:389–395
- [82] Makobongo M.O., Gancz H., Carpenter B.M., McDaniel D.P., Merrell D.S. The oligo-acyl lysyl antimicrobial peptide C₁₂K-2 β ₁₂ exhibits a dual mechanism of action and demonstrates strong *in vivo* efficacy against *Helicobacter pylori*. *Antimicrob Agents Chemother* 2012; 56(1):378–390. doi:10.1128/AAC.00689-11
- [83] Epand R.F., Sarig H., Mor A., Epand R.M. Cell-wall interactions and the selective bacteriostatic activity of a miniature oligo-acyl-lysyl. *Biophys J* 2009; 97(8):2250–2257. doi:10.1016/j.bpj.2009.08.006
- [84] Radziszewsky I.S., Kovachi T., Porat Y., Ziserman L., Zaknoon F., Danino D., Mor A. Structure-activity relationships of antibacterial acyl-lysine oligomers. *Chem Biol* 2008; 15(4):354–62. doi:10.1016/j.chembiol.2008.03.006
- [85] Giuliani A., Rinaldi A.C. Beyond natural antimicrobial peptides: multimeric peptides and other peptidomimetic approaches. *Cell Mol Life Sci* 2011; 68(13):2255–2266. doi:10.1007/s00018-011-0717-3
- [86] Radziszewsky I., Krugliak M., Ginsburg H., Mor A. Antiplasmodial activity of lauryl-lysine oligomers. *Antimicrob Agents Chemother* 2007; 51:1753–1759
- [87] Fields G.B., Noble R.L. Solid phase peptide synthesis utilizing 9-fluorenylmethoxycarbonyl amino acids. *Int J Pept Protein Res* 1990; 35(3):161–214

- [88] Drotleffa S., Lungwitz U., Breuniga M., Dennisa A., Blunka T., Tessmarc J., Göpferich A. Biomimetic polymers in pharmaceutical and biomedical sciences. *European Journal of Pharmaceutics and Biopharmaceutics* 2004; 58:385–407
- [89] Hermanson G.T. Bioconjugate techniques, 2nd ed. Academic Press: London, UK; 2008
- [90] Das T., Ramaswamy G.N. Enzyme treatment of wool and specialty hair fibers. *Textile Res J* 2006; 76(2):126–133. doi:10.1177/0040517506063387
- [91] Polaina J., MacCabe A.P. Industrial Enzymes: structure, function and applications. Dordrecht: Springer, 2007
- [92] DeJong G.A.H., Koppelman S.J. Transglutaminase catalyzed reactions: Impact on food applications. *J Food Sci* 2002; 67(8):2798–2806
- [93] Harvey D. Modern analytical chemistry (1st ed.). New York: McGraw Hill, 1999
- [94] Lakowicz J.R. Principles of fluorescence spectroscopy, 3rd edition, Springer, New York, 2006
- [95] Molecular luminescence spectrometry. In Skoog D.A., Holler F.J., Crouch S.R. *Principles of Instrumental Analysis*, International student edition. Thomson Brooks/Cole, 2007. p.399–429
- [96] O'Donnell C.P., Fagan C. Cullen P.J. Process analytical technology for the food industry. New York: Springer, 2014
- [97] Le Breton N., Martinho M., Mileo E., Etienne E., Gerbaud G., Guigliarelli B., Belle V. Exploring intrinsically disordered proteins using site-directed spin labeling electron paramagnetic resonance spectroscopy. *Front Mol Biosci* 2015. 2(21). doi:10.3389/fmolb.2015.00021
- [98] Kwon J.H., Shahbaz H.M., Ahn J.J. Advanced electron paramagnetic resonance spectroscopy for the identification of irradiated food. *American Laboratory* 2014; 46(1):1–4
- [99] Sheehan D. Physical biochemistry: Principles and applications. 2nd edition, Wiley, 2009
- [100] Weil J.A., Bolton J.R. Electron paramagnetic resonance spectroscopy: Elementary theory and applications, 2nd Edition. Wiley-Interscience, 2007
- [101] Hunter R.J. Zeta potential in colloid science. London: Academic Press, 1981

- [102] Costa A.L., Galassi C., Greenwood R. Alpha-alumina-H₂O interface analysis by electroacoustic measurements. *J. Colloid Interface Sci* 1999; 212(2):350–356. doi:10.1006/jcis.1998.6070
- [103] Hanaor D., Michelazzi M., Leonelli C., Sorrell C. C. The effects of carboxylic acids on the aqueous dispersion and electrophoretic deposition of ZrO₂. *J Eur Ceram Soc* 2012; 32(1):235–244. doi:10.1016/j.jeurceramsoc.2011.08.015
- [104] Brett C.M.A., Brett A.M.O. Electrochemistry; principles, methods and applications. New York, Oxford University Press Inc., 1993
- [105] Liese A., Hilterhaus L. Evaluation of immobilized enzymes for industrial applications. *Chem Soc Rev* 2013; 42:6236–6249. doi:10.1039/C3CS35511J
- [106] Vincent B. The effect of adsorbed polymers on dispersion stability. *Adv Colloid Interf* 1974; 4(2-3):193–277. doi:10.1016/0001-8686(74)85002-5
- [107] Skoog D.A., West D.M., F. Holler J., Crouch S.R. Fundamentals of analytical chemistry, 8th Ed., Brooks Cole, 2003
- [108] Chapter 2: Potentiometric titrations, http://www.cffet.net/sia-e/2_Pot_titr.pdf
- [109] Barth A., Zscherp C. What vibrations tell us about proteins. *Q Rev Biophys* 2002; 35(4):369–430
- [110] Stuart B.H. Infrared spectroscopy: Fundamentals and applications. Wiley, 2004
- [111] Trathnigg B. Size-exclusion chromatography of polymers in *Encyclopedia of Analytical Chemistry* (ed. Meyers R.A.) p.8008–8034. John Wiley & Sons, Ltd, Chichester, 2006
- [112] Separation methods. High-performance liquid chromatography. In *Principles of instrumental analysis*; Skoog D.A., Holler F.J., Crouch S.R (Eds.). 5th edition. Thomson Brooks/Cole, 2007
- [113] Glynn J.R., Belongia B.M., Arnold R.G., Ogden K.L., Baygents J.C. Capillary electrophoresis measurements of electrophoretic mobility for colloidal particles of biological interest. *Appl Environ Microbiol* 1998; 64(7):2572–2577
- [114] Landers J.P. Handbook of capillary electrophoresis; CRC Press: Boca Raton, 1994
- [115] Swofford W. An overview of antimicrobial testing for textile applications, AATCC Review; (10)6, 2010
- [116] Balouiri M., Sadiki M., Ibensouda S.K. Methods for *in vitro* evaluating antimicrobial activity: A review. *J Pharma Anal* 2016; 6(2):71–79. doi:10.1016/j.jpha.2015.11.005

- [117] Bauer A.W., Kirby W.M., Sherris J.C., Turck M. Antibiotic susceptibility testing by a standardized single disk method. *Am J Clin Pathol* 1966; 45(4):493–496
- [118] Klančnik A., Piskernik S., Jersek B., Mozina S.S. Evaluation of diffusion and dilution methods to determine the antibacterial activity of plant extracts. *J Microbiol Methods* 2010; 81:121–126
- [119] Moreno S., Scheyer T., Romano C.S., Vojnov A.A. Antioxidant and antimicrobial activities of rosemary extracts linked to their polyphenol composition. *Free Radic Res* 2006; 40:223–231
- [120] E2149-10: Standard test method for determining the antimicrobial activity of immobilized antimicrobial agents under dynamic contact conditions. ASTM International. West Conshohocken, PA 19428-2959: US
- [121] Gabriel G.J., Som A., Madkour A.E., Eren T., Tew G.N. Infectious disease: connecting innate immunity to biocidal polymers. *Materials Science and Engineering Reports* 2007; 57(1–6):28–64
- [122] Arndt-Jovin D.J., Jovin T.M. Fluorescence labeling and microscopy of DNA. *Methods Cell Biol* 1989; 30:417–448
- [123] Haugland R.P. Handbook of fluorescent probes and research chemicals, 7th ed., Molecular Probes, Eugene, Oreg., 1999
- [124] Molecular probes-Invitrogen. Product information; LIVE/DEAD[®] BacLight[™] bacterial viability Kits. Revised 2009
- [125] Stiefel P., Schmidt-Emrich S., Maniura-Weber K., Ren Q. Critical aspects of using bacterial cell viability assays with the fluorophores SYTO 9 and propidium iodide. *BMC Microbiol* 2015; 15(1):36. doi:10.1186/s12866-015-0376-x
- [126] Loos B., Engelbrecht A.M. Cell death: a dynamic response concept. *Autophagy* 2009; 5:590–603
- [127] Riss T.L., Moravec R.A., Niles A.L., Duellman S., Benink H.A., Worzella T.J., Minor L. Cell Viability Assays. In *Assay Guidance Manual*; Sittampalam G.S., Coussens N.P., Nelson H., Arkin M., Auld D., Austin C., Bejcek B., Glicksman M., Inglese J., Iversen P.W., Li Z., McGee J., McManus O., Minor L., Napper A., Peltier J.M., Riss T., Trask O.J. Jr., Weidner J., Eds; Eli Lilly & Company and the National Center for Advancing Translational Sciences: Bethesda, MD, USA, 2004

- [128] Johnson M.B., Criss A.K. Fluorescence microscopy methods for determining the viability of bacteria in association with mammalian cells. *J Vis Exp* 2013; 5(79). doi:10.3791/50729
- [129] ISO 3074:2014: Wool – Determination of dichloromethane-soluble matter in combed sliver
- [130] Minko S. Polymer surfaces and interfaces. Chapter 11: Grafting on solid surfaces: "Grafting-to" and "Grafting-from" methods. Stamm M: Springer, Berlin; 2008
- [131] Wong, S.S. Chemistry of protein conjugation and cross-linking, CRC Press, USA; 2000
- [132] Griffin M., Cortez J., Bonner P.L.R. Application of transglutaminases in the modification of wool textiles. *Enzyme Microb Tech* 2004; 34(1):64–72. doi:10.1016/j.enzmictec.2003.08.004
- [133] Nakajima N., Ikada Y. Mechanism of amide formation by carbodiimide for bioconjugation in aqueous-media. *Bioconjugate Chem* 1995; 6(1):123–130. doi:10.1021/bc00031a015
- [134] Bradford M. A rapid and sensitive method for the quantification of microgram quantities of protein utilizing the principles of protein-dye binding. *Anal Biochem* 1976; 72:248–254
- [135] McDonald R. Colour physics for industry, SDC, Bradford: England; 1997
- [136] Cayot P., Tainturier G. The quantification of protein amino groups by the trinitrobenzenesulfonic acid method: A reexamination. *Analytical Biochemistry* 1997; 249:184–200. doi:10.1006/abio.1997.2161
- [137] Grotzky A., Manaka Y., Fornera S., Willeke M., Walde P. Quantification of α -polylysine: A comparison of four UV/Vis spectrophotometric methods. *Analytical Methods* 2010; 2:1448–1455
- [138] Gyarmati B., Hegyesi N., Pukánszky B., Szilágyi A.F. A colourimetric method for the determination of the degree of chemical cross-linking in aspartic acid-based polymer gels. *Express Polymer Letters*; 9(2):154–164
- [139] Bubnis W.A., Ofner 3rd C.M. The determination of epsilon-amino groups in soluble and poorly soluble proteinaceous materials by a spectrophotometric method using trinitrobenzenesulfonic acid. *Anal. Biochem* 1992. 207(1):129–133
- [140] Habeeb A.F. Determination of free amino groups in protein by trinitrobenzene sulfonic acid. *Anal. Biochem.* 1966; 14(3):328–336

- [141] Shimo S.S., Smriti S.A. Color co-ordinates and relative color strength of reactive dye influenced by fabric gsm and dye concentration. *Int J Innov Res Sci Eng Technol* 2015; 4(2):192–197. doi:10.15623/ijret.2015.0402025
- [142] Čakara D., Fras L., Bračič M., Kleinschek-Stana K. Protonation behavior of cotton fabric with irreversibly adsorbed chitosan: a potentiometric titration study. *Carbohydrate Polymers* 2009; 78(1):36–40. doi:10.1016/j.carbpol.2009.04.011
- [143] Bukšek H., Luxbacher T., Petrinič I. Zeta potential determination of polymeric materials using two differently designed measuring cells of an electrokinetic analyser. *Acta Chim Slov* 2010; 57:700–706
- [144] Diress A., Lorbetskie B., Larocque L., Li X., Alteen M., Isbrucker R., Girard M. Study of aggregation, denaturation and reduction of interferon alpha-2 products by size-exclusion high-performance liquid chromatography with fluorescence detection and biological assays; *J Chromatogr A* 2010; 1217(19):3297–3306
- [145] Hong P., Koza S., Bouvier E.S.P. Size-exclusion chromatography for the analysis of protein biotherapeutics and their aggregates. *Journal of Liquid Chromatography & Related Technologies* 2012; 35(20):2923–2950. doi:10.1080/10826076.2012.743724
- [146] Huang X., Guo X.F., Wang H., Zhang H.S. Analysis of catecholamines and related compounds in one whole metabolic pathway with high performance liquid chromatography based on derivatization. *Arabian Journal of Chemistry* 2014; 1878–5352. doi:10.1016/j.arabjc.2014.11.038
- [147] Ji J., Feng L., Qiu Y., Yu X. ESR spectroscopy to determine the molecular mobility of poly(ethylene oxide) grafts in amphiphilic graft copolymers. *Macromol Rapid Comm* 1998; 19(9):473–477. doi:10.1002/(SICI)1521-3927(19980901)19:9<473::AID-MARC473>3.0.CO;2-X.
- [148] Stopar D., Štrancar J., Spruijt R.B., Hemminga M.A. Exploring the local conformational space of a membrane protein by site-directed spin labelling. *J Chem Inf Model* 2005; 45(6):1621–1627. doi:10.1021/ci0501490
- [149] LIVE/DEAD BacLight bacterial viability kit. L-7007: Molecular Probes; 2004

- [150] Susceptibility testing of Antimicrobials in liquid media. In "Antibiotics in Laboratory Medicine", Lorian, V., 5th Edition, pp. 52–111. Williams and Wilkins, Philadelphia, USA, 2005
- [151] ISO 105-D01:2010: Textiles – Tests for colour fastness
- [152] Timar-Balazsy A., Eastop D. Chemical principles of textile conservation. Oxford: Butterworth-Heinemann; 1998
- [153] Jordan C.E., Frutos A.G., Thiel A.J., Corn R.M. Surface plasmon resonance imaging measurements of DNA hybridization adsorption and streptavidin/DNA multilayer formation at chemically modified gold surfaces. *Anal Chem* 1994; 69(24):4939–4947. doi:10.1021/ac9709763
- [154] Cardamone J.M. Keratin transamidation. *Int J Biol Macromol* 2008; 42(5):413–419. doi:10.1016/j.ijbiomac.2008.02.004
- [155] Cardamone J.M, Nuñez A., Garcia R.A., Aldema-Ramos M. Characterizing wool keratin. *Mater Sci+* 2009, Article ID 147175, 5pages. doi:10.1155/2009/147175
- [156] Gholizadeh H., Naserian A., Valizadeh R., Tahmasbi A.M, Yu P. Detecting chemical molecular structure differences among different Iranian barley cultivators using Fourier Transform infrared spectroscopy. *Annu Res Rev Biol* 2014; 4(1):258–268
- [157] Grdadolnik J. Saturation effects in FTIR spectroscopy: Intensity of amide I and amide II bands in protein spectra. *Acta Chim Slov* 2003; 50(4):777–788
- [158] Akhyar Farrukh M. Advanced Aspects of Spectroscopy, INTECH Open Access Publisher, 2012; Chapter 3: Urbaniak-Domagala W. The Use of the Spectrometric Technique FTIR-ATR to Examine the Polymers Surface. doi:10.5772/48143
- [159] Kong J., Yu S. Fourier transform infrared spectroscopic analysis of protein secondary structures. *Acta Bioch Bioph Sin* 2007; 39(8):549–559. doi:10.1111/j.1745-7270.2007.00320.x
- [160] Hsu S.C., Ph D. Infrared spectroscopy. In Settle F.A. Handbook of instrumental techniques for analytical chemistry, p. 247–284. Prentice-Hall, New Jersey, 1997
- [161] Cardamone J.M. Investigating the microstructure of keratin extracted from wool: Peptide sequence (MALDI-TOF/TOF) and protein conformation (FTIR). *J Mol Struct* 2010; 969:97–105. doi:10.1016/j.molstruc.2010.01.048

- [162] Surewicz W.K., Mantsch H.H., Chapman D. Determination of protein secondary structure by Fourier transform infrared spectroscopy: a critical assessment. *Biochemistry* 1993; 32(2):389–394. doi:10.1021/bi00053a001
- [163] Barlow D.J., Thornton J.M. Helix geometry in proteins. *J Mol Biol* 1988; 201(3):601–619
- [164] Biswas R., Kühne H., Brudvig G.W., Gopalan V. Use of EPR spectroscopy to study macromolecular structure and function. *Sci Prog* 2001; 84(1):45–68. doi:10.3184/003685001783239050
- [165] Cameron G.G. ESR spectroscopy. *Comprehensive Polymer Science*. Oxford: Pergamon Press, p. 517; 1989
- [166] Millhauser G.L., Fiori W.R., Miick S.M. Electron spin labels. *Meth Enzymol* 1995; 246:589–610. doi:10.1016/0076-6879(95)46026-8
- [167] Mirtič A., Grdadolnik J. The structure of poly-L-lysine in different solvents. *Biophys Chem* 2013; 175-176:47–53. doi:10.1016/j.bpc.2013.02.004
- [168] Biswas B., Rogers K., McLaughlin F., Daniels D., Yadav A. Antimicrobial activities of leaf extracts of Guava (*Psidium guajava* L.) on two Gram-negative and Gram-positive bacteria. *Int J Microbiol* 2013; Article ID 746165. doi:10.1155/2013/746165
- [169] Berney M., Hammes F., Bosshard F., Weilenmann H.U., Egli T. Assessment and interpretation of bacterial viability by using the LIVE/DEAD BacLight Kit in combination with flow cytometry. *Appl Environ Microbiol* 2007; 73(10):3283–3290. doi:10.1128/AEM.02750-06
- [170] Zhou J., Guo A., Qi X. Cell envelope disruption of *E. coli* exposed to ϵ -polylysine by FESEM and TEM technology. *Scanning* 2013; 35(6):412–417. doi:10.1002/sca.21086
- [171] GRAS Notice: ϵ -Polylysine For Addition To Specified Foods. doi:http://www.fda.gov/downloads/Food/IngredientsPackagingLabeling/GRAS/NoticeInventory/UCM267372
- [172] Brack N., Lamb R., Pham D., Turner P. Non-ionic surfactants and the wool fibre surface. *Colloids Surf A* 1999; 146:405–415. doi:10.1016/S0927-7757(98)00863-2
- [173] Musnickas J., Rupainytė V., Treigienė R. Dye migration influences on colour characteristics of wool fiber dyed with acid dye. *Fibers and Textiles in Eastern Europe* 2005; 13(6):65–69. doi:www.fibtex.lodz.pl/54_19_65.pdf

- [174] Morimoto K., Chono S., Kosai T., Seki T., Tabata Y. Design of cationic microspheres based on aminated gelatin for controlled release of peptide and protein drugs. *Drug Deliv.* 2008; 15(2):113–117. doi:10.1080/10717540801905124
- [175] Adhirajan N., Thanavel R., Naveen N., Uma Mary Babu T.S. Functionally modified gelatin microspheres as a growth factor's delivery system: Development and characterization. *Polymer Bulletin* 2014; 71(4):1015–1030
- [176] Flanagan J., FitzGerald R.J. Characterisation and quantification of the reaction(s) catalyzed by transglutaminase using the o-phthaldialdehyde reagent. *Molecular Nutrition & Food Research* 2003; 47(3):207–212 doi:10.1002/food.200390047
- [177] Jaros D., Partschefeld C., Henle T., Rohm H. Transglutaminase in dairy products: Chemistry, physics, applications. *J. Texture Stud.* 2006; 37:113–155
- [178] Smerdel B., Pollak L., Novotni D., Čukelj N., Benković M., Lušić D., Čurić D. Improvement of gluten-free bread quality using transglutaminase, various extruded flours and protein isolates. *J Food Nut Res* 2012; 51(4):242–253
- [179] Yokoyama K., Nio, N., Kikuchi, Y. Properties and applications of microbial transglutaminase. *Applied Microbiology and Biotechnology* 2004; 64:447–454.
- [180] Heck T., Faccio G., Richter M., Thöny-Meyer L. Enzyme-catalyzed protein crosslinking. *Appl Microbiol Biotechnol*, 2013; 97(2):461–475
- [181] Nielsen S.S. Food Analysis 4th ed., Springer, New York, 2010
- [182] Cole C.G.B., Roberts J.J. Gelatine fluorescence and its relationship to animal age and gelatine colour. *S Afr Food Aci Nutr* 1996; 8(4):139–143
- [183] Issa R., Meikle S.T., James S., Cooper I.R. Poly(ϵ -lysine) dendrons as modulators of quorum sensing in *Pseudomonas aeruginosa*. *J Mater Sci Mater Med* 2015; 26(5):176. doi:10.1007/s10856-015-5508-1
- [184] Ostolska I., Wiśniewska M. Application of the zeta potential measurements to explanation of colloidal Cr_2O_3 stability mechanism in the presence of the ionic polyamino acids. *Colloid Polym Sci* 2014; 292(10):2453–2464. doi:10.1007/s00396-014-3276-y
- [185] Volodkin D., Ball V., Schaaf P., Voegel J.C., Mohwald H. Complexation of phosphocholine liposomes with polylysine. Stabilization by surface coverage versus aggregation. *Biochim Biophys Acta* 2007; 1768(2):280–290. doi:10.1016/j.bbamem.2006.09.015

- [186] Epand R.F., Sarig H., Ohana D., Papahadjopoulos-Sternberg B., Mor A., Epand R.M. Physical properties affecting cochleate formation and morphology using antimicrobial oligo-acyl-lysyl peptide mimetics and mixtures mimicking the composition of bacterial membranes in the absence of divalent cations. *J Phys Chem B* 2011; 115(10):2287–2293. doi:10.1021/jp111242q
- [187] Sadako T. Pullulan as molecular weight standard for gelatin. *Journal of the Society of Photographic Science and Technology of Japan* 2001; 64(4):264–266
- [188] Kafkova B., Bosakova Z., Tesarova E., Suchankova J., Coufal P., Stulik K. System peaks observed in capillary liquid chromatography with eluents containing trimethylamine. *Chromatographia* 2002; 56(7):445–447
- [189] Levin S., Grushka E. System peaks in liquid chromatography: their origin, formation, and importance. *Anal Chem* 1986; 58(8):1602–1607. doi:10.1021/ac00121a004
- [190] Pritchett T., Schwartz H. Separation of proteins and peptides by capillary electrophoresis. *Application to Analytical Biotechnology* 1994, Beckman Coulter
- [191] Kuhn W.G., Monning C.A. Capillary electrophoresis. *Analytical Chemistry* 1992; 64:389–407
- [192] Hideg K., Kalai T., Sar C.P. Recent results in chemistry and biology of nitroxides. *J Heterocycl Chem* 2005; 42:437–450
- [193] Dathe M., Wieprecht T. Structural features of helical antimicrobial peptides: their potential to modulate activity on model membranes and biological cells. *Biochim Biophys Acta* 1999; 1462:71–87
- [194] Hancock R.E., Patrzykat A. Clinical development of cationic antimicrobial peptides: from natural to novel antibiotics. *Curr Drug Targets Infect Disord* 2002; 2:79–83
- [195] Hancock R.E., Rozek A. Role of membranes in the activities of antimicrobial cationic peptides. *FEMS Microbiol Lett* 2002; 206:143–149
- [196] Yoshida T., Nagasawa T. e-Poly-l-lysine: microbial production, biodegradation and application potential. *J Appl Microbiol Biotechnol* 2003; 62(1):21–26. doi:10.1007/s00253-003-1312-9
- [197] Shi C., Zhao X., Liu Z., Meng R., Chen X., Guo N. Antimicrobial, antioxidant and antitumor activity of epsilon-poly-l-lysine and citral, alone or in combination. *Food Nutr Res* 2016; 60:31891. doi:10.3402/fnr.v60.31891

- [198] Alves C.S., Melo M.N., Franquelim H.G., Ferre R., Planas M., Feliu L., Bardají E., Kowalczyk W., Andreu D., Santos N.C., Fernandes M.X., and Castanho M.A.R.B. *Escherichia coli* cell surface perturbation and disruption induced by antimicrobial peptides BP100 and pepR. *J. Biol. Chem.* 2010; 285(36):27536–27544. doi:10.1074/jbc.M110.130955
- [199] Arakha M., Saleem M., Mallick B.C., Jha S. The effects of interfacial potential on antimicrobial propensity of ZnO nanoparticle. *Sci. Rep.* 5 2015; 9578. doi:10.1038/srep09578
- [200] Halder S., Yadav K.K., Sarkar R., Mukherjee S., Saha P., Haldar S., Karmakar S., Sen T. Alteration of Zeta potential and membrane permeability in bacteria: a study with cationic agents. *Springerplus* 2015; 4(1):672. doi:10.1186/s40064-015-1476-7
- [201] Hancock R.E., Chapple D.S. Peptide antibiotics. *Antimicrob Agents Chemother* 1999; 43:1317–1323
- [202] Hancock R.E. The bacterial outer membrane as a drug barrier. *Trends Microbiol.* 1997; 5:37–42
- [203] Tossi A., Sandri L., Giangaspero A. Amphipathic, alpha-helical antimicrobial peptides. *Biopolymers* 2000; 55:4–30
- [204] Kang S., Mauter M.S., Elimelech M. Microbial cytotoxicity of carbon-based nanomaterials: implications for river water and wastewater effluent. *Environ Sci Technol* 2009; 43(7):2648–2653
- [205] Li Y.Q., Han Q., Feng J.L., Tian W.L., Mo H.Z. Antibacterial characteristics and mechanisms of ϵ -poly-lysine against *Escherichia coli* and *Staphylococcus aureus*. *Food Control* 2014; 43:22–27. doi:10.1016/j.foodcont.2014.02.023
- [206] Najjar M.B., Kashtanov D., Chikindas M.L. Natural antimicrobials ϵ -polyL-lysine and Nisin A for control of oral microflora. *Probiotics & Antimicro. Prot.* 2009; 1(2):143–147. doi:10.1007/s12602-009-9020-0
- [207] ISO 10993-5:2009(E). Biological evaluation of medical devices – Part 5: Tests for in vitro cytotoxicity
- [208] O. Makobongo M., Gancz H., M. Carpenter B., P. McDaniel D., Merrell D.S. The Oligo-Acyl Lysyl antimicrobial peptide C₁₂K-2 β ₁₂ exhibits a dual mechanism of action and demonstrates strong *in vivo* efficacy against *Helicobacter pylori*. *Antimicrob. Agents Chemother.* 2012; 56(1):378–390

- [209] Maher S., McClean S. Investigation of the cytotoxicity of eukaryotic and prokaryotic antimicrobial peptides in intestinal epithelial cells in vitro. *Biochem Pharmacol* 2006; 71:1289–1298
- [210] Vaucher R.A., Teixeira M.L., Brandelli A. Investigation of the cytotoxicity of antimicrobial peptide P40 on eukaryotic cells. *Curr Microbiol* 2010; 60:1–5
- [211] Zaknoon F., Goldberg K., Sarig H., Epanand F.R., Epanand M.R., Mor A. Antibacterial properties of an Oligo-acyl-lysyl hexamer targeting Gram-negative species. *Antimicrob Agents Chemother* 2012; 56(9):4827–4832. doi:10.1128/AAC.00511-12
- [212] Postupalenko V.Y., Shvadchak V.V., Duportail G., Pivovarenko V.G., Klymchenko A.S., Mély Y. Monitoring membrane binding and insertion of peptides by two-color fluorescent label. *Biochim Biophys Acta Biomembr* 2011; 1808(1):424–432. doi:10.1016/j.bbamem.2010.09.013

8 SUPPLEMENTARY DATA

8.1 Curriculum vitae



OSEBNI PODATKI

KAISERSBERGER VINCEK MAJA

 Ruška cesta 71, 2000 Maribor (Slovenija)

Spol [Ženski](#) | Datum rojstva [17/9/1986](#) | [Državljanstvo](#) slovensko

ŽELENO PODROČJE DELA

R&D v kemijski industriji, farmacija, zdravstvo (kozmetična nega, dentalna industrija), trženje in skrbništvo za ključne stranke

DELOVNE IZKUŠNJE

1/10/2009–15/6/2010

Diplomsko delo

Perutnina Ptuj, d.d.
Potrčeva cesta 10, 2250 Ptuj (Slovenija)

Funkcionalizacija površine PET (polietilen tereftalatne) folije za doseg protimikrobnih lastnosti

[Vrsta dejavnosti ali 117ector](#) R&D v prehrabeni industriji

17/4/2010–10/4/2011

Predstavnik podjetja Danone v okviru projekta Medical Visits

Danone d.o.o., (Slovenija)

- promocija zdravega načina življenja v okviru obiskov zdravnikov, predstavitev izdelkov in njihovih znanstveno dokazanih pozitivnih učinkov na zdravje
- predstavitev izdelkov in tiskovin na strokovnih srečanjih – zdravniških kongresih

1/11/2011–2017

UM – Fakulteta za strojništvo – doktorska disertacija

UM, Fakulteta za strojništvo, Oddelek za tekstil
Smetanova ulica 17, 2000 Maribor (Slovenija)

Vpliv specifične in selektivne vezave peptidov na protimikrobno aktivnost materiala in njegovo biokompatibilnost

[Vrsta dejavnosti ali sektor](#) R&D v industriji medicinskih tekstilij

1/3/2012–v teku **Organizacija tečajev – vodenje in izobraževanje skupin v okviru popoldanskega s.p.**

Trideks, poučevanje plesa in druge storitve, Maja Kaisersberger Vincek s.p., Maribor (Slovenija)

- mentorstvo plesnim skupinam
- izobraževanje na licenčnih seminarjih za strokovne delavce v plesni rekreaciji
- animacija družabnih dogodkov

15/12/2015–v teku **Krka d.d. – samostojni tehnolog v Sektorju za proizvodnjo zdravil**

Krka, tovarna zdravil, d. d., Novo mesto
Šmarješka cesta 6, 8501 Novo mesto(Slovenija)

- vodenje posameznih področij v obratu
- reševanje tekoče tehnološke in tehnične problematike
- sodelovanje pri uvajanju novih izdelkov
- sodelovanje pri razvoju in uvajanju tehnologij in tehnoloških postopkov za nove izdelke
- spremljanje tehnologij pri pogodbenih partnerjih
- priprava in usklajevanje tehnološke dokumentacije za pogodbene partnerje
- vodenje prenosov tehnologij v Sloveniji in tujini

Vrsta dejavnosti ali sektor Farmacija

IZBRAŽEVANJE IN USPOSABLJANJE

1/10/2005–15/6/2010 **uni.dipl.ing.kem.tehnol.**

University of Maribor
Smetanova ulica 17, 2000 Maribor (Slovenija)
www.fkkt.um.si

- strokovno znanje iz področja kemije, biokemije, kemijske tehnologije, biotehnologije in inženirstva
- razvita sposobnost učenja na svojem strokovnem področju
- iniciativnost in samostojnost, ki je potrebna pri odločanju ter vodenju zahtevnejših del, laboratorijev ali obratov

KOMPETENCE

Materni jezik slovenščina

Drugi jeziki	RAZUMEVANJE		GOVORJENJE		PISNO SPOROČANJE
	Slušno razumevanje	Bralno razumevanje	Govorno sporazumevanje	Govorno sporočanje	
angleščina	C2	C2	C1	C1	C1
nemščina	A2	A2	A2	A2	B1
hrvaščina	C2	C2	C1	C1	C1
ruščina	A2	A2	A1	A1	A1

Stopnja: A1 in A2: Osnovni uporabnik - B1 in B2: Samostojni uporabnik - C1 in C2: Usposobljeni uporabnik

Komunikacijske kompetence	<ul style="list-style-type: none">▪ sposobnost za vključevanje v skupinsko delo▪ komunikacija s sodelavci in strokovnjaki drugih disciplin, kar omogoča sodelovanje pri multidisciplinarnih projektih▪ sposobnost strokovnega komuniciranja na domačem ter mednarodnem terenu
Organizacijske/vodstvene kompetence	<ul style="list-style-type: none">▪ vodenje skupine sodelavcev (trenutno sem odgovorna za proizvodnjo 20 različnih izdelkov, ki jih v različnih fazah proizvaja 400 ljudi)▪ organizacijske sposobnosti sem pridobila kot članica Športnega društva Moškanjci ter strokovni vodja Plesnega centra Mambo▪ ukvarjam se z organizacijo dogodkov, na katerih nastopa do 100 udeležencev▪ dobre vodstvene spretnosti sem pridobila tudi v procesu usposabljanja strokovnih delavcev v športu, v katerega sem vključena
Strokovne kompetence	<ul style="list-style-type: none">▪ usposobljenost za kvalitetno in varno delo v laboratoriju s poznavanjem laboratorijske opreme ter uporabe različnih postopkov analize in karakterizacije snovi od enostavnejših analiz do kompleksnih inštrumentalnih metod▪ analiza proteinskih substratov s pomočjo kapilarne elektroforeze, UV-Vis spektrofotometrije, FTIR, HPLC-GPC kromatografije, EPR spektroskopije▪ testiranje protimikrobne aktivnosti▪ optimizacija tehnoloških postopkov proizvodnje zdravil▪ GMP (dobra proizvodna praksa)
Digitalna pismenost	MS Office, MS Power point
Vozniško dovoljenje	B

8.2 Bibliography

Maja Kaisersberger Vincek [34493]

Personal bibliography for the period 2010-2017

PAPERS AND OTHER COMPONENTS

1.01 Original research articles

1. KAISERSBERGER VINCEK, Maja, ŠTRANCAR, Janez, KOKOL, Vanja. Antibacterial activity of chemically versus enzymatic functionalized wool with [xi]-poly-L-lysine. *Textile research journal*, ISSN 0040-5175, Published online before print July 5, 2016, str. 1-16. <http://trj.sagepub.com/content/early/2016/07/05/0040517516657060>, doi:[10.1177/0040517516657060](https://doi.org/10.1177/0040517516657060). [COBISS.SI-ID [19666710](https://www.cobiss.si/record/19666710)], [JCR, SNIP] kategorija: 1A1 (Z, A', A1/2); uvrstitev: SCI, Scopus, MBP; tipologija ni verificirana točke: 37.12, št. avtorjev: 3
2. GORGIEVA, Selestina, MODIC, Martina, DOVGAN, Barbara, KAISERSBERGER VINCEK, Maja, KOKOL, Vanja. Plasma-activated polypropylene mesh-gelatin scaffold composite as potential implant for bioactive hernia treatment. *Plasma processes and polymers*, ISSN 1612-8850, 2015, vol. 12, issue 3, str. 237-251, doi: 10.1002/ppap.201400125. [COBISS.SI-ID 28159271], [JCR, SNIP, WoS do 27. 4. 2015: št. citatov (TC): 0, čistih citatov (CI): 0, normirano št. čistih citatov (NC): 0, Scopus do 6. 4. 2015: št. citatov (TC): 0, čistih citatov (CI): 0, normirano št. čistih citatov (NC): 0]

1.08 Published scientific conference contribution

3. KAISERSBERGER VINCEK, Maja, GORGIEVA, Selestina, KOKOL, Vanja. Specific functionalization of wool with [epsilon]-poly-L-lysine ([epsilon]-PL) for tunable antimicrobial properties. V: MÉNDEZ-VILAS, A. (ur.). *Worldwide research efforts in the fighting against microbial pathogens: from basic research to technological developments*. [S. l.]: Formatex; Boca Raton: BrownWalker Press, cop. 2013, str. 239-243. [COBISS.SI-ID 17038102]

1.10 Published scientific conference contribution (invited lecture)

4. KAISERSBERGER VINCEK, Maja, KOKOL, Vanja. Biochemical functionalization of wool proteinaceous polymer with e-poly-L-lysine and its antimicrobial activity. V: 9th International Conference on Industrial Tools and Material Processing Technologies [also] ICIT & MPT, Ljubljana, Slovenia, April 9th - 11th 2014. HANČIČ, Aleš (ur.), et al. *Conference proceedings*. Celje: TECOS, Slovenian Tool and Die Development Centre, 2014, str. 103. [COBISS.SI-ID 17761302]

1.12 Published summary of scientific conference contribution

5. GORGIEVA, Selestina, KAISERSBERGER VINCEK, Maja, KOKOL, Vanja. Coating of polypropylene mesh with micro-structured gelatine as potential biomimetic composite for active hernia treatment. V: 26th Annual Conference European Society for Biomaterials, ESB, 31st August - 3rd September 2014, Liverpool, UK : final programme. [S. l.: s. n.], 2014, str. 46-2 [325]. http://esb2014.org/full_programme.pdf. [COBISS.SI-ID 18062614]

6. KAISERSBERGER VINCEK, Maja, KOKOL, Vanja, MOR, Amram, ŠTRANCAR, Janez. The effect of specific and selective binding of newly-structured oligo-acyl-lysyl peptides on wool fibre, its antimicrobial activity and biocompatibility. V: 8th International Conference on Polymer and Fiber Biotechnology, Baraga, Portugal, 25-27 May 2014. *IPFB 2014 : book of abstracts*. Baraga, Portugal: IPFB: Centre of Biological Engineering, 2014, str. [43]. [COBISS.SI-ID [17864726](#)]

7. KAISERSBERGER VINCEK, Maja, GORGIEVA, Selestina, PODLIPEC, Rok, ŠTRANCAR, Janez, KOKOL, Vanja. Specific functionalization of protein materials (wool and gelatin) with [epsilon]-poly-L-lysine ([epsilon]-PL) for tunable antimicrobial properties. V: II International Conference on Antimicrobial Research (ICAR2012), Lisbon, Portugal, 21-23 November 2012. *Book of abstracts*. [S. l.]: Formatex, 2012, str. 522. <http://www.formatex.org/icar2012/files/AbstractsBook.zip>. [COBISS.SI-ID [16468758](#)]

8. KAISERSBERGER VINCEK, Maja, GORGIEVA, Selestina, PODLIPEC, Rok, ŠTRANCAR, Janez, KOKOL, Vanja. Functionalization of protein polymers with antimicrobial peptide (AMPs) for tuneable antimicrobial properties. V: *E-MRS 2012 fall meeting, September 17-21, Warsaw University of Technology*. Strasbourg: European Materials Research Society, 2012, [1] str. http://www.emrs-strasbourg.com/index.php?option=com_abstract&task=view&id=183&year=2012&Itemid=&id_season=8. [COBISS.SI-ID [16271126](#)]

9. KAISERSBERGER VINCEK, Maja, GORGIEVA, Selestina, KOKOL, Vanja. Functionalization of wool fabric with [epsilon]-poly-L-Lysine for tuneable antimicrobial properties. V: Third International Symposium on Antimicrobial Peptides [also] Antimicrobial Peptide Symposium [also] AMP 2012, June 13-15, 2012, Lille (Villeneuve d'Ascq), France. *Today knowledge and future applications*. [S. l.: s. n.], 2012, str. A-13. [COBISS.SI-ID [16110358](#)]

MONOGRAPHS AND OTHER COMPLETED WORKS

2.11 Undergraduate Thesis

10. KAISERSBERGER VINCEK, Maja. Funkcionalizacija površine PET (polietilen tereftalatne) folije za doseg protimikrobnih lastnosti : diplomsko delo. Maribor: [M. Kaisersberger], 2010. XV, 42 f., graf. prikazi. <http://dkum.uni-mb.si/lzpisGradiva.php?id=16069>. [COBISS.SI-ID [2294863](#)]

2.13 Elaborate, preliminary study

11. KOKOL, Vanja, KAISERSBERGER VINCEK, Maja, GORGIEVA, Selestina, BOŽIČ, Mojca, VOGRINČIČ, Robert, MAJERIČ, Martina, VIVOD, Vera. Prilaganje *protimikrobne aktivnosti materialov z novo strukturiranimi peptidi = Targeting of material's antimicrobial activity by newly engineered peptides : končno poročilo o delu na projektu ERA-NET MATERA PLUS, 01.10. 2010 - 30. 09. 2013*. Maribor: Fakulteta za strojništvo, 2013. 17 str., ilustr., graf. prikazi. [COBISS.SI-ID [17812758](#)]

IZJAVA

Podpisana Maja KAISERSBERGER VINCEK, vpisna številka S3000481

izjavljam,

da je doktorska disertacija z naslovom **Vpliv vezave peptidov na protimikrobno aktivnost in biokompatibilnost proteinskih substratov**

- rezultat lastnega raziskovalnega dela,
- da predložena disertacija v celoti ali v delih ni bila predložena za pridobitev kakršnekoli izobrazbe po študijskem programu druge fakultete ali univerze,
- so rezultati korektno navedeni,
- nisem kršil-a avtorskih pravic in intelektualne lastnine drugih.

Podpis: _____